Master´s thesis

Realization and Evaluation of a Remotely Controlled Mobile Robot with Shared Control and Underactuated Hand to Improve the Unlatching of Doors

A.Ö. Sverrisson

Delft, February 13, 2012

Report Number: 1241
Student Number: 4039580

Delft University of Technology
Faculty of 3mE
Department of BioMechanical Engineering

Realization and Evaluation of a Remotely Controlled Mobile Robot with Shared Control and Underactuated Hand to Improve the Unlatching of Doors

Atli Örn Sverrisson

Committee:

Prof. Dr. F.C.T. van der Helm	Department of BioMechanical Engineering, 3mE
Dr.Ir. D.A.Abbink	Department of BioMechanical Engineering, 3mE
Dr. Ir. J.M.P. Geraedts	Department of Design Engineering, IO

Coach:
Dr.Ir. D.A.Abbink

Preface

The thesis is about a remotely controlled mobile robot that was able to open doors, the road that was taken to realize the complete system and the evaluation of improvements; haptic shared control and underactuated hand to ease the unlatching of doors.

For this thesis, a number of research areas were combined that are conducted at TU Delft. Two different robots, that had never been connected to another robot, were used as the master (PentaGriph1) and slave (DPR1) devices for a teleoperation. The slave device was equipped with the Delft Hand 3, an underactuated hand, and a new wrist joint specially designed for the purpose of this thesis. To top it off, a haptic guidance was created to assist the human operator while executing the task of opening doors. I believe that the search for combining researches is always beneficial and creates a greater synergy.

The focus of this study as mentioned before is the realization and evaluation of a remotely controlled mobile robot that is improved to open doors faster. The research paper provides a compact evaluation of the experiment performed with the system while the appendix describes the realization of the system and experimental results in more detail.

All relevant data used during the thesis (literature, software and measured data) have been submitted to the BioMechanical Engineering depository and are available on request.

I want to thank everyone that contributed to this study. Special thanks to Cor Meijneke, Guus Liqui Lung, Jan van Frankenhuyzen, Wouter Caarls and the guys at the Machine Shop. To my coach David, you always knew what to say to inspire me and get me back on my feet. Finally I want to thank my wife Eva, your support made all this possible.

Realization and Evaluation of a Remotely Controlled Mobile Robot with Shared Control and Underactuated Hand to Improve the Unlatching of Doors

Atli Örn Sverrisson
BioMechanical Engineering
Delft University of Technology

Abstract

Opening doors with a remotely controlled robot (telemanipulator) is a challenging task. The perceptual limitation of the telemanipulator system significantly increases the task difficulty, resulting in a higher completion time to open a door remotely. This paper focuses on three phases of opening a door: approaching the door, grasping the handle and unlatch the door. The main challenge of the task is to accurately follow the narrow trajectory of a rotating door handle without going astray and causing high force build-ups. Two improvements are presented and evaluated that enable the operator to more easily open a door remotely, haptic shared control that increases precision and an underactuated hand that decreases the need for precision. An experiment was performed to test the hypotheses that haptic shared control increases task performance of the human operator during approaching and unlatching of a door by guidance, while an underactuated hand increases task performance during grasping and unlatching of the door by increasing end-effector compliance. Subjects operated a 5 degrees of freedom mobile telemanipulator under 4 configurations: with or without haptic shared control, and with two levels of compliance in the end-effector. Results indicate that haptic shared control improves task performance significantly for both levels of end-effector compliance; in time to complete for the entire task, mainly in the grasping subtask, and in reduced number of grasps with an underactuated hand, while with a less compliant hand the guidance improved the control effort and workload. Without guidance, a decreased compliance in the end-effector significantly improved task performance towards the configuration with guidance and an underactuated hand; in time to complete the grasping subtask and reducing the amount of grasps, although the control effort is increased.

Index Terms - Teleoperation, Telemanipulation, Remotely Controlled, Mobile Robot, Haptics, Guidance, Haptic Shared Control, Underactuated Hand, Task Performance

1 Introduction

Remote controlled robots allow human operators to execute tasks at a remote location (teleoperation) which can be very beneficial if the task location is unknown and possibly dangerous to human lives. Recent disasters, the nuclear meltdown of the Fukushima reactors and the Gulf of Mexico oil spill, have shown us the importance of teleoperation in such dangerous environments and how humans are still limited to quickly scout and restrain such disasters.

Ideally humans want to see things for themselves or do maintenance with their bare hands but sometimes the environment is too dangerous for the human to enter. Therefore a robot will replace the human at the remote environment. Remotely controlled robots are constantly in the human operators' service and executes their commands at the remote environment [1]. The human operator controls the robot with a master device, through which a controller will communicate between the master device and a slave robot located in the remote environment (figure 1). Reflecting forces from the remote environment through a feedback loop provides the human operator with better sensation of what is happening there. The feedback is called transparent force feedback and if fully transparent, the human operator would feel like he is directly performing the task in the remote environment [24]. Still, the task performance is degraded because of system limitations (limited force [11] and visual [3] feedback) causing every day human tasks, e.g. opening doors, to be very time-consuming [23][19].

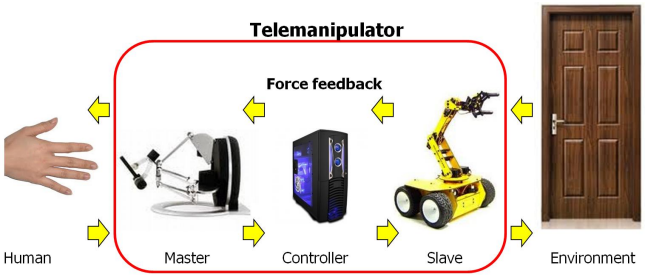

Figure 1 – A scheme of a remotely controlled robot (telemanipulator). The human operates the master device to control the slave device which is situated at a remote location.

According to a senior vice president at iRobot, the majority of the training of operators controlling two PackBots to go into the Fukushima power plant was spent on opening doors [5]. Since the first research on remotely opening doors in 1995 [23], the challenge of opening doors has been recognized. The research concluded that a remotely controlled robot needed improvements to successfully open doors in less than two minutes. In 2004, it took operators 5 times longer to complete the task of opening doors with a mobile robot than doing the task without a robot [19] (Table 1). Both studies [23][19] reached the conclusion that compliance in the system would allow operators to more easily open doors.

Research on autonomously opening doors, which is a much larger field than remotely opening doors, has acknowledged the challenge of opening doors as well, a challenge that still remains [12]. The most advanced state-of-the-art robot in opening doors, is probably the Willow Garage's autonomous robot, PR2 [16], which unlatches doors in about 15 seconds (starting ~60 cm away from the door). PR2 has a large variety of sensors, a compliance control that actively complies to environmental constraints and supplemented with a passive compliance in the arms. All successful autonomous robots are equipped with a force sensor in the wrist or fingers [18][22][12][20][26][16][13][4] to allow for an active compliance control. This is in accordance with the research on remotely opening doors to have compliance in the robot to ease the task. Remotely controlled robots are preferred in unknown and dangerous environments because the human is in the control loop and contributes its intelligence and the creativity of problem solving [25]. This paper will therefore only focus on opening doors with a remotely controlled mobile robot.

Previous studies on remotely controlled robots have shown that improved force feedback increases task performance [7][9]. Although, improving the quality of force feedback yields only marginal improvements [27]. Other studies have also tried to improve and optimize the transparency [11][15][17] by increasing the natural feeling of the device. Substantial improvements have been made but optimized transparency has not yet been realized.

Instead of focusing on improving the system transparency by reducing the limitations, that might result in a greater task performance, the task performance can be directly improved by assisting the operator to deal with the constraints of the task. That approach has shown to increase task performance more than transparent force feedback towards direct control [3].

This study will focus on the task of approaching, grasping and unlatching a door, a task that is both challenging and relevant. The constraints of the door, which rotate around an external axis, make the task a challenge for robots, which are usually rigid, and require them to accurately follow the trajectories of the constraints. The subtask of unlatching a door is a constrained force task and requires a high degree of precision given that the handle is firmly grasped. The constraint of the door handle forces the operator to move the robot along an arc of a rotating handle while rotating the hand as well. The trajectory is therefore very narrow and complicated, and if it is not accurately followed, forces will increase excessively. Improvements can therefore either assist the human operator to increase his precision or to allow him to be less precise in his movements.

Shared control, an automated control, can help the operator increase the precision of his movements by influencing the control input. Although Shared control has never been used to assist with opening doors it has been shown to be quite useful in e.g. obstacle avoidance [6][25], path following [3] and force control [8]. Shared control is different from transparent force feedback and can be divided into two types; mixed control, where the control signal is a mixture of the human intention and the automated control's intentions, and haptic shared control, where the human is in control but receives guidance force to complete the task.

An underactuated hand is a hand that has more degrees of freedom (DOF) than actuated DOF. The motor torque is equally distributed to the fingers which results in a grasp that forms very well around the object being grasped [2]. High forces acting on one or more fingers would only rearrange the fingers. The need for accuracy during the unlatching of a door is therefore redundant as the compliance in the fingers allow for a larger positional error before forces start to build up. A study [21] designed a low-cost underactuated hand with only one motor and attached to a wheelchair to open a variety of doors. With the designed hand the success rate was 71% and it was cabable of handling a variety of door handles and knobs.

Two improvements to ease the task of unlatching a door for human operators remotely controlling a robot are therefore realized:

- Shared Control
- Underactuated Hand

Table 1 – Experimental results (adapted from [19]) of the required time to open a door, for direct human interaction (direct), and interaction with a mobile teleoperator for novice users (tele a) and experienced users (tele b).

	direct	*tele a*	*tele b*	*ratio a*	*ratio b*
open door (ii)	4.3	59.9	21.1	14.1	5.0
passing door (iii)	1.3	69.6	24.1	54.3	18.8
open box (v)	13.5	82.1	45.9	6.1	3.4
total	23.5	413.0	173.8	17.6	7.4

The main objective of this research is to evaluate the influence of haptic shared control (HSC) and underactuated hand (UH) on task performance while operating a remotely controlled, non-holonomic, non-redundant service robot during the unlatching of a door. A non-holonomic robot is a robot that has less controllable degrees of freedom than the total degrees of freedom. This means that a non-holonomic

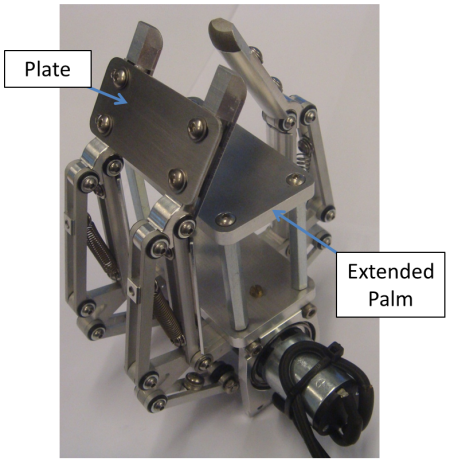

Figure 2 – Delft Hand 3 (DH3), where the palm has been extended for the purpose of door opening. A plate has been added to reduce the compliance and the degrees of freedom from 6 to 3.

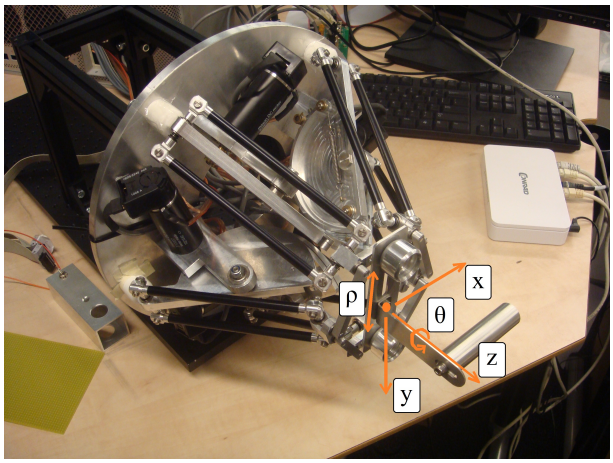

Figure 3 – The master device used for the experiment was Penta-Griph1 (PG1), a 5 DOF haptic parallel device. The orange arrows represent the 5 DOF to control the slave device, x for moving left and right, y for moving up and down, z for moving forward and backward, θ for rotation and ρ for gripping.

mobile robot is able to go straight and turn but unable to go sideways. A robot is non-redundant when the dimensions of joint space are equal to the dimensions of end-effector space. Meaning that one end effector position can only result in one configuration of the joints in the robot. To test the influence of HSC and UH, an experiment was performed on a door where subjects received haptic shared control, HSC on and off, and differently compliant end-effectors, UH and LUH. Less-underactuated hand (LUH) was realized by decreasing the number of DOF from 6 to 3 and by decreasing the rotational compliance of the fingers (figure 2). A simple plate was attached between two of the fingers to accomplish that. It was hypothesized for the 4 configurations LUH, UH, LUH-HSC and UH-HSC (table 2) that while approaching the door, HSC would improve the task performance with LUH and even more with UH. The level of underactuation would neither hinder or benefit the approaching. During the grasping phase, the level of compliance would benefit performance, but haptic shared control is not expected to do so. During the unlatching and opening, both compliance and shared control are expected to benefit the task.

Table 2 – Hypothesis, haptic shared control (HSC) is expected to improve task performance while less-underactuated hand (LUH) should decrease task performance when compared to the baseline, the underactuated hand (UH). '0' denotes no difference from the baseline.

	LUH	UH	LUH-HSC	UH-HSC
Approach	0	0	+	++
Grasp	-	0	0	0
Unlatch and open	-	0	+	++

2 Methods

2.1 Subjects

16 right handed subjects performed the experiment, both male and female (14 and 2 respectively), with an average age of 27.25 (std: 3.44). 5 of the subjects (subjects 1, 5, 6, 7 and 11) had previous experience with remotely controlling a robot. However, no significantly improved performance from those subjects was seen, see Appendix C.2.2.

2.2 Experimental Setup

The experiments were performed on a 5 DOF mobile telemanipulator setup that was constructed by combining previously developed technologies in our lab and adapting them for the purpose of door opening. The master robot, Penta-Griph 1 (PG1) is a 5 DOF haptic parallel device with movements in x, y, z, rotation around z and a gripping movement (figure 3). The device was intended for micro-assembly but is well suited for other purposes. The workspace of PG1 is approximately a cube with all sides equal to 25cm. The slave robot is the TU Delft Personal Robot 1 (DPR1) which is a non-holonomic non-redundant service robot (figure 4). The controller maps the movement of the human operator to Cartesian movements of the slave's end-effector, two DOFs actuate the mobile base for driving and turning and the other DOFs actuate the arm, wrist and hand. The mobile base is velocity controlled (axis x and z) for driving and turning the slave robot. A force field is applied to the master device similar to driving a car. Without any force from the operator the device will find an equilibrium which results in a stationary mobile base, a neutral position. The slave's end-effector is an underactuated three fingered hand, Delft hand 3 (DH3) [14], a 6 DOF hand which is actuated by only one motor and is constantly kept horizontal with a parallelogram mechanism

Figure 4 – Delft Personal Robot 1 (DPR1), the slave device used for the experiment, a 5 DOF non-holonomic, non-redundant service robot with an underactuated hand. In front of the robot is the table top door that was constructed for the experiment.

in the arm. The hand was modified for the purpose of door opening by extending the palm towards the distal phalanges to enable a firm grip on the handle (figure 2). The hand is current-controlled by sensing the current over the motor and actuated by a virtual spring of the gripping displacement on the master device. Because of the underactuation the exact position of the hand's fingers are inevitably hard to measure. Therefore the state of the grasp is determined by the electrical current over the motor, see Appendix D. The slave's arm and wrist joints are position controlled. The rotational point of the arm is at the hip of the robot causing a additional forward motion when the arm is moved downwards. This forward motion was counteracted by moving the base backwards. As the base was velocity controlled it was difficult to accurately move the arm vertically without any horizontal displacement. The end-effector moved therefore slightly forward when the arm was lowered. On the slave there is a 5MP Ethernet camera with up to 119 fps. The location of the camera is in the slave's 'head' (figure 4). This causes poor depth perception for operators. The global positioning of the slave was calculated from the velocity of the two wheels on the base, see Appendix A.2.2. The positional accuracy of the slave robot was estimated to be $\pm$ 1 cm in linear direction.

The master device was connected to a real-time xPC Target computer through a Quanser Q8 control board and running at 200 Hz. The slave was connected through a USB port to a 2.6 GHz dual-core laptop running non-real-time on Ubuntu 10.04. The inherently unpredictable communication speed of the USB port caused quite a delay-jitter which forced the running speed of the slave to be 10 Hz to minimize all jitter. The operator could therefore more easily learn on how to handle the delay in the system. The slave's code was running in the Robot Operating System (ROS-electric) which gathered commands from the master device and sent back the slave's positional information through an Ethernet cable using UDP packages. UDP is faster but less reliable than TCP because it does not confirm successful transfer of data.

For the purpose of the experiment, a small table top door was created to better manage the forces acting on the door (figure 4). The door had a L-shaped door handle (ellipse extrusion with the smaller diameter of 15 mm) on the left side of the door. The underactuated hand was not designed to withstand high torsional forces, therefore the handle had a 1 kg counterweight (8.5 cm from the rotational axis) at the other side of the door to counteract about $2/3$ of the internal spring force of the handle. A structure was created to let the counterweight always act orthogonally on the handle even though it had been rotated, see Appendix A.2. The principal remains the same as the handle still needs to be rotated but with less force. A safety measure was taken to allow the door to slide away from the robot if the forces were too high. The door was mounted on top of a 50-by-50 cm wooden particle board, centered at 11 cm from one end and the plate sat on top of a plastic coated office desk. This resulted in a handle height of 1.04 m from the ground, which is approximately the normal height. A 16 kg weight was placed behind the door to increase the friction between the wooden plate and the desk. A force of approximately 50 N onto the door handle was needed to start moving the door.

Two sensors were added to the experimental setup to provide visual feedback to help the operator perform the task. The first sensor was a pull-up resistor connected to the slave's end-effector. When the robot made contact with the grounded door handle a signal was sent to the operator in a form of an LED light. The second sensor was a switch that indicated a open door and the end of the task.

2.3 Task Instructions

The task was to operate the telemanipulator to approach the door, grasp and unlatch the handle and slightly open the door until a switch turned on, which marked the end of the task. Subjects were only able to watch the remote environment on a computer screen using a video stream from the camera on the slave and listen to the action due to the closeness of the master and slave. There were two starting locations of the slave robot, 130 cm away from the door and $\pm$ 37 cm sideways from the middle of the door handle (figure 5). The reason for two starting location was to prevent the subjects from performing the task without thinking but rather use force, visual and audio feedback to decide what to do. The robotic arm and wrist started in their initial position. The subjects were told to try to approach the door straight on and touch the handle before grasping it. They were also told to grasp the handle as far away as possible from its rotational axis but without letting the fingers fall off the handle. The task was counted as a failure if the handle was not grasped with a firm grip with the handle on the palm or the door had

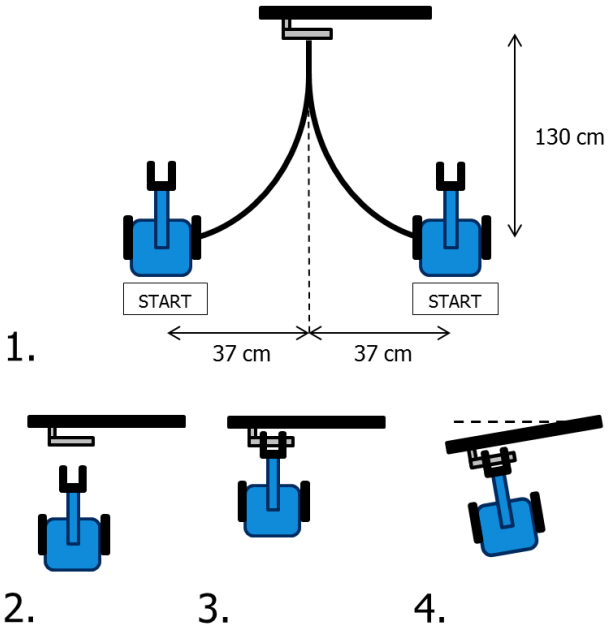

Figure 5 – Task instruction, 1. Drive as fast as possible to the door, 2. Drive gently close to the door, 3. Grasp the handle, 4. Unlatch and open the door.

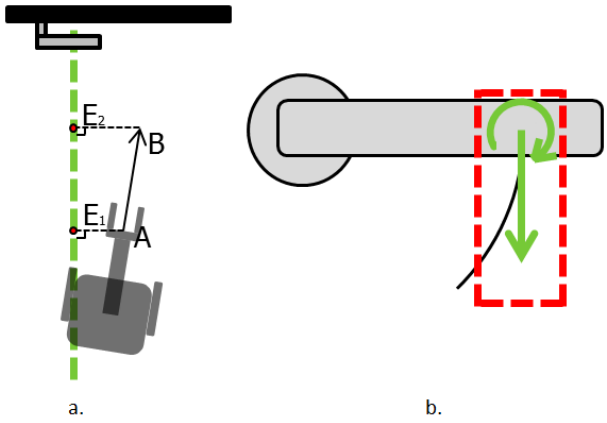

Figure 6 – Design of the haptic shared control. **a)** A guidance force was provided to subjects at point A where the magnitude of the guidance force was defined by E_2, a path error from a future position B after a certain time, $\vec{AB} = \dot{z} \cdot t_{lookahead}$, where $\dot{z}$ is the velocity of the robot. **b)** Subjects were restrained inside a box and received a linked rotational and vertical force for guidance.

been moved. Therefore, a successful completion of the task required at least one grasp on the handle.

2.4 Haptic Shared Control Design

Haptic shared control relies on information about the environment, sensed or known beforehand, in order to define the ideal path to the goal position. In this case, the control needs the global position of the mobile robot to robustly guide the operator towards the path. For the experiment, a perfect knowledge of the environment was assumed at the start of each trial and the ideal path had been defined. Haptic shared control was provided during the approach and for the unlatching of the door (figure 6). Because of positional errors in the mobile base of the slave, 4 test runs from each starting location were performed to calibrate the defined ideal path of the approach. The slave was therefore driven from the starting locations toward the correct location on the door handle. From the acquired data the end location was averaged and used for calibration. The positional error of the mobile base was estimated as $\pm$ 2 cm when the slave was driven towards the door but mainly depended on how much turning was involved. No knowledge about the exact trajectory of the path was supplied to the subjects before or during the experiment except for what subjects learned from the guidance.

The design of the haptic shared control during the approach was based on attractive guiding were the two starting positions were outside the optimal path. Subjects were attracted to an orthogonal path to the door and to the height of the door handle as well. Guidance force was only provided for rotating the slave robot (x-direction) and the height of the arm (y-direction). The further the slave robot was away from the path the higher force was provided to the operator in the direction towards the path. Instead of superimposing the guidance force on top of the equilibrium forces (acting along the x-direction) the equilibrium was moved corresponding to the path error and was no larger than the workspace of the master device, $\pm$ 0.096 m with an error gain of $g_x = -0.36$ and $g_y = -108$. That approach gave a much clearer intention of the guidance. The velocity $\dot{z}$ of the slave was taken into an account by calculating a future position B of the robot after a certain time, a look-ahead time of $t_{lookahead} = 0.1$ s, before measuring the distance E_2 to the path, $\vec{AB} = \dot{z} \cdot t_{lookahead}$ (figure 6.a). The look-ahead time seemed to increase the stability of the guidance.

For the unlatching task, the operator was constrained inside a vertical box when a grasp had been made, illustrated in figure 6.b. The operator was therefore restrained from moving the robot's base or moving the arm upwards. The only remaining degrees of freedom were linked to help the operator to both rotate and decrease the height of the hand. The height corresponded to a certain rotation of the hand and the guidance forces were approximated according to an arc with a radius of 6.5 cm. If the arm was moved downwards a clockwise rotational force was felt that would result in a rotated wrist. The error gain on the height and rotation was $g_y = -100$ and $g_\theta = -5$, respectively. The high gains in the y-direction of both designs is due to the weight compensation of the master device which needed to be overruled.

2.5 Experimental Protocol

Subjects performed the task 8 times for each of the 4 configurations (UH, LUH, UH-HSC, LUH-HSC). Starting with or without HSC was randomized for each subject and LUH was

fixed on the 2^{nd} and 3^{rd} configurations, mainly because of the time it took to change UH to become LUH.

2.6 Data Acquisition & Task Performance Metrics

During the experiment, a great amount of raw data was acquired at 200 Hz that later served to determine the metrics for the performance and control effort of the operator performing the task for the 4 configurations. The metrics were as follows:

Performance metrics:

***ttc** [s]* Time to complete, the time it takes a subject to finish the (sub)task.

$\boldsymbol{n}_{grasps}$ *[-]* Number of grasps, the amount of grasps before successively finishing the task.

***d** [m]* Distance traveled, the driven distance of the mobile robot during the approach to the door.

Control effort metric:

$\boldsymbol{r}_{rate}$ *-x [-]* Reversal rate of the turning command on the master device, determining the amount of steering corrections during the approach subtask. The number of corrections were found calculating the amount of zero crossings per minute along the x-axis. This is a good measure of how often the operator needs to correct the alignment of the robot before reaching the door handle.

Additionally, for all 4 configurations, subjective measures were recorded with a self reported mental workload using the NASA Task Load Index (NASA-TLX) questionnaire [10]. NASA-TLX provides a good measure of the workload during the execution of the task on the scale from 0 to 100, where higher numbers indicate higher workload.

2.7 Data Analysis

To statistically analyze the acquired data, a repeated measurement design was used. A paired t-test determined the significance of the 4 configurations (LUH, UH, LUH-HSC and UH-HSC). 8 repetitions were averaged for each of the 16 subjects before the differences were evaluated between the configurations and then compared to the hypotheses. Results with $p \leq 0.05$, 95% confidence, were regarded as statistically significant. The marks $(\bullet\bullet\bullet)$, $(\bullet\bullet)$ and $(\bullet)$ denote the significance of $p \leq 0.001$, $p \leq 0.01$ and $p \leq 0.05$, respectively, and $(-)$ denotes no significant difference.

3 Results

A general overview of the results are provided in figure 7 and 8. Figure 7 shows a stacked boxplot of the averaged

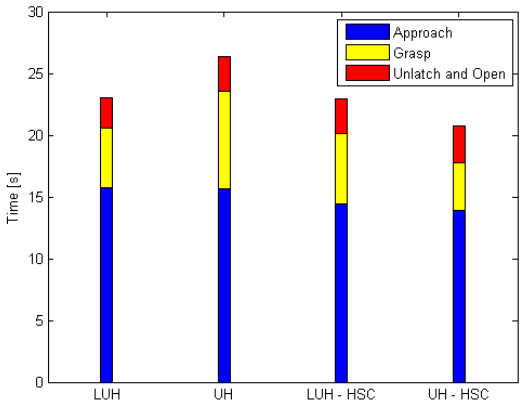

Figure 7 – Time to complete for the entire task, separated for the 3 subtasks, average of the 16 subjects were each had 8 repetitions.

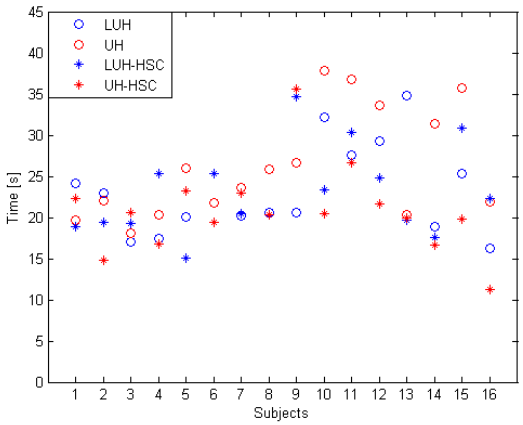

Figure 8 – Time to complete metric for the entire task for all configurations, average of 8 repetitions for each of the 16 subjects.

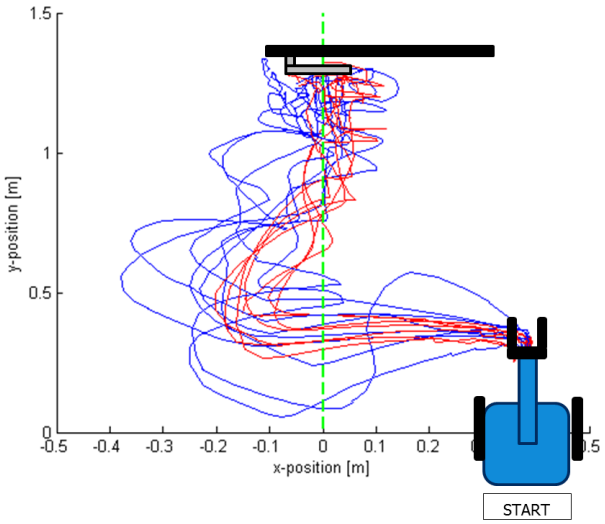

Figure 9 – End-effector path of a typical subject that benefited from haptic shared control when performing the entire task from one starting point with both end-effector types, for 8 repetitions without HSC (blue) and 8 with HSC (red). The green dashed line marks the reference for the haptic shared control.

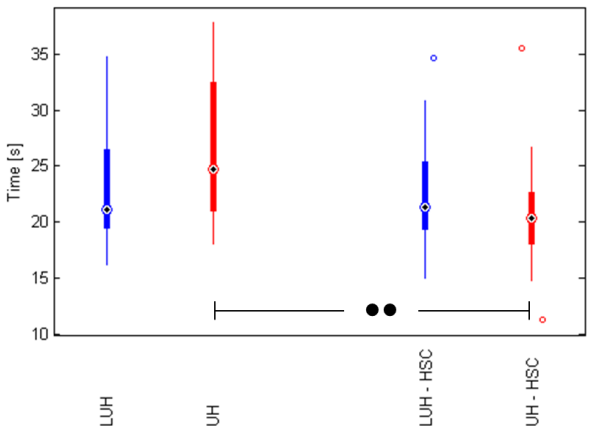

Figure 10 – Time to complete for the entire unlatching a door task, averaged from 8 repetitions for 16 subjects. The boxplot presents a median, 25^{th} and 75^{th} percentiles, and whiskers for all configurations. Significant differences of p $\leq$ 0.05, p $\leq$ 0.01 or p $\leq$ 0.001 are presented with a mark of (•),(••) or (• • •) on the plot, respectively

time to complete (ttc) for the entire task of unlatching a door, separated for the 3 subtasks (approach; grasp; unlatch and open). The average approach times for the two cases with HSC are approximately equal and the same can be said about the two cases without HSC, as was expected. Figure 8 shows the average time to complete for the 4 configurations for each of the 16 subjects. The variability between subjects can be clearly seen in the image and how the 4 configurations affect each subject differently. Subjects 9 and 10 are a good example of the variability as subject 10 performed better with HSC while subject 9 did not and they both started with HSC.

In the following sections the influence of the 4 configurations on the measured metrics, described in section 2.6, on each of the 3 subtasks (approach; grasp; unlatch & open) and on the subjective measures is presented.

3.1 Influence on Task Performance and Control Effort

The effect of the 4 configurations on task performance and control effort can be viewed in figures 9, 10, 11 and 12 and in tables 3 and 4. Figure 10 shows the time to complete for the task of unlatching a door. All configurations decreased in time with regard to the baseline (UH). Haptic shared control (HSC) improved the time of LUH-HSC by 3.37 s (p = 0.056) and UH-HSC by 5.57 s (p = 0.009). With fewer DOF and less compliant end-effector (LUH) the time was reduced by 3.28 s (p = 0.057). The fastest completion times recorded were 10.93 s, 11.77 s, 11.03 and 7.3 seconds for configurations LUH, UH, LUH-HSC and UH-HSC, respectively. Looking at the amount of grasps before a successful unlatching (figure 11), subjects tended to grasp more with UH than any other configuration and least amount of grasps with UH-HSC. With guidance, the amount is decreased by 29% (p = 0.013) for UH-HSC and 15% (0.091) for LUH-HSC when compared to UH. A significant difference was found between the two HSC configurations, UH-HSC resulted in 11% (p = 0.039) less grasps than LUH-HSC. Comparing UH with LUH, the number of grasps is decreased by 24% (p = 0.011). The distance traveled to the door yielded no significant difference although figure 9, path taken by a typical subject for 8 repetitions with and without HSC, clearly presents a large difference in travelled distance and consistency. The control effort of each of the subjects are presented in figure 12, where the reversal rate, the amount of steering corrections per minute, is displayed for the 4 configurations in turning command (x-direction) on the master device. The reversal rate in driving command (z-direction) yielded similar results, see Appendix C.2. Reversal rate for LUH is increased when compared to UH by 15% (p = 0.031), but when LUH is compared to the two cases with HSC the significant difference is slightly less, LUH-HSC by 23% (p = 0.039) and UH-HSC by 19% (p = 0.066). Tables 3 and 4 provide a comprehensive overview of the analysis.

3.2 Influence per Subtasks

Looking more closely at the 3 subtasks (approach; grasp; unlatch & open) with figure 13 and tables 5 and 6, the differences between configurations are easier to distinguish. As can be seen in table 6 there are no significant differences during the approach subtask, although the differences between UH and UH-HSC of 1.75 s (p = 0.139) and LUH and UH-HSC of 1.83 s (p = 0.070) come close. The averaged completion time for the grasping subtask can be seen in figure 13. When compared to UH, the UH-HSC decreases the

Table 3 – Overview of the analyzed differences between configurations. The metrics being analyzed are; Time to complete (*ttc*), number of grasps (n_{grasps}), distance traveled (*d*) and the reversal rate (r_{rate}). The table shows the difference in mean, the 95% confidence interval and the significance (p-value). Statistical significance is shaded.

	ttc [s]		n_{grasps} *[-]*		*d [m]*		r_{rate} *-x [-]*	
Configuration	Diff. mean (95% CI)	p value	Diff. mean (95% CI)	p value	Diff. mean (95% CI)	p value	Diff. mean (95% CI)	p value
UH - LUH	3.28 (-0.12; 6.68)	0.057	0.31 (0.08; 0.54)	0.011	-0.81 (-2.51; 0.89)	0.327	-2.70 (-5.12; -0.27)	0.031
UH - UH-HSC	5.57 (1.59; 9.54)	0.009	0.36 (0.09; 0.63)	0.013	0.02 (-0.14; 0.18)	0.786	0.18 (-2.71; 3.07)	0.896
UH - LUH-HSC	3.37 (-0.10; 6.83)	0.056	0.21 (-0.04; 0.46)	0.091	0.05 (-0.05; 0.15)	0.315	0.63 (-2.65; 3.92)	0.688
LUH - LUH-HSC	0.085 (-3.67; 3.84)	0.962	-0.10 (-0.24; 0.04)	0.138	0.86 (-0.88; 2.59)	0.310	3.33 (0.20; 6.46)	0.039
LUH - UH-HSC	2.28 (-1.41; 5.98)	0.208	0.05 (-0.08; 0.17)	0.432	0.83 (-0.92; 2.57)	0.328	2.88 (-0.22; 5.97)	0.066
UH-HSC - LUH-HSC	-2.20 (-5.00; 0.61)	0.115	-0.15 (-0.29; -0.01)	0.039	0.03 (-0.10; 0.15)	0.624	0.45 (-3.27; 4.17)	0.800

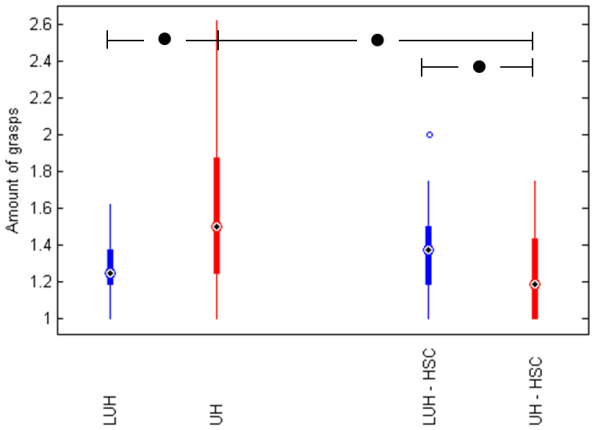

Figure 11 – Amount of grasps before a successful completion of the unlatching a door task, averaged from 8 repetitions for 16 subjects. At least 1 grasp is required for a successful task completion The boxplot presents a median, 25^{th} and 75^{th} percentiles, and whiskers for all configurations. Significant differences of $p \leq 0.05$, $p \leq 0.01$ or $p \leq 0.001$ are presented with a mark of (•),(••) or (• • •) on the plot, respectively

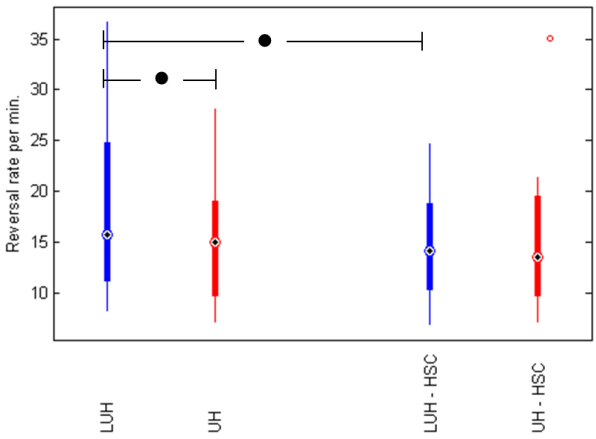

Figure 12 – Reversal rate of the master device, for the turning command, during the approach subtask, averaged from 8 repetitions for 16 subjects. The boxplot presents a median, 25^{th} and 75^{th} percentiles, and whiskers for all configurations. Significant differences of $p \leq 0.05$, $p \leq 0.01$ or $p \leq 0.001$ are presented with a mark of (•),(••) or (• • •) on the plot, respectively

Table 4 – Performance and control effort metrics are presented in this table with a mean and standard deviation for all configurations

	Mean (std)			
Metric	LUH	UH	LUH-HSC	UH-HSC
ttc [s]	23.06 (5.47)	26.34 (6.62)	22.97 (5.35)	20.77 (5.35)
n_{grasps} *[-]*	1.28 (0.17)	1.59 (0.46)	1.38 (0.26)	1.23 (0.25)
d [m]	2.50 (3.25)	1.69 (0.29)	1.65 (0.21)	1.67 (0.15)
r_{rate} *-x [-]*	17.98 (8.51)	15.28 (6.75)	14.65 (5.33)	15.10 (7.14)

time by 4.01 s (p = 7.1e-4). The time difference between UH and LUH-HSC is also worth mentioning as the time difference is 2.20 (p = 0.080). If the two HSC configurations are compared a significant difference is found as UH-HSC takes 1.81 s (p = 0.050) less time in grasping the door. LUH configuration decreases the time of grasping by 3.08 s (p = 0.006) when compared to UH. The third subtask showed no significant difference and is the only time when both HSC configurations have a higher mean than the two configurations without HSC.

Table 5 – Subtasks are presented in this table with a mean and standard deviation of the time to complete for all configurations

	Time to complete (ttc) Mean (std)			
Subtask	LUH	UH	LUH-HSC	UH-HSC
Approach	15.72 (3.56)	15.64 (3.84)	14.43 (2.86)	13.89 (3.03)
Grasp	4.82 (2.68)	7.90 (4.01)	5.70 (4.59)	3.88 (2.76)
Unlatch & Open	2.52 (1.17)	2.80 (1.16)	2.84 (1.01)	3.00 (1.71)

3.3 Subjective Measures

The workload scores (NASA-TLX) given by the subjects after each of the configurations are presented in table 6 and figure 14. Subjects found a 13% (p = 0.075) increase in workload

Table 6 – Overview of the analyzed differences between configurations for time to complete (ttc) for each of the subtasks and the subjective measure (NASA-TLX). The table shows the difference in mean, the 95% confidence interval and the significance (p-value). Statistical significance is shaded.

	Approach - ttc [s]		*Grasp - ttc [s]*		*Unlatch & Open - ttc [s]*		*NASA-TLX [0-100]*	
Configuration	Diff. mean (95% CI)	p value	Diff. mean (95% CI)	p value	Diff. mean (95% CI)	p value	Diff. mean (95% CI)	p value
UH - LUH	-0.09 (-1.65; 1.48)	0.908	3.08 (1.05; 5.11)	0.006	0.29 (-0.25; 0.83)	0.271	-7.13 (-15.06; 0.80)	0.075
UH - UH-HSC	1.75 (-0.64; 4.13)	0.139	4.01 (2.00; 6.03)	7.1e-4	-0.19 (-1.14; 0.76)	0.671	0.36 (-2.92; 3.65)	0.816
UH - LUH-HSC	1.21 (-0.69; 3.10)	0.195	2.20 (-0.29; 4.69)	0.080	-0.04 (-0.69; 0.61)	0.905	-1.14 (-6.54; 4.26)	0.659
LUH - LUH-HSC	1.29 (-0.75; 3.33)	0.197	-0.88 (-3.69; 1.93)	0.515	-0.33 (-0.83; 0.18)	0.187	5.99 (1.39; 10.59)	0.014
LUH - UH-HSC	1.83 (-0.17; 3.84)	0.070	0.93 (-0.88; 2.75)	0.290	-0.48 (-1.29; 0.32)	0.220	7.49 (-1.32; 16.30)	0.090
UH-HSC - LUH-HSC	-0.54 (-2.37; 1.29)	0.539	-1.81 (-3.63; 0.001)	0.050	0.16 (-0.51; 0.83)	0.627	-1.50 (-7.05; 4.04)	0.572

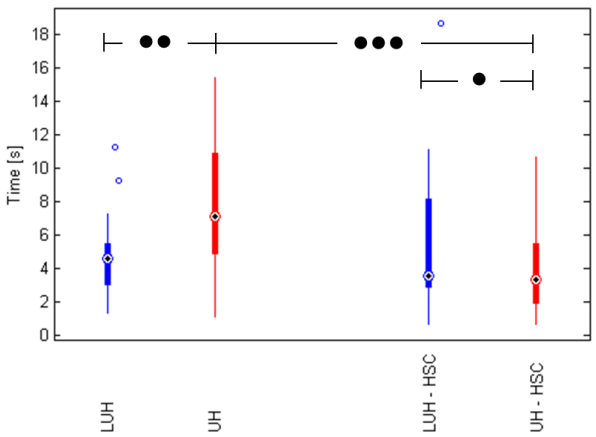

Figure 13 – Time to complete for the grasp subtask, averaged from 8 repetitions for 16 subjects. The boxplot presents a median, 25^{th} and 75^{th} percentiles, and whiskers for all configurations. Significant differences of $p \leq 0.05$, $p \leq 0.01$ or $p \leq 0.001$ are presented with a mark of (•),(••) or (• • •) on the plot, respectively

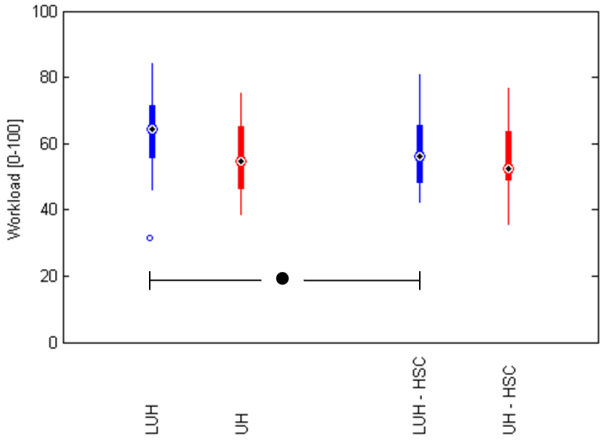

Figure 14 – NASA-TLX subjective measure, scaled from 0 to 100, where low number represents lower workload. The boxplot presents a median, 25^{th} and 75^{th} percentiles, and whiskers for all configurations. Significant differences of $p \leq 0.05$, $p \leq 0.01$ or $p \leq 0.001$ are presented with a mark of (•),(••) or (• • •) on the plot, respectively

when LUH is compared to UH, and a 11% (p = 0.014) and 14% (p = 0.090) when LUH is compared to LUH-HSC and UH-HSC, respectively. 10 out of 16 subjects found that LUH required the most workload out of the 4 configurations and only 1 subject thought the same about UH. According to 6 subjects, the configuration that required the least amount of workload was the UH-HSC configuration and another 6 subjects thought the same about LUH-HSC.

After the experiment subjects were asked to comment on their experience. Many subjects found the depth perception in the video stream very limited, which caused a large learning curve. Subjects reported a restricted view of the handle in the LUH configuration. While operating, the offset from the neutral position was hard to determine and therefore also difficult to know how much force was actually exerted on the door. Velocity control of the mobile base was not very intuitive for the operators and making fine movements was especially difficult. Some subjects did not trust in HSC and felt more in control without it but the ones who did trust it had to think less about the trajectory while approaching the door. The guidance forces during the unlatching of the door were not obvious to some subjects as they did not feel them very well. Subjects found audio feedback quite useful because they heard when the robot made contact with the door and when it was exerting too much force on the door. Also, subjects did not need to take their eyes off the screen with the audio feedback, like they did to view the status of the contact LED.

4 Discussion

Although the large variability between subjects (figure 8) complicates the analysis, the experimental results still showed that human operators could benefit from haptic shared control and compliant end-effector. The effects of the haptic shared control and the underactuated hand on the results are discussed in the following chapters.

4.1 Effects of Haptic Shared Control

The effects of haptic shared control are evident when the two configurations UH and UH-HSC are compared. A signif-

icant difference is found in time to complete (figure 10) and amount of grasps (figure 11) for the entire task, while other metrics show no indication. Subjects performed these configurations either first or last which could suggest that the learning effect might have been less for UH-HSC. When the first 4 repetitions are compared to the last 4 for both configurations the same learning curve is seen but when all subjects that started with UH-HSC are compared to all subjects starting with UH a significant difference is found. Subjects starting with HSC had reduced control effort (reversal rate) during the approach, see Appendix C.2. The reduced amount of grasps required to finish the task indicates increased task performance during the grasping subtask. The completion time of the grasping subtask is significantly lower (figure 13) as the operator is guided towards the door to the correct location on the door handle causing the operator to need less grasps and time to successfully unlatch the door.

Interestingly, haptic shared control affected subjects differently when they had a different compliant end-effector. By adding HSC to LUH, subjects had significantly lower control effort (reversal rate) and workload, as indicated by figures 12 and 14, respectively, while it had little effect on other metrics. As some subjects stated, the view was partly blocked by LUH, which might have caused a higher difficulty in aligning the end-effector onto the door handle without any guidance, causing a higher control effort and workload.

When the two HSC configurations are compared, LUH-HSC resulted in a higher completion time. It seems like HSC does not help the operator with LUH as much as it does for UH and according to figures 11 and 13, the reason is centered around the grasping. This implies that a more compliant hand (UH) will grasp the handle more securely. The guidance during the unlatching subtask might also have restrained LUH-HSC too much because it had less compliance. If the handle was grasped further away from the rotational axis of the handle the guidance box might have been too small.

There were several limitations in the design of haptic shared control, which may have reduced the possible benefits. The accuracy of the information could be distorted due to positional errors in the slave. Then haptic shared control would no longer have an accurate information about the environment causing a displacement of the ideal path. That would cause excessive and incorrect guidance forces provided to the operator who would have to counteract them to successfully finish the task. During the experiment, subjects received unintentionally incorrect guidance due to positional errors but were able to quickly detect and solve the conflict to finish the task. Subjects were more aware of positional errors every time they had to retry to grasp and unlatch the door. They reported that the task got more difficult with the incorrect guidance, especially the fine movements, and that they became more easily frustrated. This is probably the cause of the difference between LUH-HSC and UH-HSC because subjects had to re-grasp more often with LUH-HSC.

Sometimes the intentions of the shared control and the human operator are not the same. That happened during the experiment conflicting about the height of the end-effector with regard to the door handle. Subjects felt that the guidance wanted them to be higher compared to what they were used to when grasping the door handle. These were almost all subjects that did not start with HSC but acquired a certain strategy to solve the task without it and were accustomed to grasp the handle a bit lower. Such conflicts made the subjects skeptical of the benefit of haptic shared control.

4.2 Effects of an Underactuated Hand

Contrary to what was hypothesized, LUH resulted in a shorter completion time (figure 10) and a significantly less amount of grasps (figure 11) when compared to UH for the entire task. A possible explanation for this result could be that UH was too compliant for the task. The reversal rate was significantly higher for LUH (Figure 12) which could indicate that subjects that started with HSC had a more difficult time in controlling the robot when they lost the guidance force. Alternatively, it might be that those who started without HSC felt over-confident and ventured a bit more than they could handle during their 2^{nd} configuration. Those reasons are unlikely as the configuration order in which subjects performed the experiment did not matter, the reversal rates were very similar. The most likely reason is again that LUH was partly blocking the view on the door handle which supports the conclusion that haptic shared control improved the reversal rate and workload even though the end-effector was LUH.

The experimental results indicate that the rotational compliance of the Delft Hand 3 is too high. Decreased compliance with LUH has a positive influence on task performance, although the compliance might be too low for the designed haptic shared control.

Subjects often exerted high forces onto the door making it impossible to unlatch the door until these excessive forces were gone. This was caused by the slight forward motion of the slave robot arm when moving down, resulting in an even larger force on the door. The movement of the arm should have resulted in a slight backward movement instead to relieve the excessive forces. Alternatively, the source of the compliance should have been in the arm instead of the fingers.

4.3 Comparing Time to Complete to Other Researches

Comparing the average time to complete, for the entire task, to a human directly opening a door in 1.72 seconds, results in a 13.4, 15.3, 13.4 and 12.1 fold increase in time for LUH, UH, LUH-HSC and UH-HSC, respectively. If the best time performance is compared to a human, it results in an 6.4, 6.8, 6.4 and 4.2 fold increase for LUH, UH, LUH-HSC and UH-HSC, respectively. These results correspond well to results from other research [19] (table 1), where subjects experienced higher telepresence with stereo vision that moved

according to the operator's head motion, force feedback and the ability to walk themselves along with the master device. Less experienced subjects had a ratio of 14.1 and experienced subjects a ratio of 5. Haptic shared control with an underactuated hand shows improved performance compared to that study but the comparability can be questioned as subjects there did not firmly grasp the door handle but pushed it downwards, avoiding the complexity of the door handle trajectory.

When the fastest time of the configuration UH-HSC, is compared to the state-of-the-art robot in opening doors, PR2 [16], the time to complete is 7.3 s against 15 s, respectively. Although, PR2 takes more than double the time to unlatch a door and from less than half the distance, haptic shared control assumes perfect knowledge of the environment while PR2 derives it from sensor information.

4.4 Future Work

The experiment was limited to only a one door in a constructed environment where the environment, the intention of the human operator and the ideal path of the guidance was known beforehand. Because of these limitation it is impossible to implement the designed shared control where the environment is unknown. Future work involves making haptic shared control possible for unknown environments.

An unknown environment differs from a constructed environment in the way that nothing can be known before hand, everything is hard to identify and the environment is not optimal. To be able to implement shared control, the environment must be sensed and objects and possible routes identified. Then shared control needs to be able to robustly generate an ideal path that aids the operator to solve the constraints and goals of the task, given that it knows what the intentions of the operator are. Additionally, shared control should be able to revise its path, in case there is a conflict of intention between it and the operator.

For shared control to robustly assist the human operator completing the task, it requires knowledge about what the task is and how the human intends to solve it. Shared control therefore needs a way to identify them and use them for generating the ideal path and to correctly guide the human. For example if there are three doors in a hallway, which door does the human want to open? The shared control needs to analyze the input from the operator to figure out his intentions.

Shared control should be able to identify objects, e.g. a door, and be able to locate constraints, e.g. hinges (axes of rotation), because that information is required for the shared control to create the ideal path, e.g. trajectory of a rotating door handle.

To be able to perform a larger variety of tasks, not only open doors, the workspace of the master device needs to be larger because the workspace on the PentaGriph 1 is quite limited. Increasing the gains will partly solve the problem but will make the movements less intuitive and harder to operate.

5 Conclusions

For the experimental conditions studied, the following conclusions can be drawn:

- Guidance from haptic shared control allowed subjects to significantly improve their time performance during the grasping subtask and decrease the amount of grasps before successfully opening the door with an underactuated hand.
- Guidance reduced the control effort and workload with a less compliant hand.
- With guidance, an underactuated hand significantly reduced the amount of grasps and time during the grasping subtask.
- Without guidance, a less compliant hand improved time performance and decreased the amount of grasps while increasing the control effort and workload.

References

[1] D.P. Barnes and M.S. Counsell. Haptic communication for remote mobile manipulator robot operations. In *American Nuclear Society, Proc. 8th Topical Meeting on Robotics and Remote Systems*, pages 1–8, 1999.

[2] Lionel Birglen, Thierry Laliberté, and Clément Gosselin. *Underactuated robotic hands*. Springer-Verlag, Berlin, 2008.

[3] H. Boessenkool, D.A. Abbink, C.J.M. Heemskerk, and F.C.T. van der Helm. Haptic shared control improves tele-operated task performance towards performance in direct control. In *World Haptics Conference (WHC), 2011 IEEE*, number January, pages 433–438. IEEE, 2011.

[4] Sachin Chitta, Benjamin Cohen, and Maxim Likhachev. Planning for autonomous door opening with a mobile manipulator. In *Robotics and Automation (ICRA), 2010 IEEE International Conference on*, pages 1799–1806. IEEE, 2010.

[5] D.C. Denison. Packbots explore stricken reactor, 2011.

[6] N. Diolaiti and C. Melchiorri. Teleoperation of a mobile robot through haptic feedback. *IEEE International Workshop HAVE Haptic Virtual Environments and Their*, (November):67–72, 2002.

[7] JV Draper, WE Moore, JN Herndon, and BS Weil. Effects of force reflection on servomanipulator task performance. Technical report, Oak Ridge National Lab., TN (USA), 1986.

[8] Weston B. Griffin, William R. Provancher, and Mark R. Cutkosky. Feedback Strategies for Telemanipulation with Shared Control of Object Handling Forces. *Presence*, 14(6):720–731, December 2005.

[9] B. Hannaford, L. Wood, D.a. McAffee, and H. Zak. Performance evaluation of a six-axis generalized force-reflecting teleoperator. *IEEE Transactions on Systems, Man, and Cybernetics*, 21(3):620–633, 1991.

[10] S.G. Hart and L.E. Staveland. Development of NASA-TLX (Task Load Index): Results of empirical and theoretical research. *Human mental workload*, 1(11):139–183, 1988.

[11] K. Hastrudi-Zaad and S.E. Salcudean. On the use of local force feedback for transparent teleoperation. *Proceedings 1999 IEEE International Conference on Robotics and Automation (Cat. No.99CH36288C)*, (May):1863–1869, 1999.

[12] A. Jain and C.C. Kemp. Behaviors for robust door opening and doorway traversal with a force-sensing mobile manipulator. In *RSS Manipulation Workshop: Intelligence in Human Environments*, 2008.

[13] Dongwon Kim, Ju-hyun Kang, Chang-soon Hwang, and Gwi-tae Park. Mobile Robot for Door Opening in a House. *Service Robot*, pages 596–602, 2004.

[14] Gert A Kragten. *Underactuated Hands. Fundamentals, Performance Analysis and Design*. Doctoral thesis, TU Delft, 2011.

[15] D.a. Lawrence. Stability and transparency in bilateral teleoperation. *IEEE Transactions on Robotics and Automation*, 9(5):624–637, 1993.

[16] Wim Meeussen, Melonee Wise, Stuart Glaser, Sachin Chitta, Conor Mcgann, Patrick Mihelich, Eitan Marder-eppstein, Marius Muja, Victor Eruhimov, Tully Foote, John Hsu, Radu Bogdan Rusu, Bhaskara Marthi, Gary Bradski, Kurt Konolige, Brian Gerkey, Eric Berger, and Willow Garage. Autonomous Door Opening and Plugging In with a Personal Robot. *Computer*, 2010.

[17] F. Mobasser and K. Hashtrudi-Zaad. A model-independent force observer for teleoperation systems. *IEEE International Conference Mechatronics and Automation, 2005*, 2:964–969.

[18] K. Nagatani and S. Yuta. Designing strategy and implementation of mobile manipulator control system for opening door. *Proceedings of IEEE International Conference on Robotics and Automation*, (April):2828–2834, 1996.

[19] N. Nitzsche and G. Schmidt. A mobile haptic interface mastering a mobile teleoperator. *2004 IEEE/RSJ International Conference on Intelligent Robots and Systems (IROS) (IEEE Cat. No.04CH37566)*, pages 3912–3917, 2004.

[20] L. Peterson, D. Austin, and D. Kragic. High-level control of a mobile manipulator for door opening. *Proceedings. 2000 IEEE/RSJ International Conference on Intelligent Robots and Systems (IROS 2000) (Cat. No.00CH37113)*, pages 2333–2338, 2000.

[21] E.B. Rapacki, C. NiEzREcki, and H.A. Yanco. An underactuated gripper to unlatch door knobs and handles. In *Technologies for Practical Robot Applications, 2009. TePRA 2009. IEEE International Conference on*, pages 135–140. IEEE, 2009.

[22] Changju Rhee, Munsang Kim, and Hyungjin Lee. Door opening control using the multi-fingered robotic hand for the indoor service robot. *IEEE International Conference on Robotics and Automation, 2004. Proceedings. ICRA '04. 2004*, pages 4011–4016 Vol.4, 2004.

[23] M. Saitoh, Y. Takahashi, A. Sankaranarayanan, H. Ohmachi, and K. Marukawa. A mobile robot testbed with manipulator for security guard application. *Proceedings of 1995 IEEE International Conference on Robotics and Automation*, pages 2518–2523, 1995.

[24] Bruno Siciliano and Oussama Khatib. *Handbook of Robotics*. Springer-Verlag, Heidelberg, 1st edition, 2008.

[25] G.S. Sukhatme and G.J. Kim. *Haptic control of a mobile robot: a user study*. Number 2. IEEE, 2002.

[26] B J W Waarsing, M Nuttin, and H Van Brussel. Behaviour-based mobile manipulation : the opening of a door. *Mechanical Engineering*, pages 168–175, 2003.

[27] J G W Wildenbeest. Improving the Quality of Haptic Feedback Yields Only Marginal Improvements in Teleoperated Task Performance. 2010.

Appendices belonging to the Master´s thesis:

Realization and Evaluation of a Remotely Controlled Mobile Robot with Shared Control and Underactuated Hand to Improve the Unlatching of Doors

Atli Örn Sverrisson

Contents

Appendix A Unlatching Doors - Experimental Setup

The experiment is based on connecting two robots that haven´t been connected together before, the PentaGriph1 (PG1) and Delft Personal Robot 1 (DPR1), and operate them to open a door under different configurations. Because opening doors is difficult with a robot it was hypothesized that haptic shared control would improve task performance by increasing the precision of the operator while an underactuated hand would reduce the need for precision. The configurations to test are therefore with or without haptic shared control and with an underactuated hand or a less compliant hand. These conditions are thought to improve the system to make opening doors reality with a 5 DOF non-holonomic, non-redundant service robot (DPR1) operated by a 5 DOF parallel haptic robot (PG1).

First the task of opening a door will be discussed in detail to better understand what the task is, why it is so difficult for robots to finish and what the required forces are. Then the experimental setup is introduced, what was needed for the experiment and how it was designed.

A.1 Task Environment

Unlatching and opening a door is a constrained force task and this chapter describes the forces and required degrees of freedom to complete the task. The door handle type of interest is a common European L-shaped handle.

A door and a door handle have both only one degree of freedom. The door can rotate around its hinges and the door handle can be twisted around an axis centered at the handle's base, see Figure A-1. The location of the hinges will never move but the door handle's location is dependent on how much the door is open.

Figure A-1: Door rotating around its hinges

By twisting the door handle the door is unlatched from the door frame and can be rotated open. Door handles have a spring mechanism to keep the doors safely closed. Unlatching requires a certain force to overcome the internal torsional spring torque τ of about 1 - 2.5 Nm. Even though a robot can provide the required torque to overcome the spring force the direction of the force is equally important. The direction of the force needs to be orthogonal to the handle at all times to be able to rotate the handle.

There are three ways to unlatch a door;

1. Pushing the door handle downwards, while not caring about horizontal placement on the door handle. The force F required to twist a door handle is $F = \tau/r$, where r is the distance from the rotational axis of the door handle to the center of the hand. The greater the r is, the less force F is needed. The weakness of this method is that it is fairly easy to slip off the handle but the task only requires one degree of freedom.

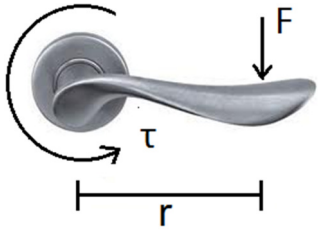

$$\tau = F \cdot r \tag{1}$$

2. Firmly grasping the door handle and rotating the hand around its center. This method requires the arm, wrist or fingers to comply with the movements of the hand because of the hand's fixed position on the door handle. The rotation of the hand creates a moment around the hand's center. The moment can be seen as two forces, F_1 and F_2, acting in opposite direction, perpendicular to the door handle and with a distance r_1 and r_2 respectively, from the rotational axis of the door handle. The distance between the two forces is determined by the width of the hand. Usually the two forces are equal, $F_1 = F_2$, which leads to an effective torque of $F_1(r_1-r_2)$ against the internal spring of the handle. This results in a very ineffective method of opening a door because of the small moment arm created by the hand rotation. Although, the wider the hand is the less moment is needed and the position on the handle does not matter except for the different radius of the arc trajectory needed to follow. Furthermore, the handle is firmly gripped which should not lead to any slippage. On the other hand the number of required task degrees of freedom is now three, one active for rotation and the other two passive to follow the door handle in vertical and horizontal direction.

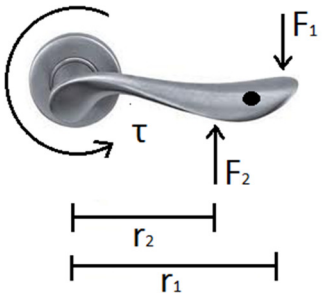

$$\tau = F_1 \cdot r_1 - F_2 \cdot r_2$$

$$\tau = F_1(r_1 - r_2) \quad (2)$$

3. The third method is what humans usually use to unlatch a door handle, a combination of the two methods before. The handle is firmly grasped, then rotated and pushed downwards. The effective torque created to overcome the internal spring in the door handle is then: $F \cdot r + F(r_1 - r_2)$. This method is optimal if it is required to limit the necessary force to unlatch a door handle but requires two active degrees of freedom, rotation and vertical movement.

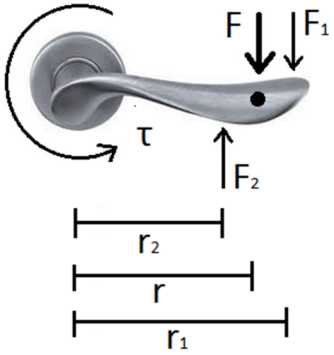

$$\tau = F \cdot r + F_1(r_1 - r_2) \quad (3)$$

Comparing the three methods by introducing the internal spring torque τ = 2,5 Nm, r = 10 cm and hand width of 5 cm in formulas (1) to (3) results in:

$$(1)\ F = 2{,}5\ Nm\ /\ 0.1\ m\ =\ 25\ N$$
$$(2)\ F = 2{,}5\ Nm\ /\ 0.05\ m\ =\ 50\ N$$
$$(3)\ F = 2{,}5\ Nm\ /\ 0.1\ m\ =\ 25\ N + F_1/2$$

These results show the magnitude of force needed to unlatch a door handle with large internal spring and set the requirements for the design of an active robotic wrist.

A.2 Experimental Setup

To execute the experiment of remotely controlling a mobile robot with haptic shared control and an underactuated hand improve the unlatching of a door the following things are required:

- Master robot
- Slave robot
- Controller
- Communication lines
- Haptic shared control
- Underactuated hand
- Webcam
- Video display
- Experimental environment: Door with a door handle

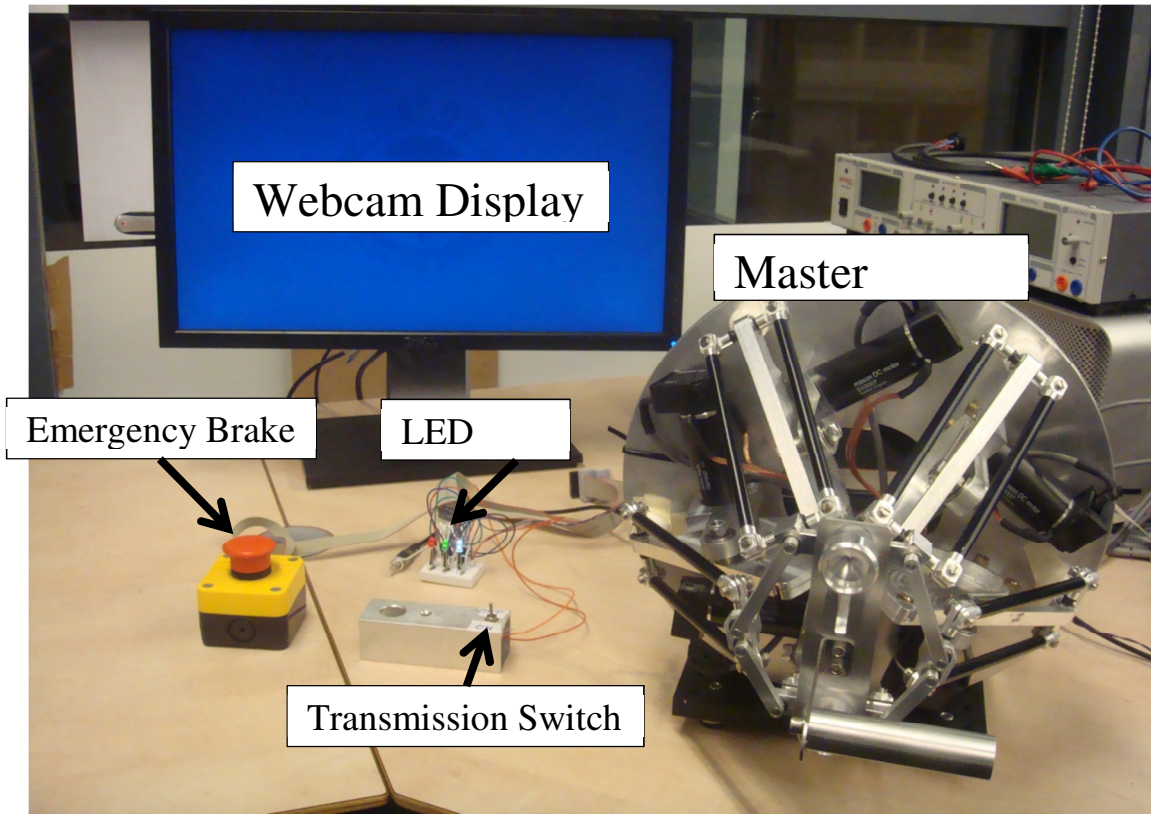

Figure A-2: Human control station for controlling a mobile slave robot

The created experimental setup consisted of a human control station, a mobile slave robot and a table top door, see Figure A-2 and Figure A-3. In the control station the human operator was able to control the slave robot. A transmission switch managed the communication between the master device and the slave device. An emergency brake was released to allow current to flow into the motors on the master device. Three LED lights indicated to the operator the task status. Red light indicated that a communication was on between the master and the slave. Green light represented contact between the slave device and the door and

white light indicated an open door and the end of the task. When controlling the human operator was only able to view the remote environment through a video stream. The master and the slave device were in the same room which allowed for audio feedback as well.

A table top door was created for the experiment. The door has an L-shaped door handle on the left side of the door and rotatable clockwise. On the back side of the door a 1 kg counterweight was placed 8.5 cm from the rotational axis of the handle. The counterweight was supposed to counteract the internal spring in the handle. The door was fastened to a 50x50cm wooden particle plate. Behind the door a 16 kg weight increased the friction between the plate and the desk which worked as a safety for the slave robot. Instead of the robot being damaged the door was simply moved if the forces were higher than approximately 50 N, which was thought to be reasonable.

Figure A-3: Delft Personal Robot 1 (DPR1), the slave device used during the experiment of opening doors and the table top door created for the purpose of the experiment

The LED lights that indicated the task status received signals from two pull-up resistors connected to the robot and the door. The door handle was grounded and if the slave made contact the signal was pulled down and the green LED lid up. The white LED was connected to a switch situated right in front of the door and if it was pulled open the switch immediately was turned on resulting in a lid white LED.

To provide an orthogonal load onto the door handle a structure was designed and manufactured. The structure was used during the experiment to let the 1 kg counterweight always act on the door handle with an equal and orthogonal force. The acting counterweight would then not vary depending on how much the handle was rotated. The structure can be seen in Figure A-4. The structure consists of 3 things, a clamp to clamp onto the door handle, support structure and a pin. A wire is then connected between the handle and the counterweight. The wire will make contact with the pin. The whole designed structure will rotate along with the handle and as the handle is rotated the counterweight will always stay vertical. The pin in the design will make sure that the part of the wire (here: plastic tie wrap) between the handle and the pin will be kept orthogonal to the handle while the angle between the pin and the weight will change depending on the rotation of the handle. That will cause the force to always act orthogonal to the handle. Optimally the pin would have a pulley to reduce friction.

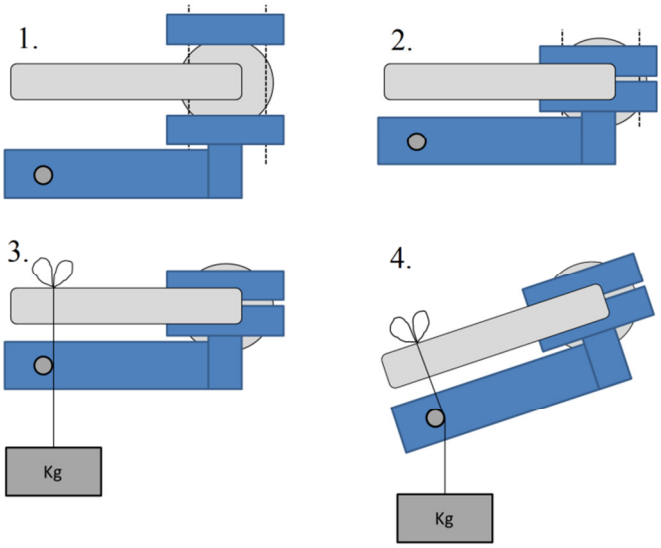

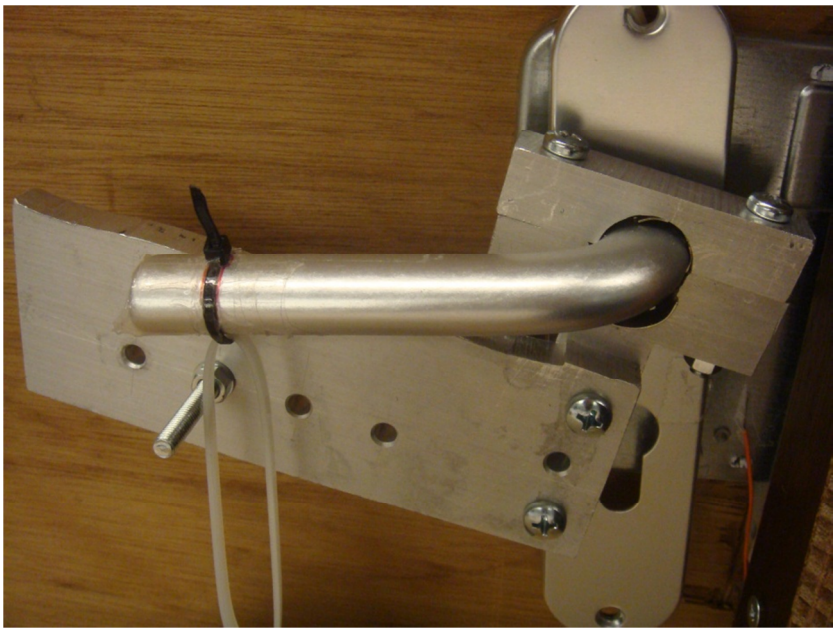

Figure A-4: Designed structure to provide orthogonal load on the door handle.

A.2.1 Master

The master device was PentaGriph 1 (PG1) designed and developed by Patrice Lambert Ph.d. The device was designed for micro-assembly but was thought perfect for the experiment because of its 5 degrees of freedom that corresponded well to the 5 degrees of freedom needed to perform the task of opening a door. The nice thing about PG1 is that all the motors do not move, they are stationed at the base and do not add unwanted inertias. PG1 is cleverly designed to incorporate all 5 degrees of freedom together in a closed loop with 5 parallelograms.

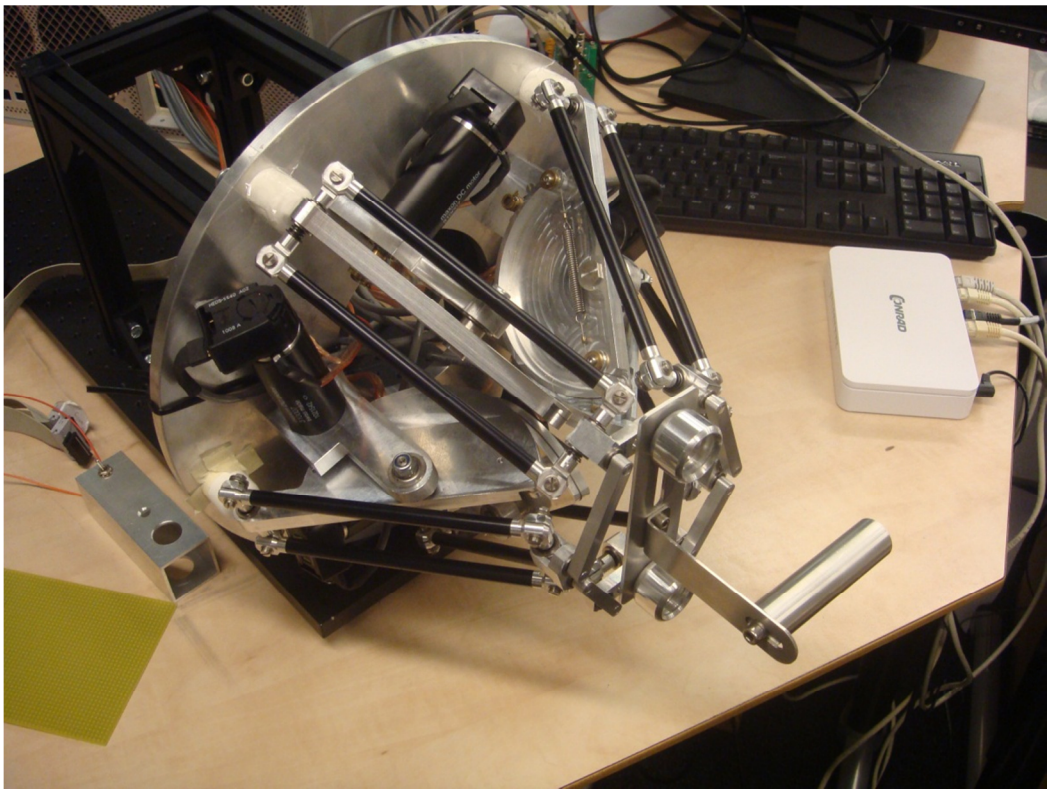

Figure A-5: PentaGriph 1, the master device used during the experiment of opening doors.

A.2.1.1 Kinematics

PG1´s kinematics is not very trivial. It is a closed loop system with 5 inputs ending in one output state. The 5 degrees of freedom are x, y, z, θ and ρ, where θ is the rotation around z-axis and ρ is the gripping motion, see Figure A-6.

The degrees of freedom correspond to the movement of the slave device as follows:

- x – turn (horizontal movement)
- y – move arm (vertical movement)
- z – drive (forward/backward)
- θ – rotate wrist
- ρ - grip

The movements are thought to be the combination of driving a car (x and z) and moving a hand (y, θ and ρ). They can be seen as the movements of the slave´s end effector and not as

separate entities (base and arm). It is not yet known if it is more difficult to operate all five degrees of freedom with only one device or if they should be divided into two devices operated by two hands or the more common driving method, a hand and a foot.

To make it easier for the operators to perform their task, the PG1 is rotated to align the degrees of freedom to match the movements of what humans are used to when opening a door. If the operators need to transpose their movements from a camera view they are much likelier to fail because of high mental load.

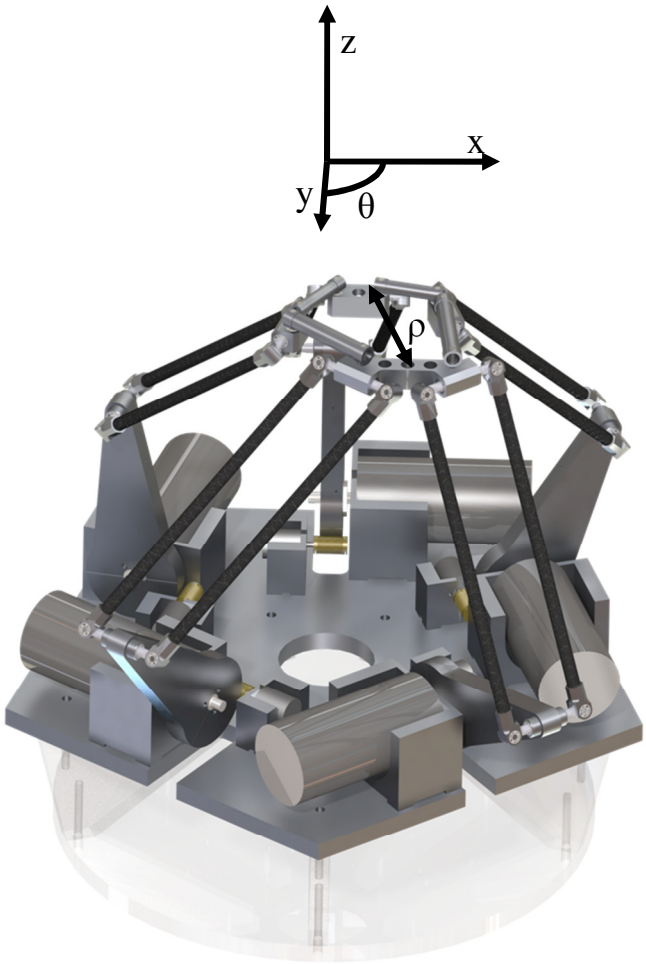

Figure A-6: The 5 degrees of freedom of the master device (x, y, z, θ, ρ)

A.2.1.2 Operation

The operation of the PG1 is through a real-time xPC target computer. Models are created on a host computer in Simulink and uploaded to the target computer. The target computer communicates then in real-time with the Quanser Q8 control board which actuates the motors and reads sensors. The control board can control up to 8 motors and read 8 encoders. The host computer starts and stops the execution of the master device.

The Simulink model used during the experiment is *Atli_model_experiment.mdl*, see Figure A-7.

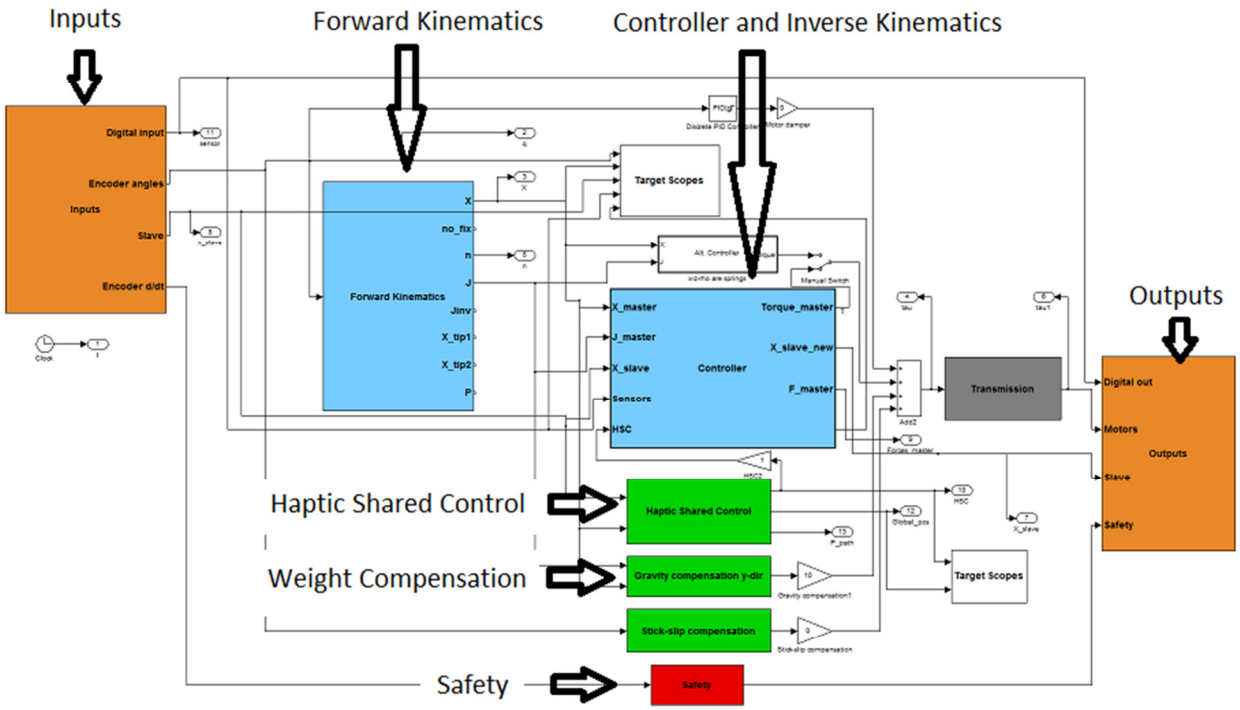

Figure A-7: The Simulink model, *Atli_model_experiment.mdl*, used during the experiment

A basic model that can operate the PG1 should have an input/output, forward/inverse kinematics and a controller. The Simulink model should read values from the encoders on the motors, use those values to determine the position of the operator´s fingertips through forward kinematics. Then send those values to a controller that decides if forces should be exerted to the operator through the master device. The inverse kinematics should then transfer the fingertip forces to motor output torque. The input/output, forward/inverse kinematics and safety module was already available for the experiment. Additional modules that were added are the controller (see chapter A.2.3), haptic shared control (see chapter A.2.1.3), weight compensation and to communicate with a slave device an input/output through UDP communication protocol (see chapter A.2.4).

The safety module is very important because it will prevent the model to send too high currents to the motors.

The weight compensation module keeps the master device extended in the position that the operator left it in, no matter how far away from the base it is. The weight of the device m is calculated and multiplied by the distance z and the gravity constant g = -9.81. The result is then placed as a force in y-direction where all other directions have no forces. The force vector is then multiplied by the transpose of the jacobian resulting in motor torques. These motor torques are then added to the motor torques of the controller.

The communication module receives the slave´s position and sends movement commands to the slave. The module utilizes xPC target´s UDP communication protocol which is already

implemented. The only thing that is needed is an IP address and a port number. The communication is discussed further in chapter A.2.4.

A.2.1.3 Haptic Shared Control Design

The haptic shared control provides a guidance force to the operator and was provided during the approach and unlatching task. Haptic shared control requires information about the environment, either by sensing or knowing beforehand. The starting positions of the slave and the position of the door were known beforehand during this experiment. The approach guidance will be described before the unlatching guidance.

The design of the approach guidance was attractive guidance where the optimum path was decided to be a straight line orthogonal to the door plane in the height of the door handle. Instead of finding the path error E_1 from the end-effector location a future position B is used for more stability, see Figure A-8.a. Point B is found by multiplying the velocity of the robot $\dot{z}$ with the so called look-ahead time $t_{lookahead}$.

$$\overrightarrow{AB} = \dot{z} \cdot t_{lookahead}$$

The path error E_2 is then calculated by finding a point on the optimal path that is orthogonal to the direction of the robot. This is found by calculating the dot product of the vector between all points on the optimal path and the direction of the robot, $\overrightarrow{AB}$. The one point that provides the absolute minimum dot product value is the point that is orthogonal to the robots direction. The further away the slave is from the path the more guidance force is provided to the operator and direction of the force is of course towards the optimal path. The direction of E_2 towards the optimal path is found by calculating the cross product of the vector that had the lowest dot product and $\overrightarrow{AB}$. The last value of the cross product will determine if the robot needs to turn left or right. The guidance force has an error gain of g_x = -0.36 in rotating the base and g_y = -108 in the height of the arm. The guidance is provided to the operator by changing the equilibrium position of the master device instead of superimposing the equilibrium force. The high gain on the height of the arm is because the gain needs to overcome the weight compensation of the master device.

The guidance design of the unlatching subtask was a bit different, see Figure A-8.b. As the slave robot is non-holonomic it cannot go sideways and makes it more difficult to design a path to follow that exactly follows the trajectory of a rotating handle. Therefore an guidance was implemented that made it harder for the operator to go in unwanted directions. A box was created that the operator could feel if the handle was grasped. Additionally, linked rotational and vertical forces were provided that if the operator would only rotate the handle he would feel a downward force as well. The link between the forces was designed to correlate to an arc with a radius of 6.5 cm. Certain rotation of the hand corresponded to a certain height which was calculated by first finding a line that passed through the center of the arc and to a point on the arc that had the same angle as the rotated hand. The point then defined the height from the zero angled line.

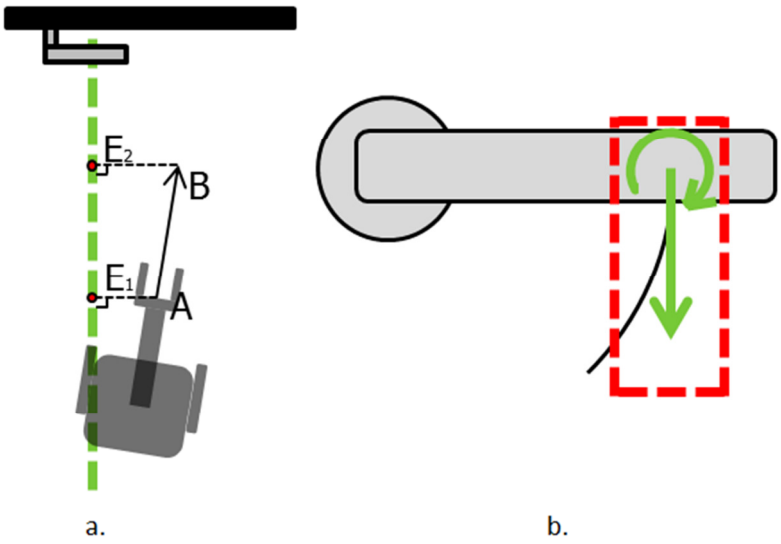

Figure A-8: a. Guidance during the approach subtask is found by calculating a future position B of the end-effector and its corresponding path error E_2 with the robot's direction AB, velocity, and the look-ahead time of 0.1 seconds. b. Guidance during the unlatching subtask. Subjects were constrained inside a box while receiving a linked rotational and vertical force.

A.2.1.3.1 How to get the PentaGriph1 running

The following is a small how-to, to get the master device up and running.

Step 1 Turn on the host and target computers, turn on the amplifiers and power supply for the motors.

Step 2 Open Matlab R2010b and then open the simulink model 'atli_model_experiment.mdl', found here: Experiments\Master\Master device\XPC\

Step 3 Select the model and press 'ctrl+b' to upload the model to the xPC target computer. You know it's finished when the xPC target displays the target scopes on the screen.

Step 4 Start running the master device by typing '+tg' in the command line in Matlab. You know it's running if the xPC target displays increasing time. Now the master device is already trying to send and receiving data from the slave.

Step 5 To activate the motors on the master release the safety button by twisting it.

Step 6 To turn the master device off, press the safety button and type '-tg' in Matlab's command line.

Step 7 To restart the master go to Step 4

Step 8 To shut down the master device, close Matlab and shut down the host computer. On the xPC target hit the turn on/off button and turn off the amplifiers and power supply.

A.2.1.4 Designed Parts

A.2.1.4.1 Handle for the Operator

To ease the maneuver of the master device for the operator, several parts were designed and manufactured. The parts make up a handle for the operator that provide him with easier movements for 4 DOF and leave the 5th DOF, the gripping, just for the thumb and the index finger. The handle is connected to the master device with a plate that is mounted under the finger placements. The smart design of the plate adds constraints to the movements of the platform of the master device. If the platform is rotated too much it ends up in a strange lock which is hard to undo and the same happens when the grip DOF is too large or too small. The plate therefore restrains the movement of over-twisting and restricts the gripping motion to only 50 mm. In between the handle and the plate is a bracket that connects the two parts. The slit on the bracket was increased to 25 mm to allow for larger variety of hand sizes. The parts were designed as light as possible while keeping it low-cost and retaining the integrity of the master device´s stiffness. The weight of the handle assembly is 85.78 g.

The three parts are presented as part drawings for manufacture and the first drawing is the movement constraining plate, the second drawing is the bracket and last the handle.

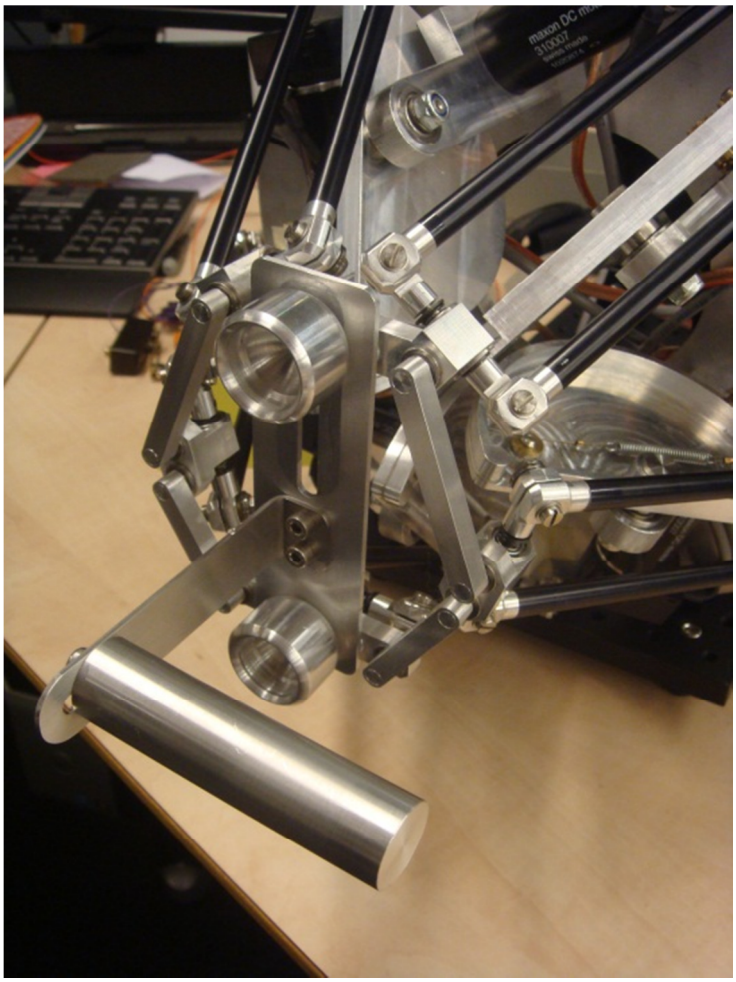

Figure A-9: Operator handle for the PentaGriph 1 haptic master device. Operators would graps the handle and place their index finger and thumb in the two finger placemenets.

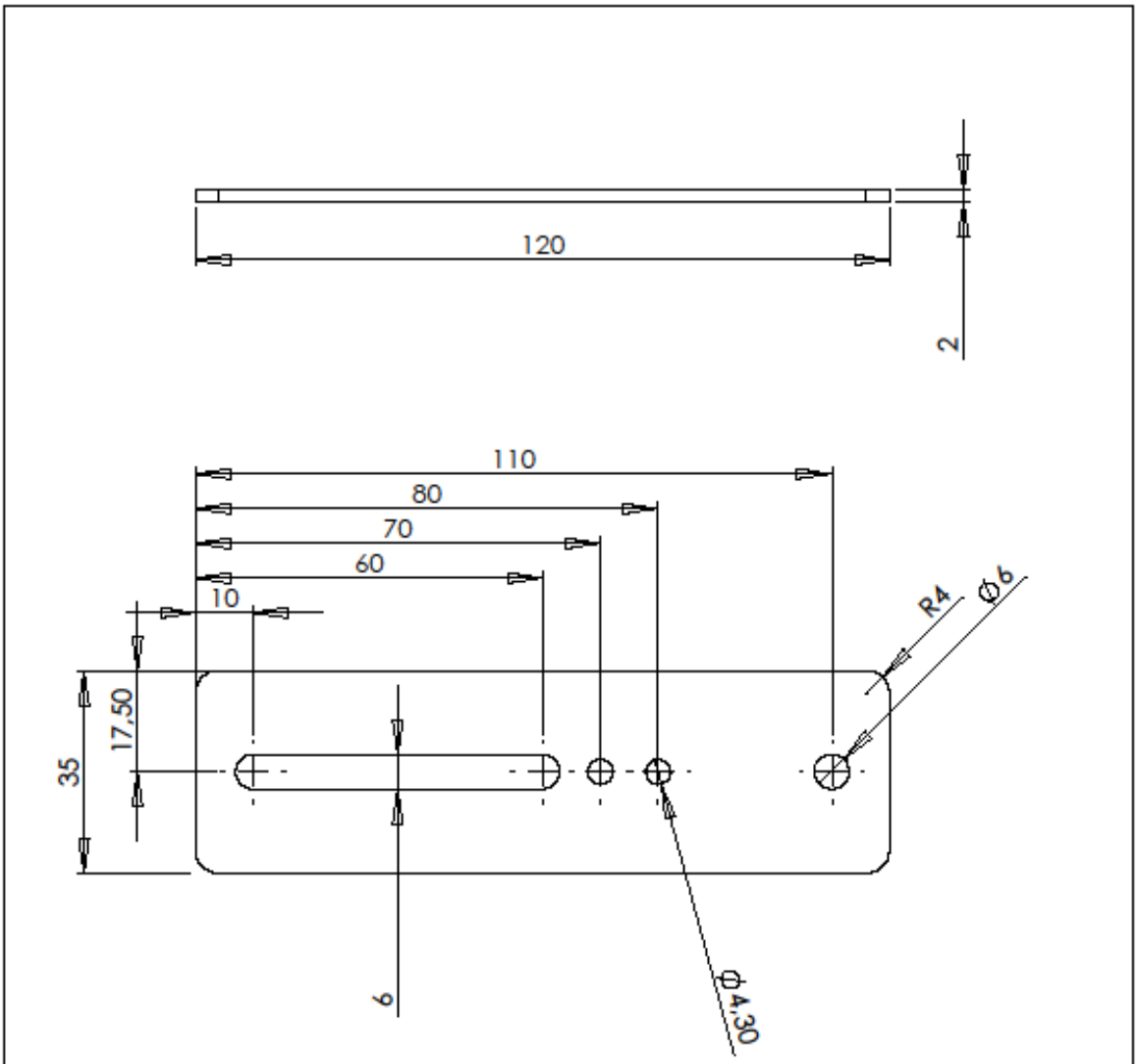

UNLESS OTHERWISE SPECIFIED: DIMENSIONS ARE IN MILLIMETERS SURFACE FINISH: TOLERANCES: LINEAR: ANGULAR:		FINISH:		DEBUR AND BREAK SHARP EDGES	DO NOT SCALE DRAWING	REVISION
	NAME	SIGNATURE	DATE		TITLE: Movement constrainer PentaGriph	
DRAWN	Alli Svantesson					
CHK'D						
APPV'D						
MFG						
Q.A				MATERIAL: Aluminum	DWG NO: Movement_constrainer_plate	A4
SolidWorks Student License Academic Use Only				WEIGHT:	SCALE:1:1	SHEET 1 OF 1

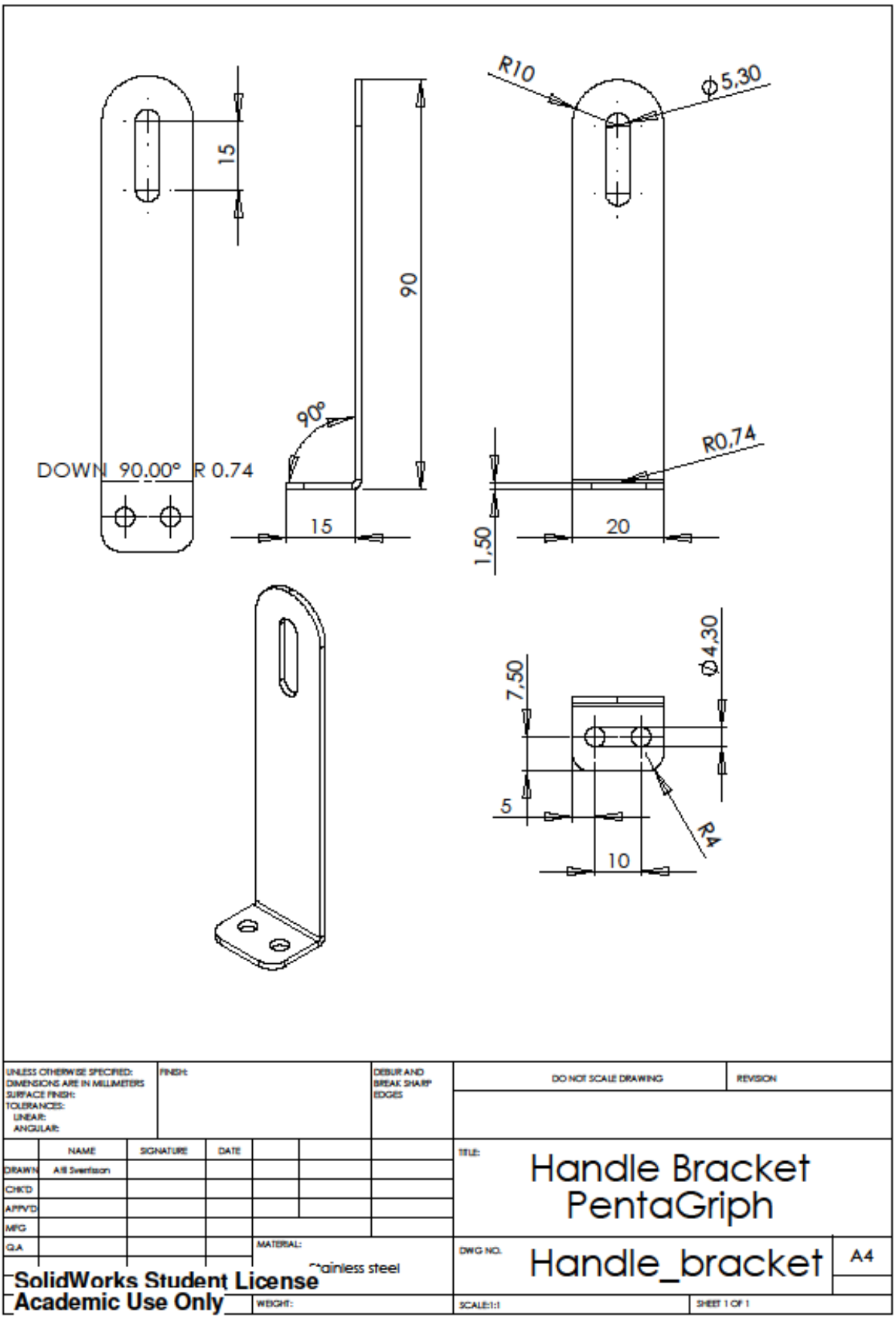
R10
ϕ5,30
15
90
90°
DOWN 90.00° R 0.74
15
R0,74
1,50
20
Ø4,30
7,50
5
R4
10
UNLESS OTHERWISE SPECIFIED:
DIMENSIONS ARE IN MILLIMETERS
SURFACE FINISH:
TOLERANCES:
LINEAR:
ANGULAR:
FINISH:
DEBUR AND BREAK SHARP EDGES
DO NOT SCALE DRAWING
REVISION
NAME
SIGNATURE
DATE
DRAWN
Alli Svantesson
CHKD
APPV'D
MFG
Q.A
MATERIAL:
Stainless steel
WEIGHT:
TITLE:
Handle Bracket PentaGriph
DWG NO.
Handle_bracket
A4
SCALE:1:1
SHEET 1 OF 1
SolidWorks Student License
Academic Use Only

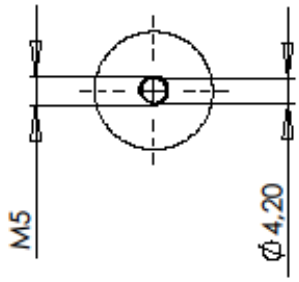

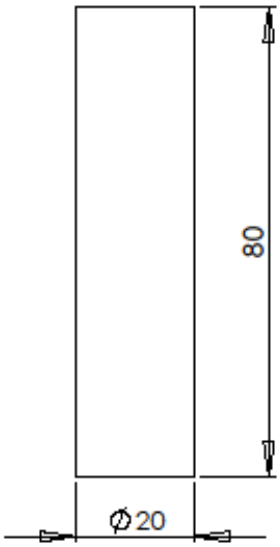

The hole is tap drilled for M5 bolt

UNLESS OTHERWISE SPECIFIED: DIMENSIONS ARE IN MILLIMETERS SURFACE FINISH: TOLERANCES: LINEAR: ANGULAR:			FINISH:			DEBUR AND BREAK SHARP EDGES	DO NOT SCALE DRAWING / REVISION
	NAME	SIGNATURE	DATE				TITLE: User handle PentaGriph
DRAWN	Alli Svantsson						
CHK'D							
APPV'D							
MFG							
Q.A							DWG NO. Handle / A4
				MATERIAL: Aluminum or plastic			
				WEIGHT:			SCALE:1:1 / SHEET 1 OF 1

A.2.2 Slave

The slave robot of the experiment was Delft Personal Robot 1 (DPR1). The robot is a non-holonomic non-redundant mobile service robot. Non-holonomic robots are mobile robots that cannot go in any direction without turning first. Those are usually robots with a two wheel drive and can turn on the spot but cannot go sideways. DPR1 being a non-redundant robot means that its axes of motion equal the achievable motion of the end effector. Only one configuration of the robot can be possible at a certain end effector position.

DPR1 was designed to autonomously serve people, by for example fetching object.

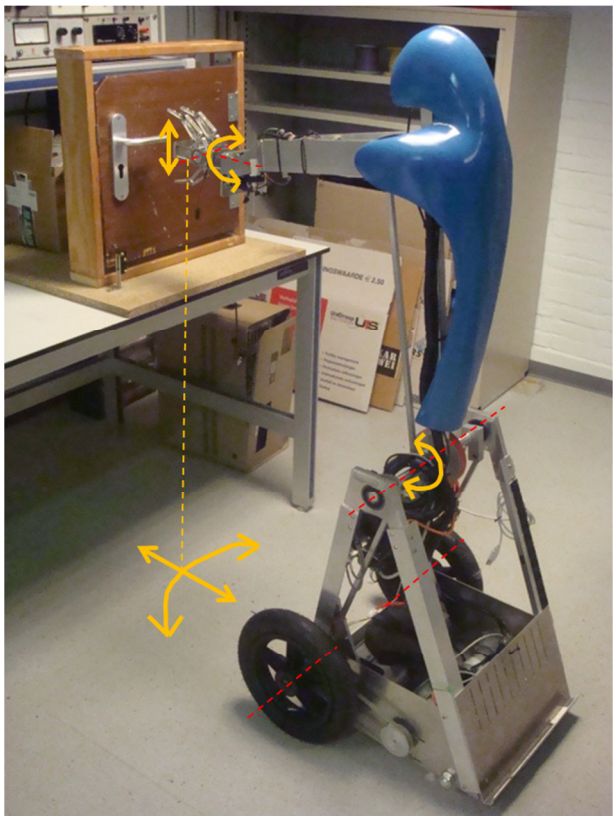

Figure A-10: Delft Personal Robot 1 (DPR1). The 5 degrees of freedom are indicated with orange arrows and axis of rotation with dashed red lines.

A.2.2.1 Kinematics

DPR1 has a mobile base, an arm, wrist and a hand. The mobile base has two active wheels and two passive. The arm is a L-shaped structure with one degree of freedom with the rotation at its base. When the arm moves, it is similar to a human that has his hand stretched forward and while keeping it like that he bends forward, rotating around his hips. For the experiment, DPR1 had only one degree of freedom in his wrist joint, roll, the rotation around the axis of the lower arm. The hand is an underactuated 3 fingered gripper, Delft Hand 3 (DH3). DH3 has only one actuator but total of 6 degrees of freedom. The underactuation mechanism created from a differentiator and a rotating motor makes it possible to divide equally the total torque from the motor to the three fingers. This is especially useful because the fingers can adapt their shape to the object and enabling the hand to encumber objects of different sizes and shapes.

The mobile base is velocity controlled and the velocities of both wheels are presented to the master for localization. It is not trivial how to calculate the location of the robot at a certain point in time because the wheels can rotate at different speeds and direction. The global position q_{global} of the mobile robot is presented as a 3x1 vector $[x\ y\ \theta]^T$. x and y are the coordinates of the local reference frame in the global reference frame and θ is the angle between the two frames.

Figure A-11: DPR1 with required measurements for the experiment

To map the motion of the robot in the global reference frame to motion in terms of the local reference frame we can use a rotation matrix R(θ). This is done by multiplying R(θ) by the global velocity $\dot{q}_{global}$ to get $\dot{q}_{local}$.

$$R(\theta) = \begin{bmatrix} cos\ \theta & sin\ \theta & 0 \\ -sin\ \theta & cos\ \theta & 0 \\ 0 & 0 & 1 \end{bmatrix}$$

As we are more interested in the global velocity to localize the robot at a certain position in time we can invert the equation and get:

$$\dot{q}_{global} = R(\theta)^{-1}\dot{q}_{local}$$

The local velocity $\dot{q}_{local} = [\dot{x}\ \dot{y}\ \dot{\theta}]^{\mathrm{T}}$ of the robot is then found. Let's say the local frame is centered between the two wheels at point P with +x direction going straight and y to the side. If we have the wheel radius of *r* and length 2*l* between the two active wheels of the robot we can find the local velocities. If one of the wheels spins forward while the other is stationary we know that point P moves at half speed compared to the moving wheel, $(1/2) \cdot r \cdot vel_{left}$ and $(1/2) \cdot r \cdot vel_{right}$. We can then add the two contributions together to get the local velocity in x-direction. As the robot is non-holonomic it cannot have a velocity in y-direction. Again if only one of the wheels is moving the center of rotation is located at the other wheel at distance 2*l*. Therefore will point P move in circles with radius 2*l* and have an angular velocity of $(1/2l) \cdot r \cdot vel_{left}$ and $(1/2l) \cdot r \cdot vel_{right}$. These can as well be added together but with different signs and complete the local velocities of the mobile robot:

$$\dot{q}_{local} = \begin{bmatrix} r\dfrac{vel_{left}}{2} + r\dfrac{vel_{right}}{2} \\ 0 \\ r\dfrac{vel_{left}}{2l} - r\dfrac{vel_{right}}{2l} \end{bmatrix}$$

The arm of DPR1 is L-shaped and rotates around DPR1 hip which is elevated about 595 mm above the ground. The arm has a vertical height of 600 mm and horizontal length of about 600 mm. The length of the arm can therefore be considered as 848.5 mm with an initial angle of 45° (0.7854 rad). When the arm is rotated, a mechanism in the arm retains the horizontal position of the wrist and hand to make it easier to pick up objects at different heights.

Figure A-12: Operator at the control station.

A.2.2.2 Camera

DPR1 has a Gigabit Ethernet camera from Allied Vision Technologies. The camera is a Prisilica GC, a very compact camera with 5MP resolution and up to 119 fps. The location of the camera is just above the body but moves along with the arms and has a view of the arm and the hand. Locating the camera at that position provides a very bad depth perception for the operator and when the arm is in initial position the operator cannot even see the palm of the hand. Fortunately, when the arm is lowered to about the height of a door handle the palm can be easily detected. The depth perception might be improved if the location of the camera

would be attached to the mobile base and would therefore not move along with the arm. That view would provide a much better overview of the task environment. Adding another camera, just showing the hand, would be ideal because when the slave robot is close to the door the operator could switch his view to have a closer view at the handle. For the experiment the camera is not moved nor is another camera added. The camera view can be seen in Figure A-12.

To operate the camera, install GigE Sample Viewer at *http://www.alliedvisiontec.com*. Download and follow the instructions online. Remember to allow the program to run in Windows firewall and set the IP address of the camera to a similar address as the computer that runs the program and the same subnet mask.

A.2.2.3 Operation

The slave is operated by a laptop with C++ programs through the 3Mxel microcontroller. ROS (Robot Operating System) is used to provide libraries and tools to better control DPR1. ROS provides a neat way to send (publish) and receive (subscribe) messages between programs and to debug programs as well.

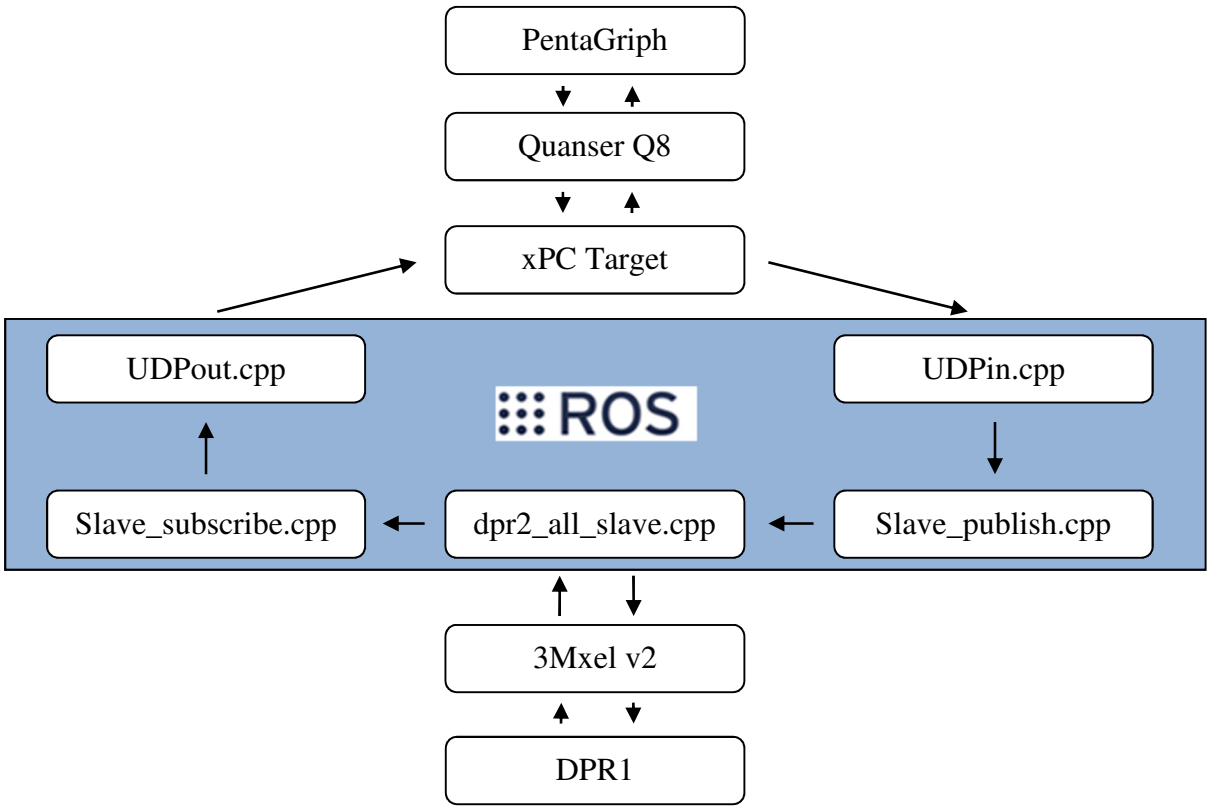

Figure A-13: An overview of how data is transmitted through the slave programs

The master device sends commands to the slave device with UDP messages through a Ethernet cable and is picked up by the UDPin.cpp program running inside the Slave_publish.cpp program. The commands are then published to all other programs that subscribe to the incoming commands. dpr2_all_slave.cpp is the main program that

communicates to the 3Mxel by subscribing to the incoming commands and setting those values as motor inputs. The program reads then positions, velocities or currents of the slave device and publishes them. Slave_subscribe.cpp subscribes to those values and forwards them to the UDPout.cpp program that delivers them to the master device.

A.2.2.3.1 How to get DPR1/DPR2 running

This is a small how to guide to get the DPR1 or DR2 running. It is assumed that Linux and ROS has been installed on a laptop and the DBL repository has been downloaded. Take a look at ros.caarls.org for a guide to set up ROS and the DBL repository.

Step 1 Turn on a laptop and choose linux as an operating system.

Step 2 Turn on DPR1, plug in the USB cable or the RS-485 express card and the Ethernet cable from the master in the laptop.

Step 3 Open a terminal and write ‘roscore’.

Step 4 Switch off the emergency stop.

Step 5 Open another terminal and write ‘roslaunch dpr2_slave dpr2_slave_all.launch’. This command will launch all motors of the DPR1. Switch all for ‘base’, ’arm’, ‘wrist’ or ’gripper’ to initiate only one part of the DPR1.

Step 6 Now DPR1 is initating and you are good to go.

Step 7 To terminate the run just it Ctrl+C on both terminals.

A.2.2.4 Designed Parts

A.2.2.4.1 DH3 – Extended Palm

To properly open a door with the DH3 the palm needed to be extended because without the extension the hand formed a caging grip around the door handle, see Figure A-14. With the extension the palm was extended about 50 mm and the hand was able to grip the handle firmly. The designed parts were two 5 mm plates, and by adding four 40 mm stand-offs in between them the extension was achieved. Two 2.5M bolts fasten the structure by using the already available threaded counterparts. The extra space in between the plates was thought as space for sensors to detect for instance: force, touch or even distance.

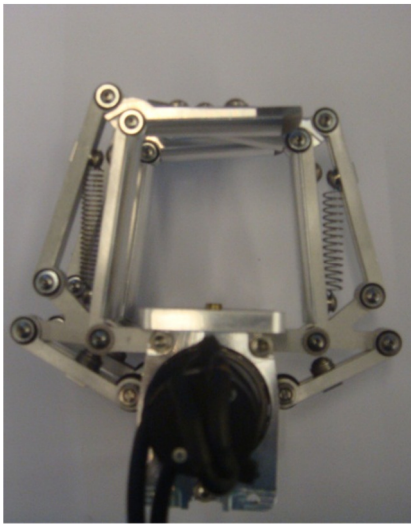

Figure A-14: Fully closed DH3

The two designed parts are presented here as part drawings

for manufacture. The plate closer to the hand is presented first and then the plate further away. The total assembly of the gripper with the extended palm can be viewed in Figure A-15.

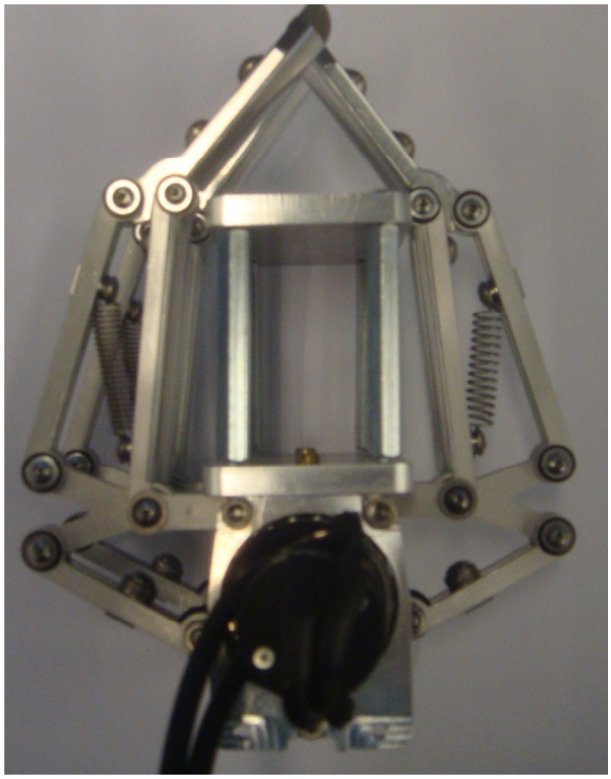

Figure A-15: DH3 with an extended palm

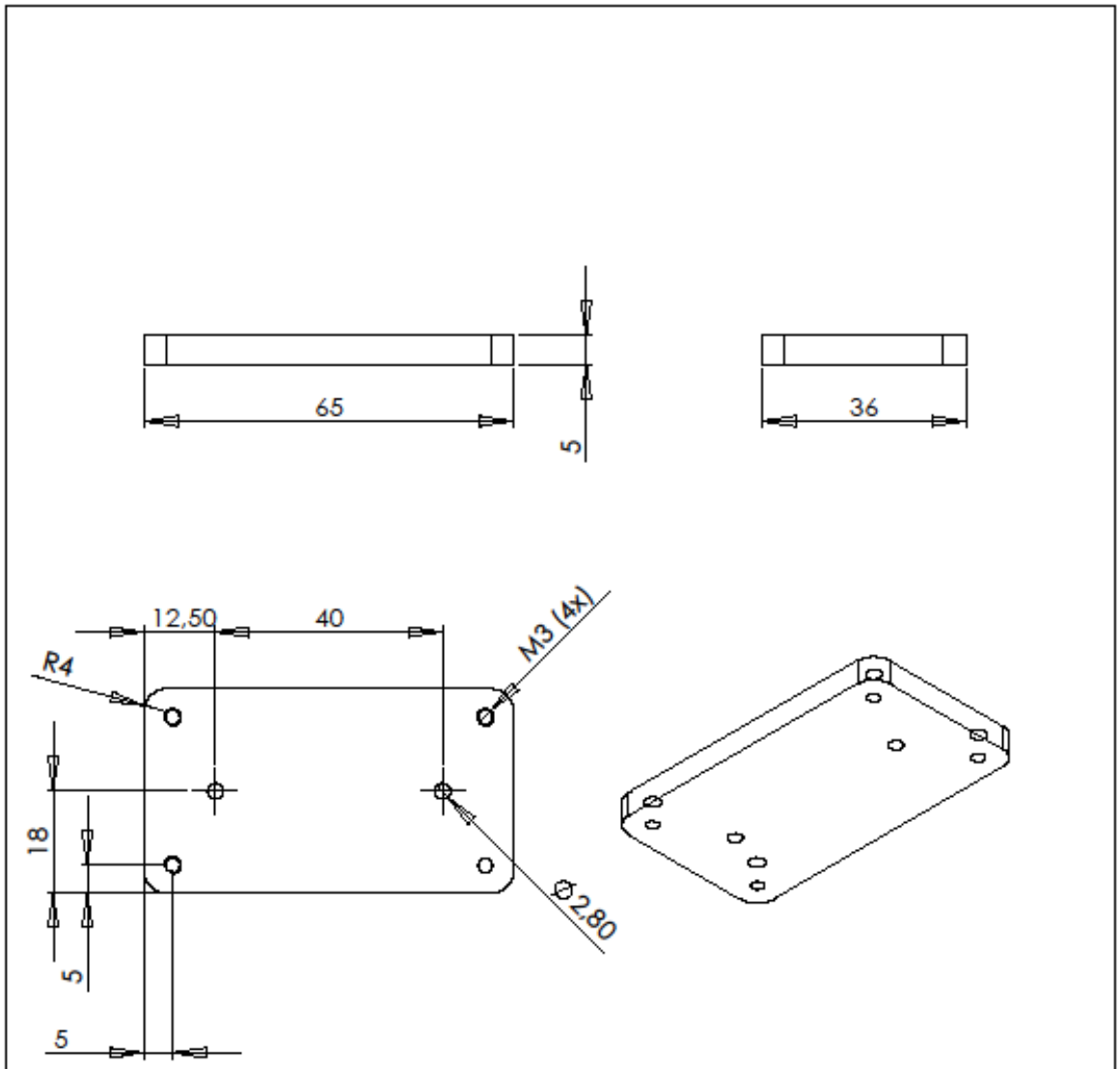

4 corner holes are tap drilled for M3 bolts

UNLESS OTHERWISE SPECIFIED: DIMENSIONS ARE IN MILLIMETERS SURFACE FINISH: TOLERANCES: LINEAR: ANGULAR:		FINISH:			DEBUR AND BREAK SHARP EDGES	DO NOT SCALE DRAWING / REVISION
	NAME	SIGNATURE	DATE			TITLE: Palm base DH3
DRAWN	Alli Svantesson					
CHK'D						
APPV'D						
MFG						
Q.A				MATERIAL: Aluminum		DWG NO. DH3_palm / A4
SolidWorks Student License Academic Use Only				WEIGHT:		SCALE:1:1 / SHEET 1 OF 1

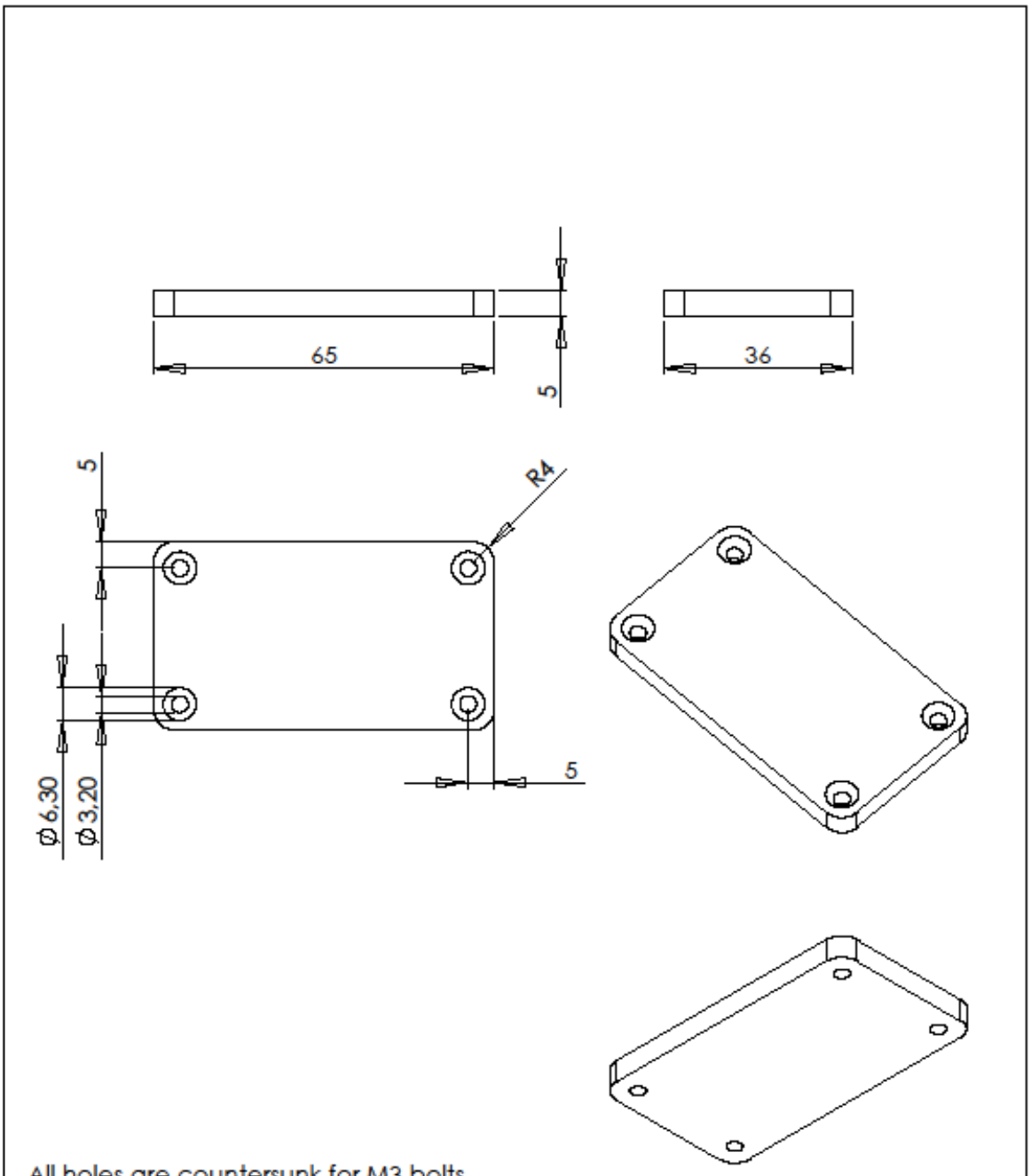

UNLESS OTHERWISE SPECIFIED: DIMENSIONS ARE IN MILLIMETERS SURFACE FINISH: TOLERANCES: LINEAR: ANGULAR:			FINISH:		DEBUR AND BREAK SHARP EDGES	DO NOT SCALE DRAWING / REVISION
	NAME	SIGNATURE	DATE			TITLE: Palm extended DH3
DRAWN	Alli Swenlsson					
CHK'D						
APPV'D						
MFG						
Q.A						DWG NO. DH3_extended_palm — A4
				MATERIAL: Aluminum		
SolidWorks Student License Academic Use Only				WEIGHT:		SCALE:1:1 / SHEET 1 OF 1

A.2.2.4.2 Wrist Joint

For the DPR1 to be able to open a door some improvements to the wrist joints was required. The wrist as it was had three consecutive Dynamixels representing the yaw, roll and pitch of the hand. The Dynamixels are a compact servo motors with integrated gearbox and encoder, and can be daisy-chained with RS485 cables. DPR1 being the slave in a telemanipulation of opening doors, the wrist joints were thought to be too weak to handle the excessive forces that might arise when colliding with the door. Although only one motor was needed and it would have provided enough torque, the collision forces would have gone directly along the rotational shaft and quickly damaged the motor's ball bearings. Another thing is that the communication to and from the Dynamixels are at 1.5 Mbaud which is at odds with the 3Mxel's communication which is either at 1 or 2 Mbaud and could cause problem for a stable telemanipulator.

From chapter Task EnvironmentA.1 the requirements of the wrist joints are calculated. The wrist joint should be able to unlatch a door by just rotating the handle (method 2) that has a high internal spring torque of 2.5 Nm. Using equation (2) in chapter A.1 and that DH3 has an effective hand width of about 4 cm, the requirement for an actuated wrist joint was found to be a torque of at least 2 Nm at grip level.

A wrist joint was designed and manufactured to be able to provide that torque and be passive as well. If the joint would be passive there would be no motor to actuate it. The joint would only have a torsional stiffness from a spring to keep it in the right orientation to grip the handle. The hand would rotate along the door handle when using method 1 in chapter A.1 to open a door. The DH3 is not asymmetric and would require a torsional spring which could provide at least 0.016 Nm without any angular displacement. This is only roughly calculated knowing that the asymmetric part of the hand is the actuator which is about 54g and sticking half way out the side of the hand. It is then assumed half of the weight is outside the hand with a center of mass at the hand´s edge creating a lever arm of 30 mm.

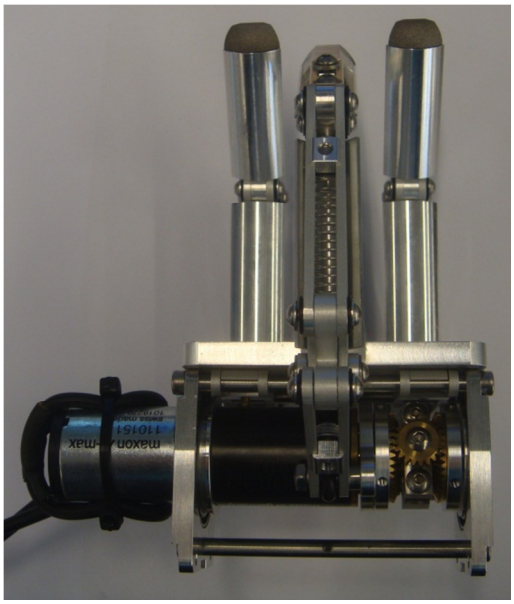

Figure A-16: DH3 showing the actuator sticking out

In the design there is a power transmission with two timing pulleys (AT3, 24 teeth) and a timing belt of 150mm. This was done to prevent any damage to the motor from collisions with the environment. Only there are two ball bearings that need to withstand the forces. To open a door it was assumed not more than 25 N was needed to unlatch a common household door. Therefore the forces on bearing 1 and 2 were found to be 108.3 N and 83.3 N, respectively, see Figure A-17. The diameter of the shaft through the two bearings and connecting the hand to the wrist was decided to be 6 mm and most bearings with that inner diameter can withstand forces higher than 200 N. The only concerns are the forces in the

axial direction caused by collisions which can be much higher than 25 N. As they are most of the time only instantaneous there should be no need to have special bearings that endure axial forces as well as radial forces.

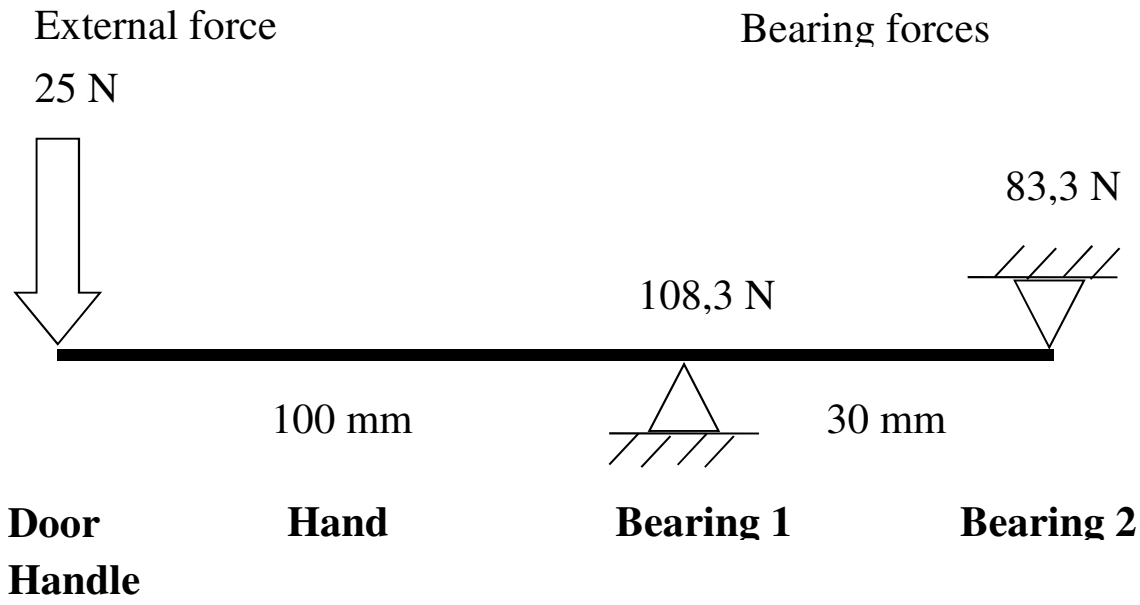

Figure A-17: Bearing force in the wrist joint to react to an external force

On top of the external force there are internal forces acting on the bearings as well. Due to the requirement of tensioning the timing belt, additional 115.6 N force will be divided between the two bearings. Tensioning is necessary so no slippage will occur between the belt and the pulleys. The amount of tensioning force was provided by the Mulco belt-pilot when provided information about the transmission system, two AT3 24 teeth pulleys with 6x150 mm timing belt, 30 r.p.m. and a torque of 2 Nm (*http://mulco.gwj.de/en/index.htm*). In the design of the wrist joint the tensioning of the belt was considered. First the triangle shaped motor plate is attached to the gearhead and then loosely fastened to the wrist backplate. Looking at the wrist backplate drawing, one can see a large hole where the motor is inserted through and the small hole above is where the motor plate is attached with a M3 screw. Connecting the motor plate to the backplate with only one screw makes the motor able to rotate around the screw. This rotation changes the distance between the motor shaft and the rotating shaft above and providing a perfect way to tension the timing belt.

A special clamping mechanism was used to securely fasten a cylindrical part to a rotating shaft. It can be very troublesome to have a robust connection between, for example, a motor shaft and a pulley. One could glue the two objects together but high torques will loosen the glue in time. Also, it can be very difficult to take off the pulley without damaging the motor if one decides to disconnect the two parts. Another method is to drill a hole in the pulley and tap, M6 for instance, then glue in a headless screw so it will hit the flat part of the motor shaft. This method is of course not perfect either as the screw can get loose. These methods are just few of many but the solution that was used was a flat block bolted to a cylindrical

part (e.g. pulley) which was clamped onto a rotating shaft (e.g. motor shaft). It is easy to assemble and dissemble and provides a very robust connection. Like the blocks are now, made out of strengthen aluminum, is probably the weakest link in the design and will wear out the fastest. Stainless steel would have been much more robust.

Because of time limitations and to save a couple of hundred euros a gearhead, motor and encoder were salvaged from a failed robot arm design project. The motor is a A-max Ø26 but more information was hard to come by. The gearhead is a planetary gearhead GP 32 A 166178 with a reduction ratio of 456:1 and has a continuous output torque of 4.5 Nm. The output torque is a lot more than was needed and the speed is slower than hoped because of the high reduction ratio.

The drawings of the parts are presented here, first the assembly drawing with the bill of materials and then following the part drawings in the same order as they appear in the bill of materials. Take care that some of the parts where already available (the pulleys and the gripper plate) but only needed some modification so there are no instructions to create the whole part, only the changes.

The position of the gear motor was designed not to interfere with other degrees of freedom of the DPR1.

Experience taught me that the distance between the pulleys should be decreased by at least 1 mm but no more than 2 mm. The timing belt was too tight, which worried us that it might damage the actuator. For the duration of the experiment, the wrist worked like a charm and with no problems. Even the aluminum clamping blocks are still holding on to the rotating shafts.

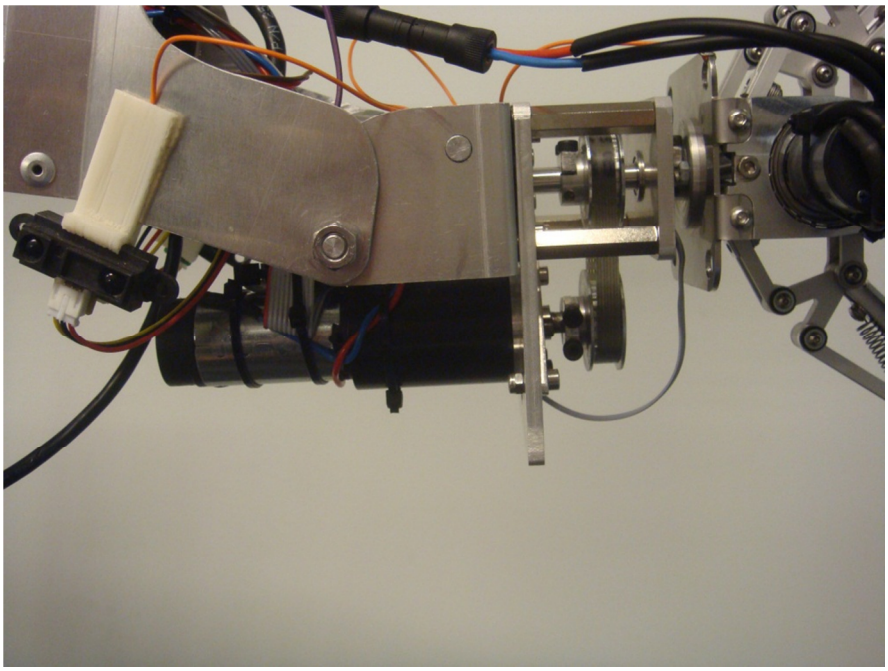

Figure A-18: The designed wrist joint connected to DPR1´s arm and to the underactuated hand, DH3.

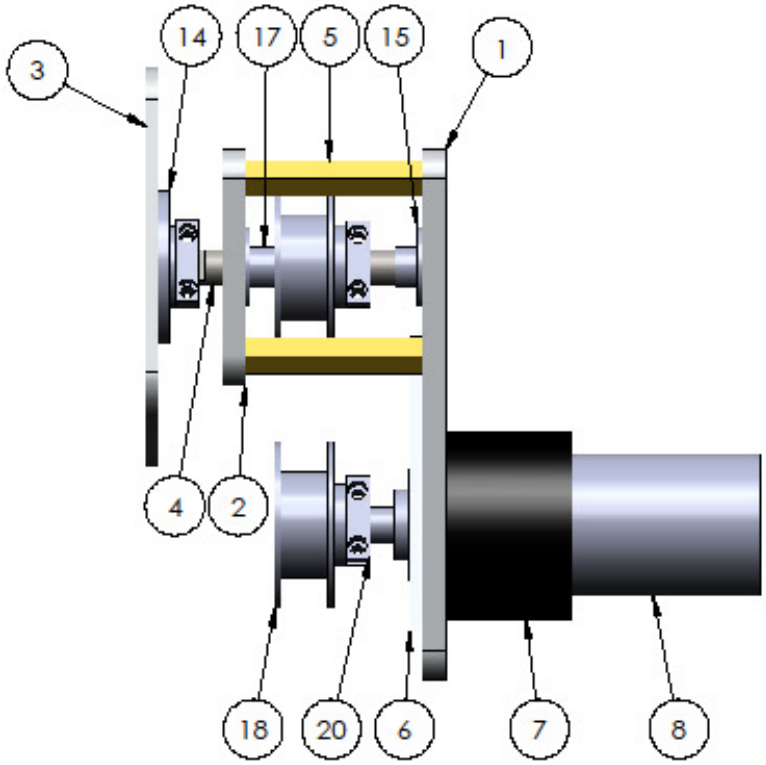

ITEM NO.	PART NUMBER	DESCRIPTION	QTY.	MAKE
1	wrist backplate		1	x
2	wrist plate		1	x
3	wrist gripper plate		1	x
4	wrist rod	Rotational shaft 48x6mm	1	/
5	wrist offset	Stand-off M4x30mm	4	BUY
6	Motor plate		1	x
7	Planetary Gearhead	GP-32-A-166178	1	BUY
8	Motor	A-max 26	1	BUY
9	Socket flat head bolt	M4x12mm	8	BUY
10	Socket head bolt	M3x6mm	7	BUY
11	Socket head bolt	M3x12mm	6	BUY
12	Hexagon bolt	M3x6mm	3	BUY
14	shaft_gripper_attach		1	x
15	Bearing	in-6 out-12 width-4	2	BUY
16	bushing_5		1	x
17	bushing_7_4		1	x
18	pulley_24teeth	AT3 24 teeth width-6mm	2	/
19	Timing Belt	AT3 150mm	1	BUY
20	Shaft_pulley_connector		3	x

UNLESS OTHERWISE SPECIFIED:
DIMENSIONS ARE IN MILLIMETERS
SURFACE FINISH:
TOLERANCES:
LINEAR:
ANGULAR:

FINISH:

DEBUR AND BREAK SHARP EDGES

DO NOT SCALE DRAWING

REVISION

	NAME	SIGNATURE	DATE
DRAWN	Alli Sventsson		
CHK'D			
APP'V'D			
MFG			
Q.A			

MATERIAL:

TITLE:

DWG NO. wrist2

A4

WEIGHT:

SCALE:1:2

SHEET 1 OF 1

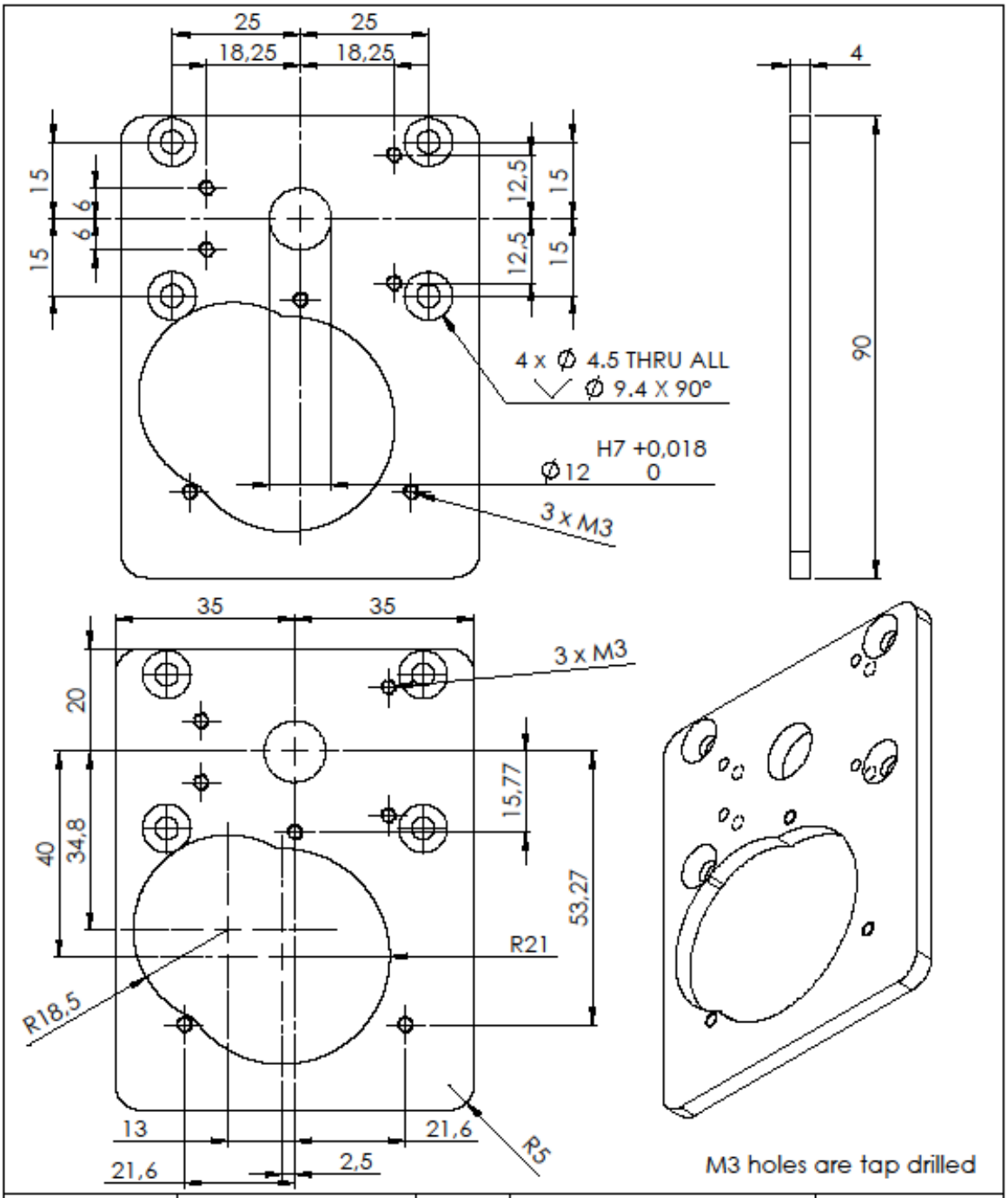
25
25
18,25
18,25
4
15
6
6
15
12,5
15
12,5
15
90
4 x Ø 4.5 THRU ALL
Ø 9.4 X 90°
H7 +0,018
Ø12 0
3 x M3
35
35
3 x M3
20
40
34,8
15,77
53,27
R21
R18,5
13
21,6
21,6
2,5
R5
M3 holes are tap drilled
UNLESS OTHERWISE SPECIFIED:
DIMENSIONS ARE IN MILLIMETERS
SURFACE FINISH:
TOLERANCES:
LINEAR:
ANGULAR:
FINISH:
DEBUR AND BREAK SHARP EDGES
DO NOT SCALE DRAWING
REVISION
NAME
SIGNATURE
DATE
DRAWN
Alli Sventsson
CHK'D
APP'V'D
MFG
Q.A
MATERIAL:
Aluminum
WEIGHT:
TITLE:
Wrist backplate
DWG NO.
wrist_backplate
A4
SCALE:1:1
SHEET 1 OF 1
SolidWorks Student License
Academic Use Only

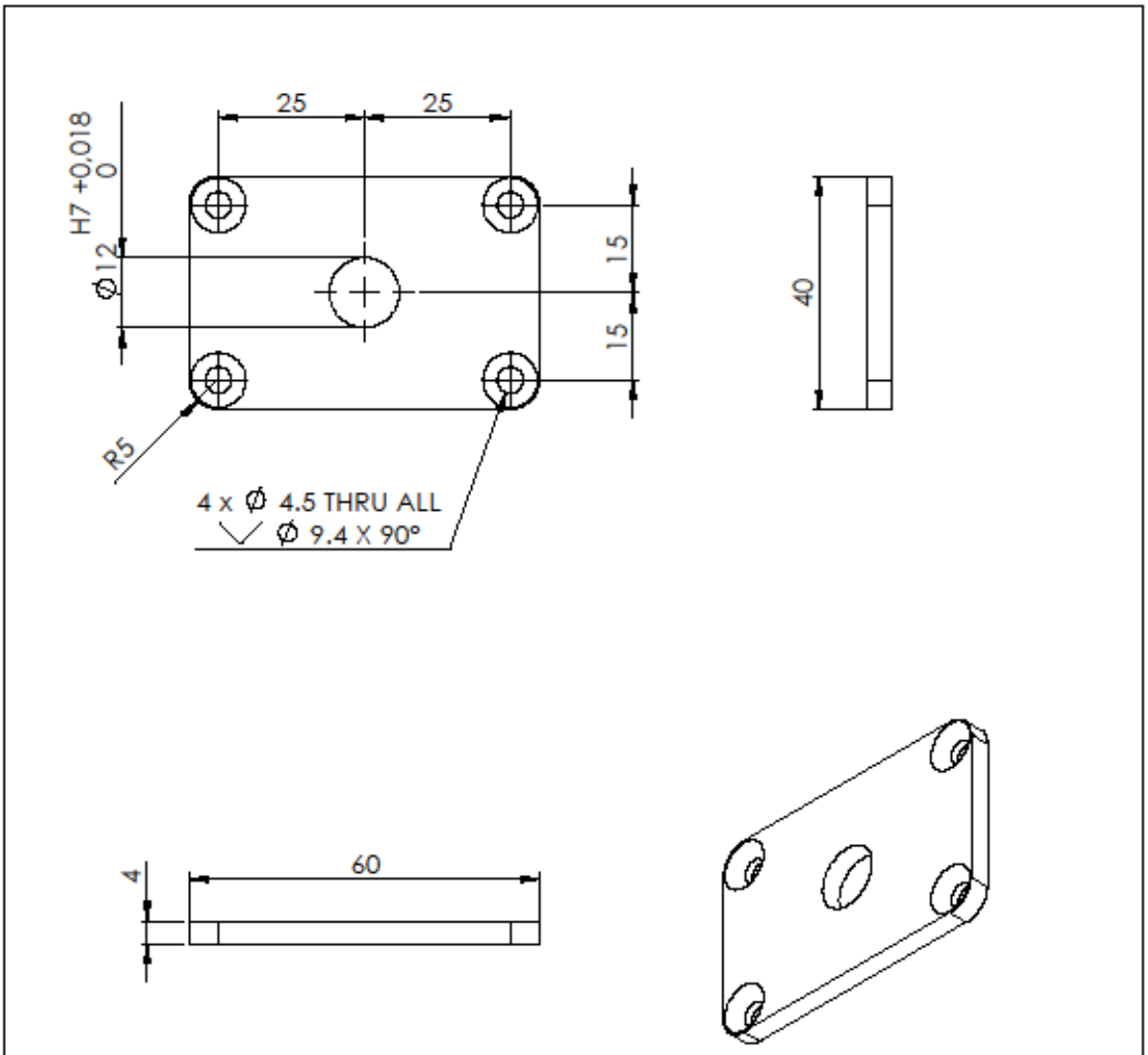

UNLESS OTHERWISE SPECIFIED: DIMENSIONS ARE IN MILLIMETERS SURFACE FINISH: TOLERANCES: LINEAR: ANGULAR:		FINISH:		DEBUR AND BREAK SHARP EDGES	DO NOT SCALE DRAWING	REVISION
	NAME	SIGNATURE	DATE		TITLE: Wrist plate	
DRAWN	Alli Sventsson					
CHK'D						
APPV'D						
MFG						
Q.A				MATERIAL: Aluminum	DWG NO. wrist_housing	A4
SolidWorks Student License Academic Use Only				WEIGHT:	SCALE:1:1	SHEET 1 OF 1

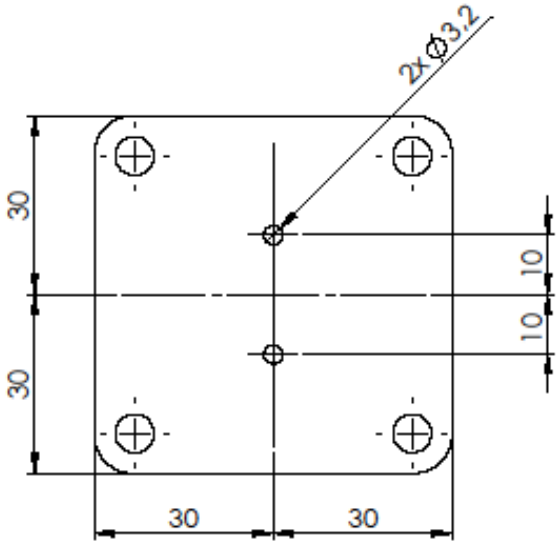

UNLESS OTHERWISE SPECIFIED: DIMENSIONS ARE IN MILLIMETERS SURFACE FINISH: TOLERANCES: LINEAR: ANGULAR:	FINISH:		DEBUR AND BREAK SHARP EDGES			DO NOT SCALE DRAWING	REVISION
	NAME	SIGNATURE	DATE			TITLE: Gripper plate	
DRAWN	Alli Sventsson						
CHK'D							
APPV'D							
MFG							
Q.A				MATERIAL: Aluminum		DWG NO. wrist_gripper_plate	A4
SolidWorks Student License Academic Use Only				WEIGHT:		SCALE:1:1	SHEET 1 OF 1

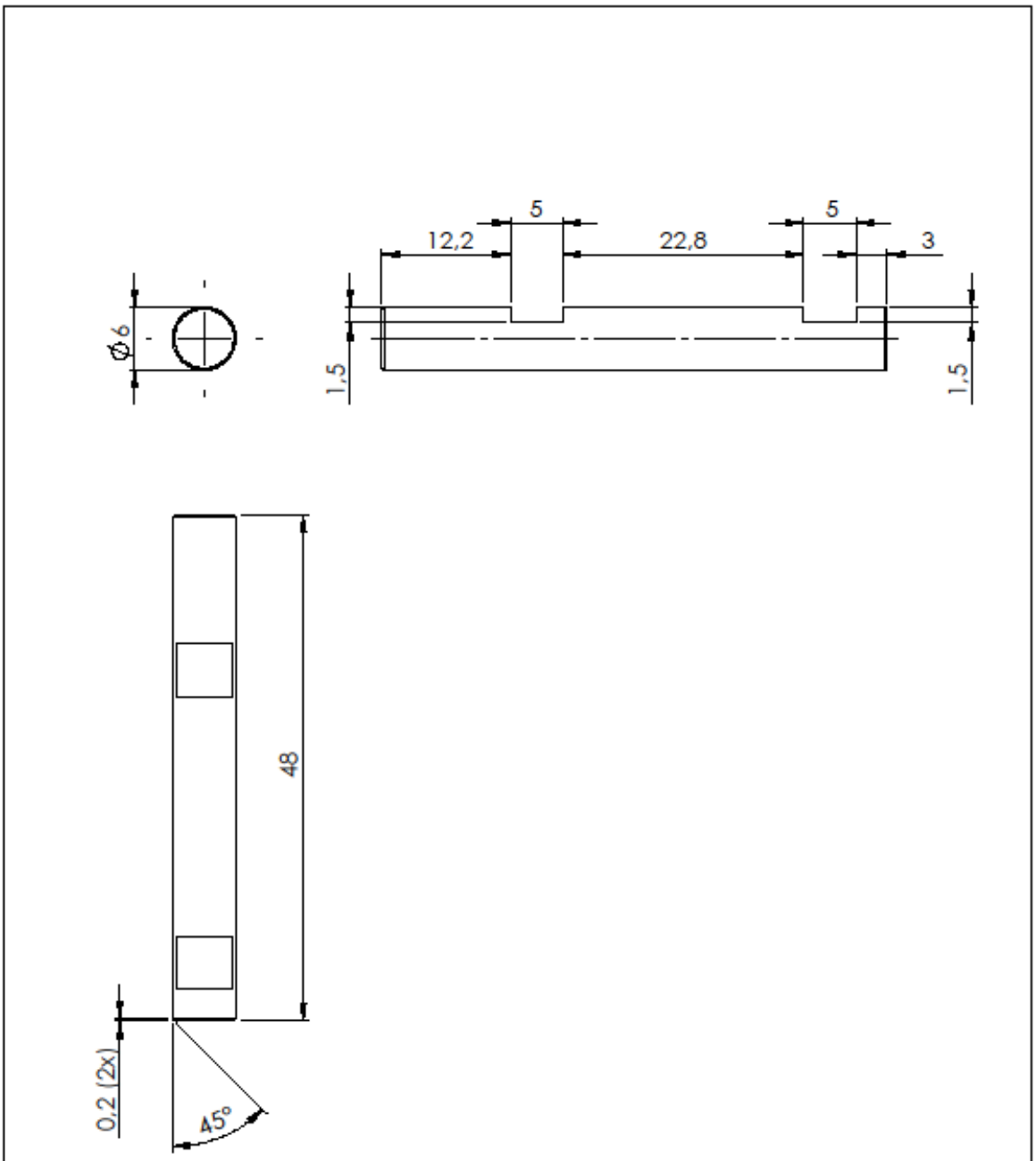

UNLESS OTHERWISE SPECIFIED: DIMENSIONS ARE IN MILLIMETERS SURFACE FINISH: TOLERANCES: LINEAR: ANGULAR:		FINISH:			DEBUR AND BREAK SHARP EDGES	DO NOT SCALE DRAWING / REVISION
	NAME	SIGNATURE	DATE			TITLE: Rotational shaft
DRAWN	Alli Sventsson					
CHK'D						
APPV'D						
MFG						
Q.A				MATERIAL:		DWG NO. wrist_rod / A4
SolidWorks Student License Academic Use Only				WEIGHT:		SCALE:2:1 / SHEET 1 OF 1

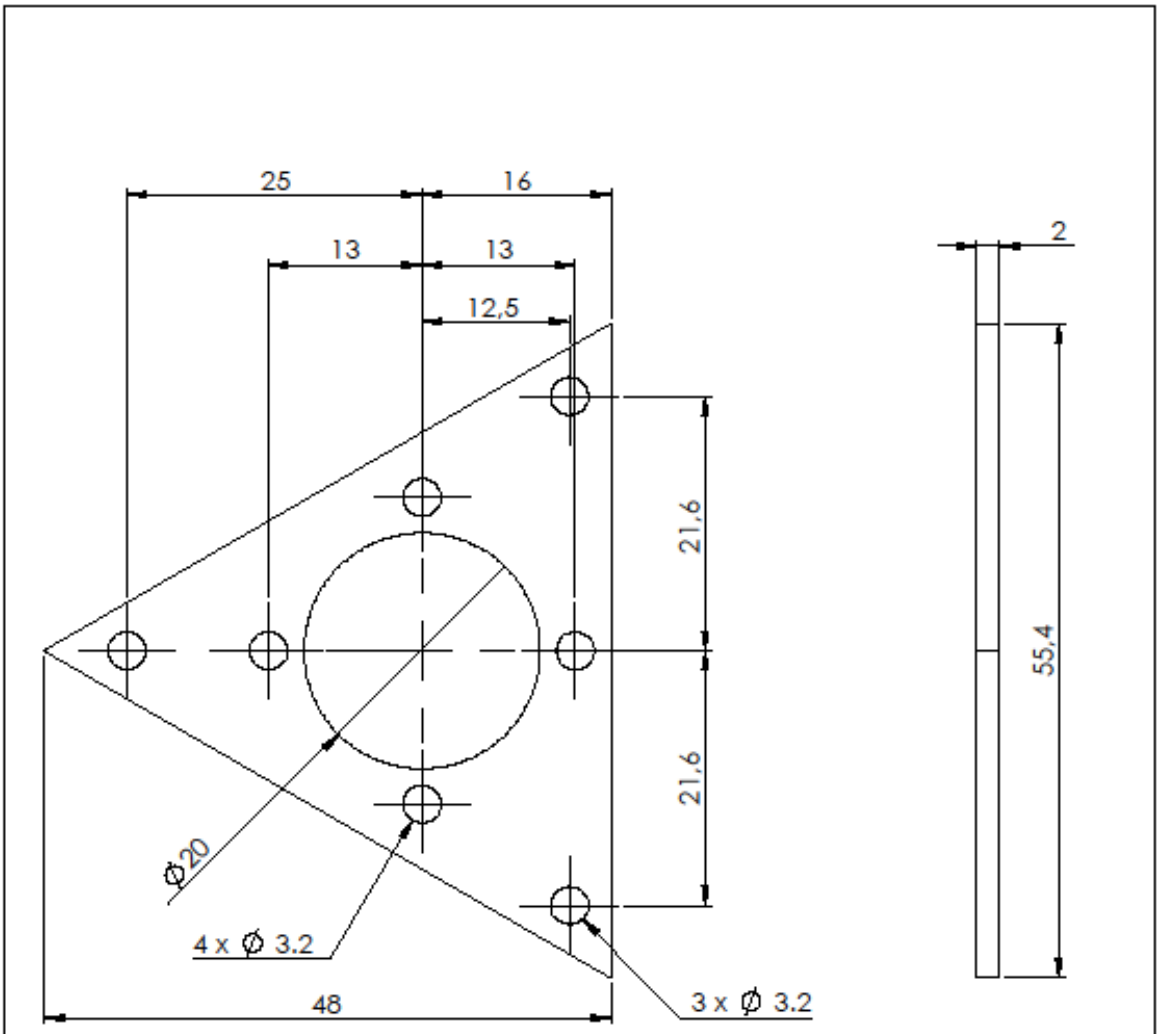

Round corners R2

UNLESS OTHERWISE SPECIFIED: DIMENSIONS ARE IN MILLIMETERS SURFACE FINISH: TOLERANCES: LINEAR: ANGULAR:	FINISH:		DEBUR AND BREAK SHARP EDGES	DO NOT SCALE DRAWING	REVISION
	NAME	SIGNATURE	DATE	TITLE: Gearhead plate Wrist DPR1	
DRAWN	Alli Svantsson				
CHK'D					
APPV'D					
MFG					
Q.A					
SolidWorks Student License Academic Use Only		MATERIAL: Aluminum		DWG NO. motor_plate_v2	A4
		WEIGHT:		SCALE:2:1	SHEET 1 OF 1

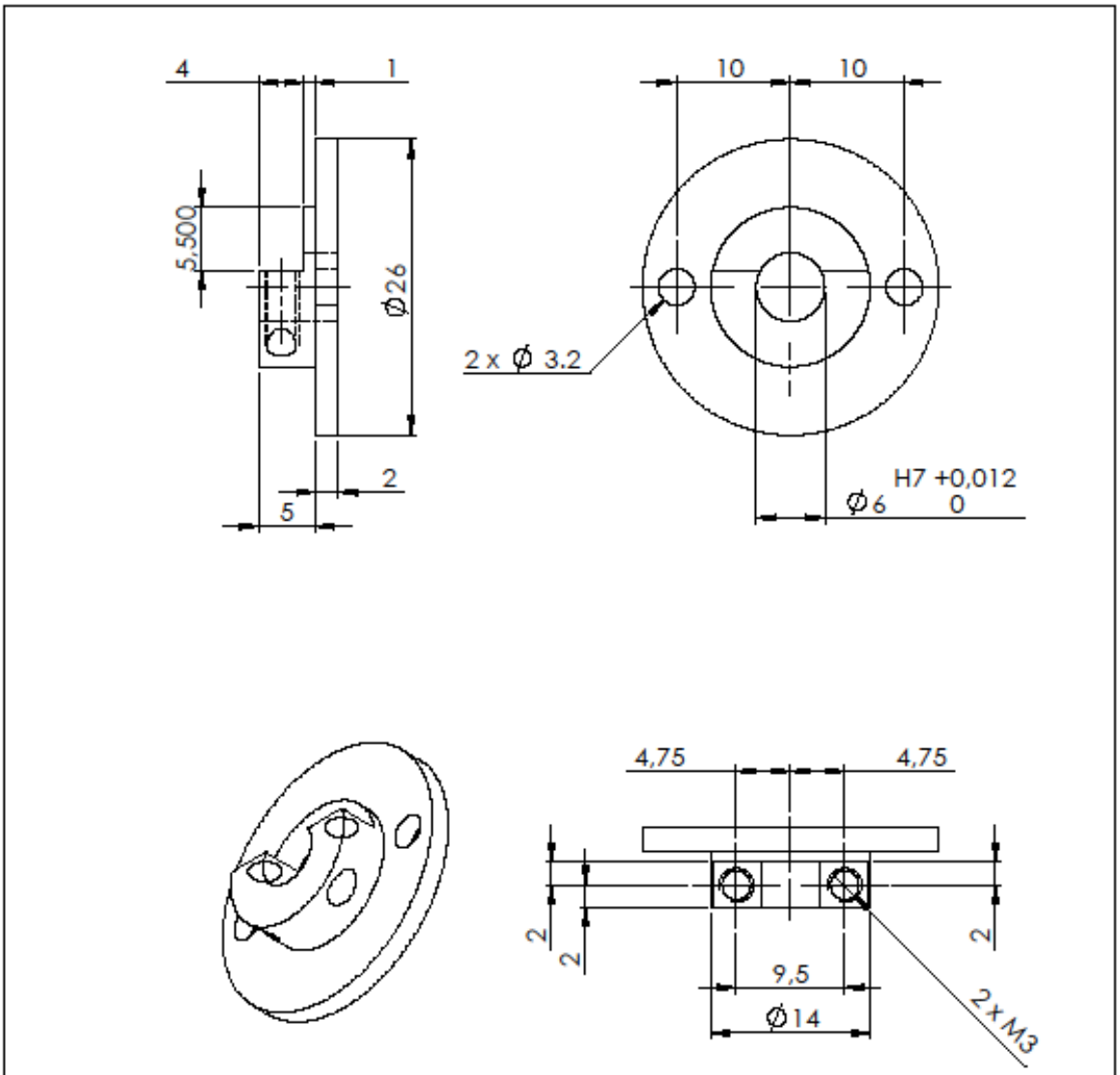

UNLESS OTHERWISE SPECIFIED: DIMENSIONS ARE IN MILLIMETERS SURFACE FINISH: TOLERANCES: LINEAR: ANGULAR:			FINISH:			DEBUR AND BREAK SHARP EDGES	DO NOT SCALE DRAWING / REVISION
	NAME	SIGNATURE	DATE				TITLE:
DRAWN	Alli Sventsson						
CHK'D							
APPV'D							
MFG							
Q.A							
MATERIAL: Aluminum							DWG NO. shaft_gripper_attach A4
WEIGHT:							SCALE:2:1 SHEET 1 OF 1

SolidWorks Student License
Academic Use Only

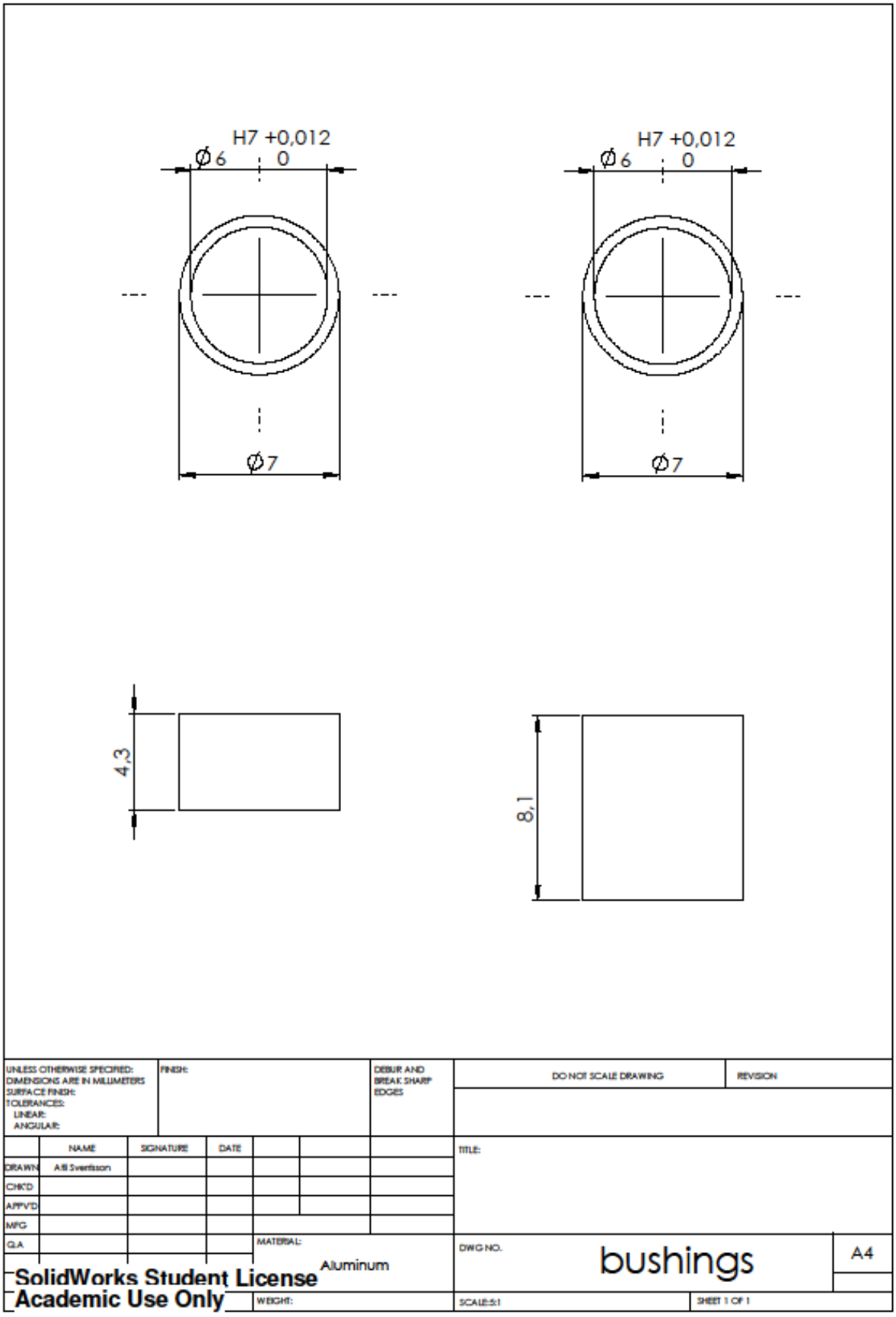
H7 +0,012
Ø6 0
Ø7
H7 +0,012
Ø6 0
Ø7
4,3
8,1
UNLESS OTHERWISE SPECIFIED:
DIMENSIONS ARE IN MILLIMETERS
SURFACE FINISH:
TOLERANCES:
LINEAR:
ANGULAR:
FINISH:
DEBUR AND BREAK SHARP EDGES
DO NOT SCALE DRAWING
REVISION
NAME
SIGNATURE
DATE
DRAWN
Alli Svantsson
CHK'D
APP'VD
MFG
Q.A
TITLE:
MATERIAL:
Aluminum
DWG NO.
bushings
A4
SolidWorks Student License
Academic Use Only
WEIGHT:
SCALE:5:1
SHEET 1 OF 1

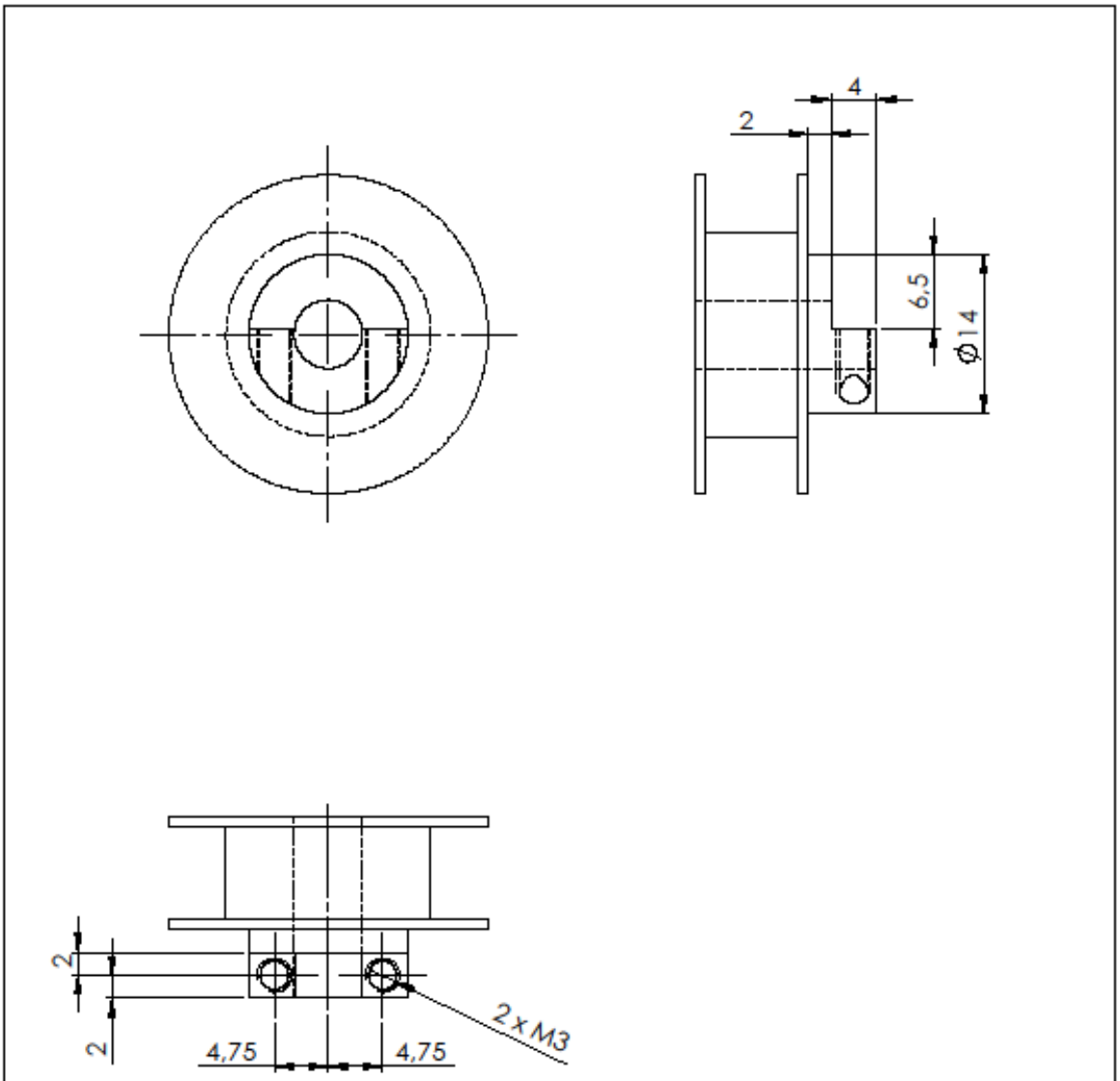

UNLESS OTHERWISE SPECIFIED: DIMENSIONS ARE IN MILLIMETERS SURFACE FINISH: TOLERANCES: LINEAR: ANGULAR:	FINISH:	DEBUR AND BREAK SHARP EDGES	DO NOT SCALE DRAWING / REVISION
NAME / SIGNATURE / DATE			TITLE: AT3 24 teeth width-6mm
DRAWN			
CHK'D			
APPV'D			
MFG			
Q.A		MATERIAL:	DWG NO. pulley_24teeth / A4
SolidWorks Student License Academic Use Only		WEIGHT:	SCALE:2:1 / SHEET 1 OF 1

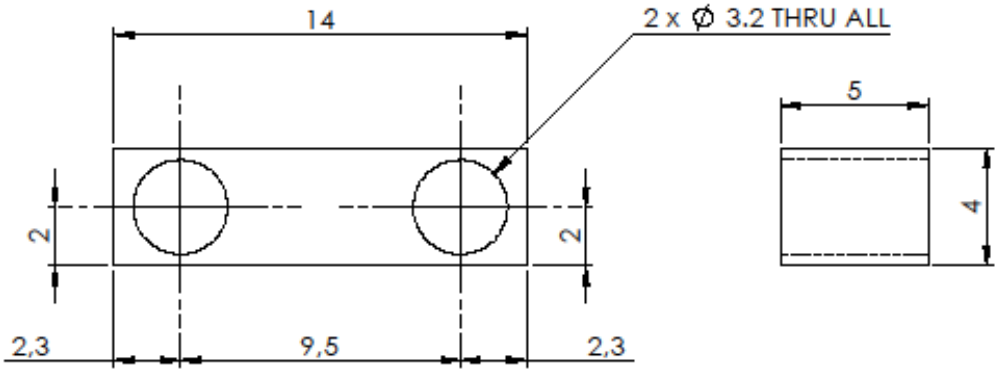

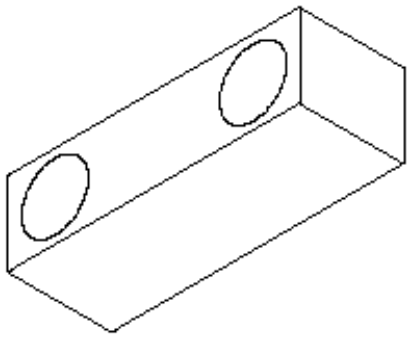

UNLESS OTHERWISE SPECIFIED: DIMENSIONS ARE IN MILLIMETERS SURFACE FINISH: TOLERANCES: LINEAR: ANGULAR:		FINISH:				DEBUR AND BREAK SHARP EDGES	DO NOT SCALE DRAWING / REVISION
	NAME	SIGNATURE	DATE				TITLE:
DRAWN	Alli Sventsson						
CHK'D							
APP'V'D							
MFG							
Q.A							
				MATERIAL: Aluminum			DWG NO. Shaft_pulley_connector / A4
SolidWorks Student License Academic Use Only				WEIGHT:			SCALE:5:1 / SHEET 1 OF 1

A.2.3 Controller

The controller for both the master and the slave (see Figure A-19) was running on the xPC target at 0.005 ms real-time. The master controller was divided due to haptic shared control into two modes that depended on whether the slave gripper was grasping or not. The master controller read the position of itself and the slave, haptic shared control intentions and sensory information. The slave controller was divided as well into two models depending on whether commands to the slave should be sent or not. If the slave should not be moving commands with zero velocity was sent to the slave. By having the master and slave controller side by side is ideal when designing a haptic feedback loop because you would need position or force from both sides to link two devices together. It was thought to be too time-consuming to implement a haptic feedback for this experiment and the time-delay of the slave was as well not ideal.

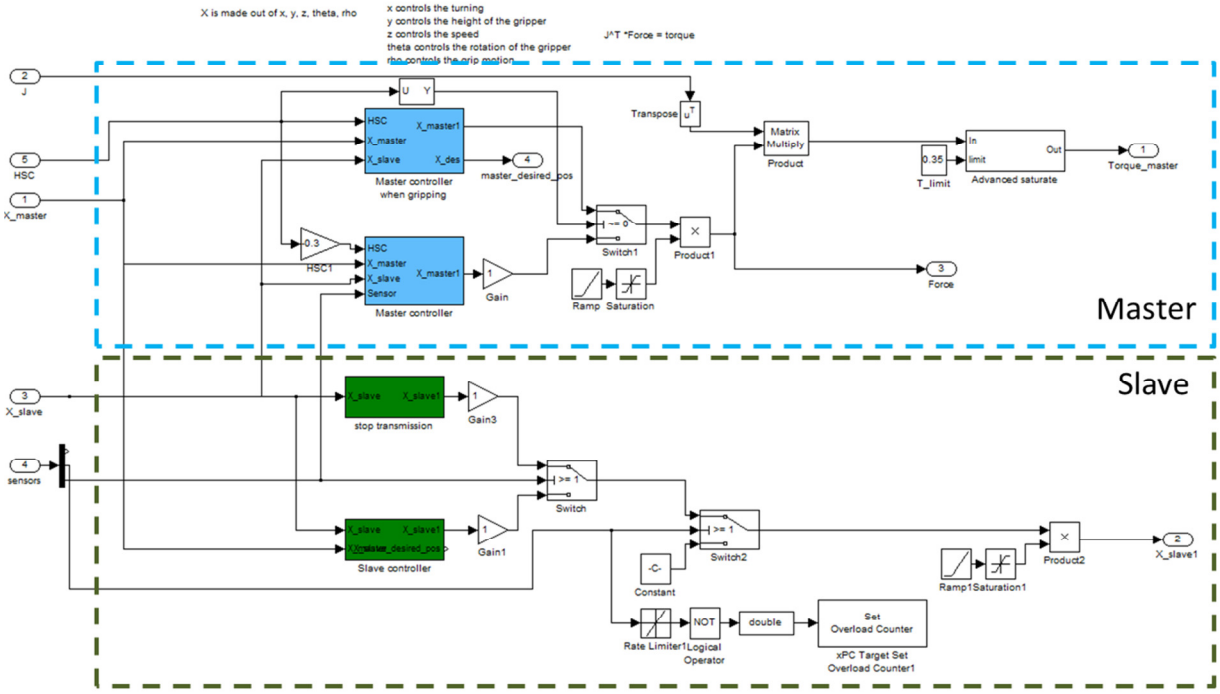

Figure A-19: The controller is divided into a master controller (blue) and a slave controller (green).

A.2.3.1 Master Controller

As said before, the master controller was divided into two modes depending on whether the slave is grasping and the slave is not grasping. Most of the time, the controller was running the mode where the slave was not grasping (see Figure A-20). The position of each of the 5 degrees of freedom (DOF) for the master, slave and haptic shared control are evaluated in separate blocks. The x and z DOF have an equilibrium force, similar to a joystick in the sense that it tries to get back to neutral position where zero velocity commands are sent. The same DOF also have a small notch implemented to make it easier for operators to find the neutral position before turning on the transmission. They were able to lean against two small notches, small virtual wall, and find where they meet. After turning on the transmission the notch was gone because it was thought that the notch could be in the way when making small delicate

movements close to the neutral position. Haptic shared control was implemented in the x and y DOF where x is the turning command and y is the arm height command. This helped the operators to find and stay on the ideal path in 3 dimensions to finish the task. θ DOF was in fact not connected because it was not used during this mode. Force was provided in the ρ DOF to help the subjects keep the grasp open but subjects were still tired keeping the grasp open, therefore the gains should be increased. To try to increase the stability of the master a damping in x, y and z DOF was implemented at the outskirts of the workspace.

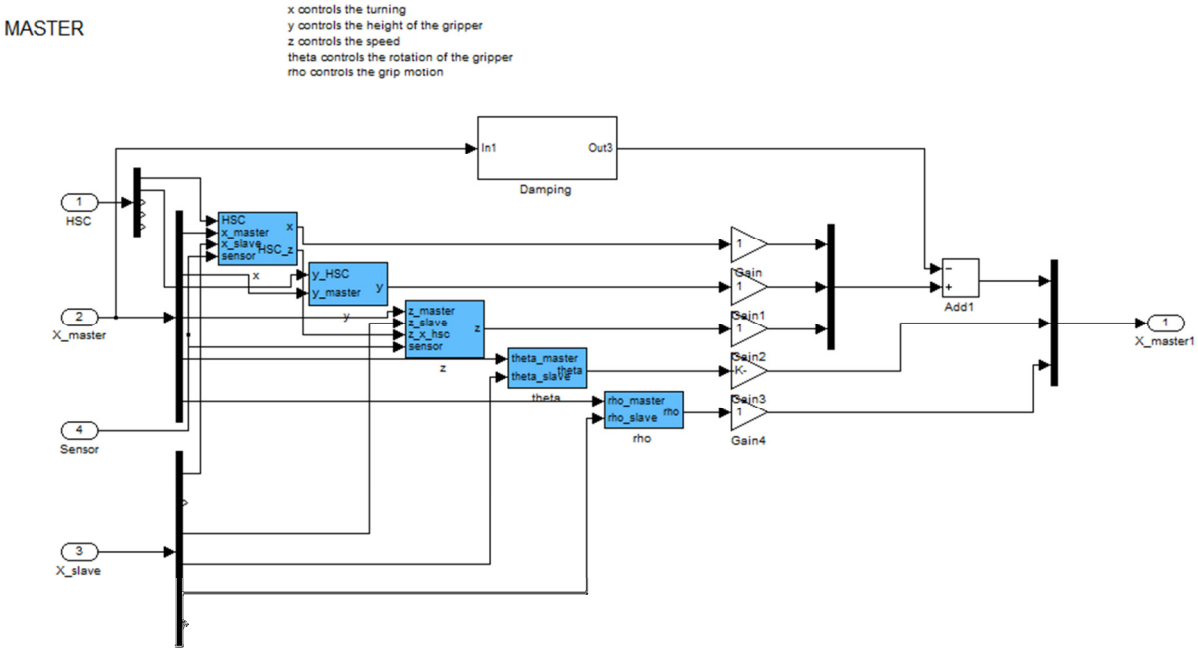

Figure A-20: Master controller when the slave is not grasping. The 5 degrees of freedom are split up for the master, slave and haptic shared control and evaluated in separated blocks.

The mode when the slave was grasping (see Figure A-21), the model looks very similar. Haptic shared control played an important role in this mode. When a grasp had been made the position of the end-effector was saved. That position was then sent to this model and compared to the actual position of the master. If the difference was large, a larger force was provided to the user in x, positive y and z direction towards the original position when the grasp had been made. The position of the y and θ were linked to an equation of a circle with radius of 0.065 which was supposed to mimic a rotating handle. So if the operator would only move downwards (y) without rotating (θ), he would feel a rotating force acting in a clockwise-direction. The same would happen if the operator would only rotate he would feel a downwards force. The force would grow larger with a larger deviation from the trajectory of a door handle.

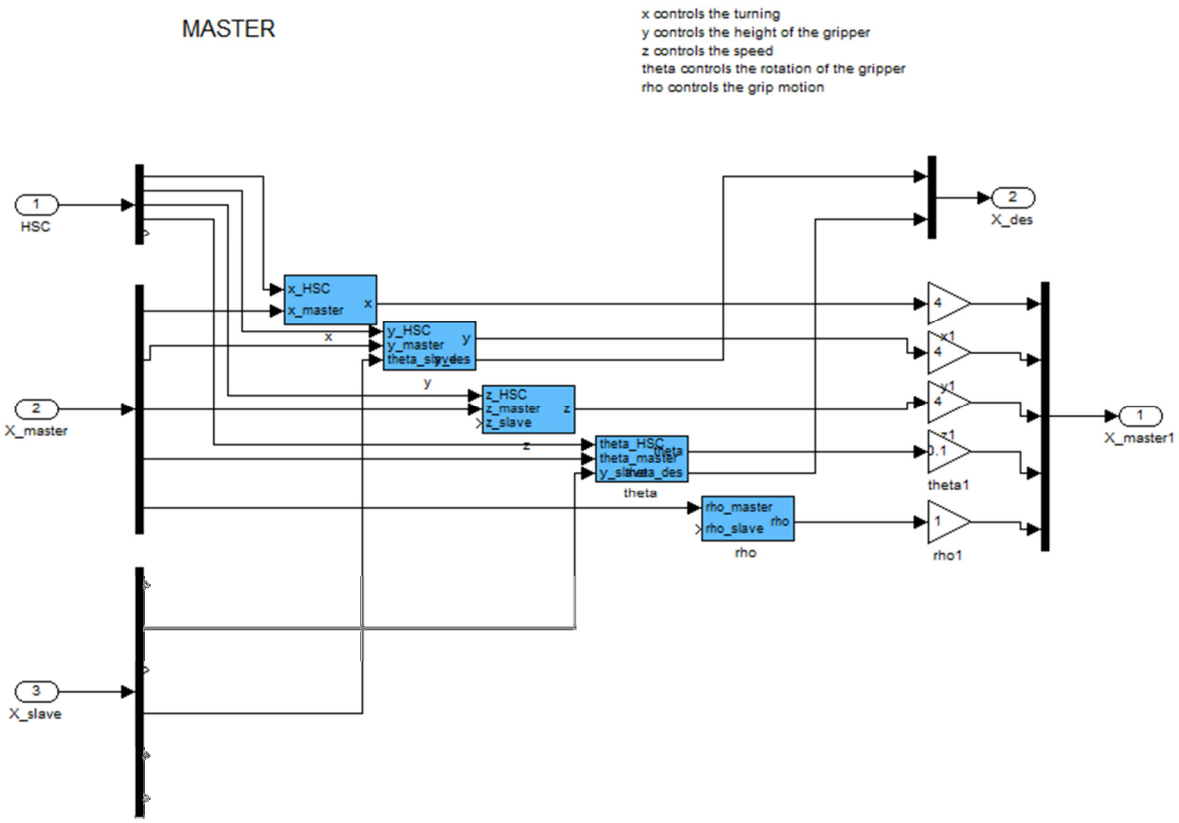

Figure A-21: Master controller when the slave is grasping. The 5 degrees of freedom are split up for the master, slave and haptic shared control and evaluated in separate blocks.

A.2.3.2 Slave Controller

The slave controller when the transmission was on is illustrated in Figure A-22. x and z DOF are velocity controlled and only use the position of the master to determine the velocity commands to the slave. The farther the operator moved the master device from the neutral position the higher velocity was sent to the slave, although with a maximal 3 rad/s of the wheel speed. The y, θ and ρ DOF are position controlled where the position of the master is compared to the position of the slave and outcome is sent as a velocity to the slave. The reason for why a velocity was sent to the slave is because the 3mxel control board on the slave can still not handle position commands at high frequency. In the y block, where the height of the arm is calculated, the horizontal movement of the arm is added to the z DOF to counteract the horizontal motion of the arm. Experience though us that the z movement should be more than less because subjects tended to push the door too much. It was optimized to be as small as possible but still resulted in a small forward motion.

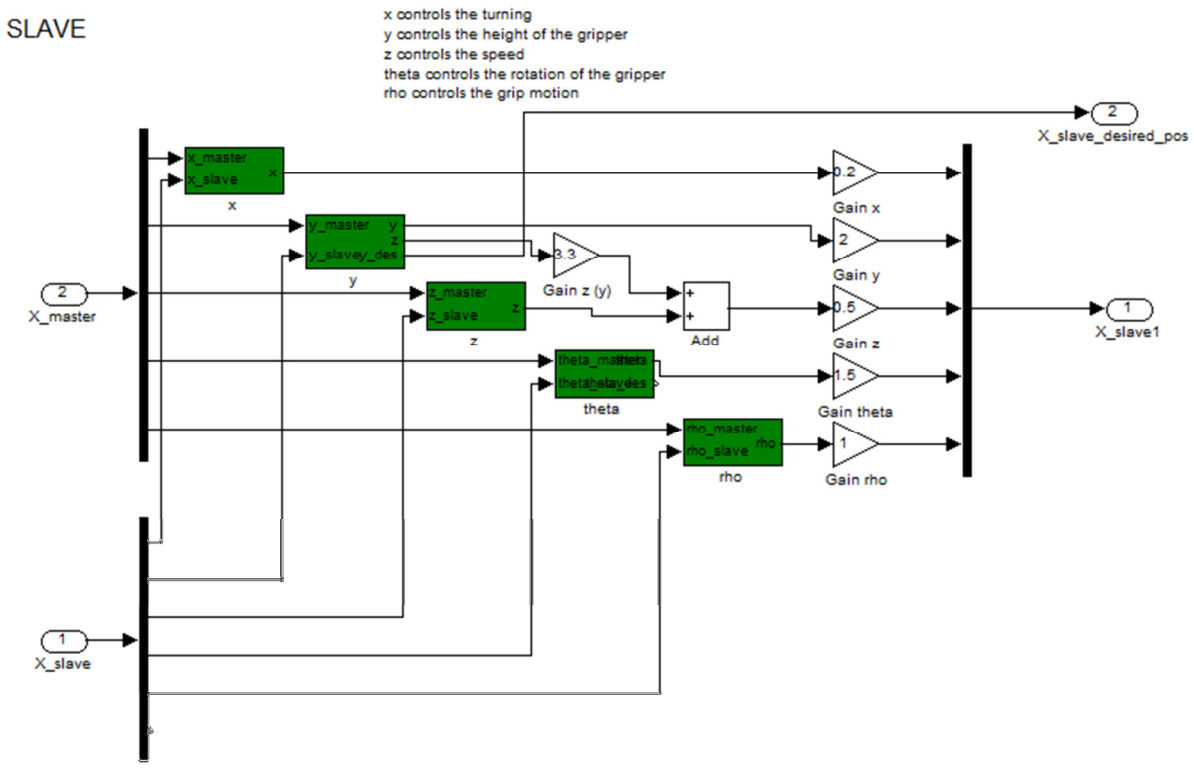

Figure A-22: Slave controller when the transmission is on. The 5 degrees of freedom are split up for the master and slave and evaluated in separate blocks.

A.2.4 Communication

The master device is running on a xPC target machine through a Quanser Q8 board. A Simulink model is uploaded to the target. The best communication protocol to and from the target machine is UDP through an Ethernet cable, see chapter A.2.4.1. The Slave is operated by a local laptop through a 3Mxel v2 microcontroller. The host, target and the slave laptop should all be connected by Ethernet cable through a multiport switch, see Figure A-23.

For a smooth and robust control of the master-slave setup a proper architecture is needed. Figure A-24 presents that architecture and one can see that the slave controller has been merged with the master controller and is situated at the master side. Master-slave setups usually have only one controller where all position/force data is gathered from master and slave and processed. Having all that data at the same place gives the ability to provide force feedback and since the xPC target is definitely running at real-time at the master side it is preferable to keep the controller there. The data is transferred between master and slave with the UDP communication protocol.

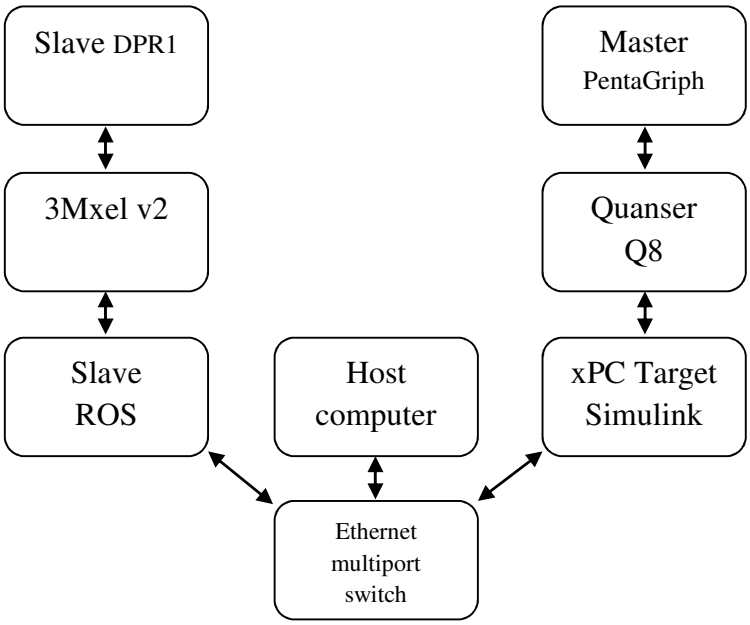

Figure A-23: Master - Slave communication

Originally the communication between the slave laptop and the slave was done through a USB port. That setup had a really bad communication speed. The time it took 5 messages to be received from the 3mxl was on average 12.5 ms (see Figure A-25). After receiving data from the motor, signals would be sent to the motors as well but that can be done faster with the SyncWrite function, where all motor signals can be sent at the same time. Although, because of time pressure the SyncWrite function was not implemented.

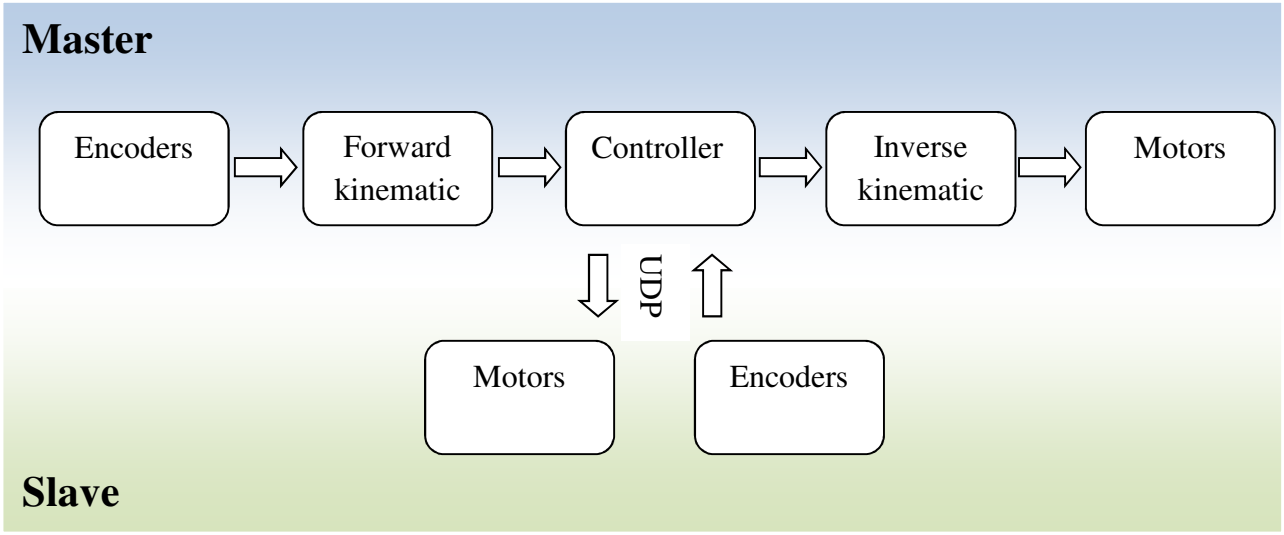

Figure A-24: Master - Slave configuration

The delay was thought to be too large because initially haptic feedback was intended to be provided to the operator. Therefore a RS-485 express card was purchased that can communicate directly to the laptop´s processor and immensely decrease the time it takes to receive values from all of the motors. Unfortunately, delivery got postponed and when it

finally arrived we found out that we received the wrong card, a PCMCIA card, it did not work properly and the Linux drivers were as well too old. Therefore, I was stuck with the USB connection.

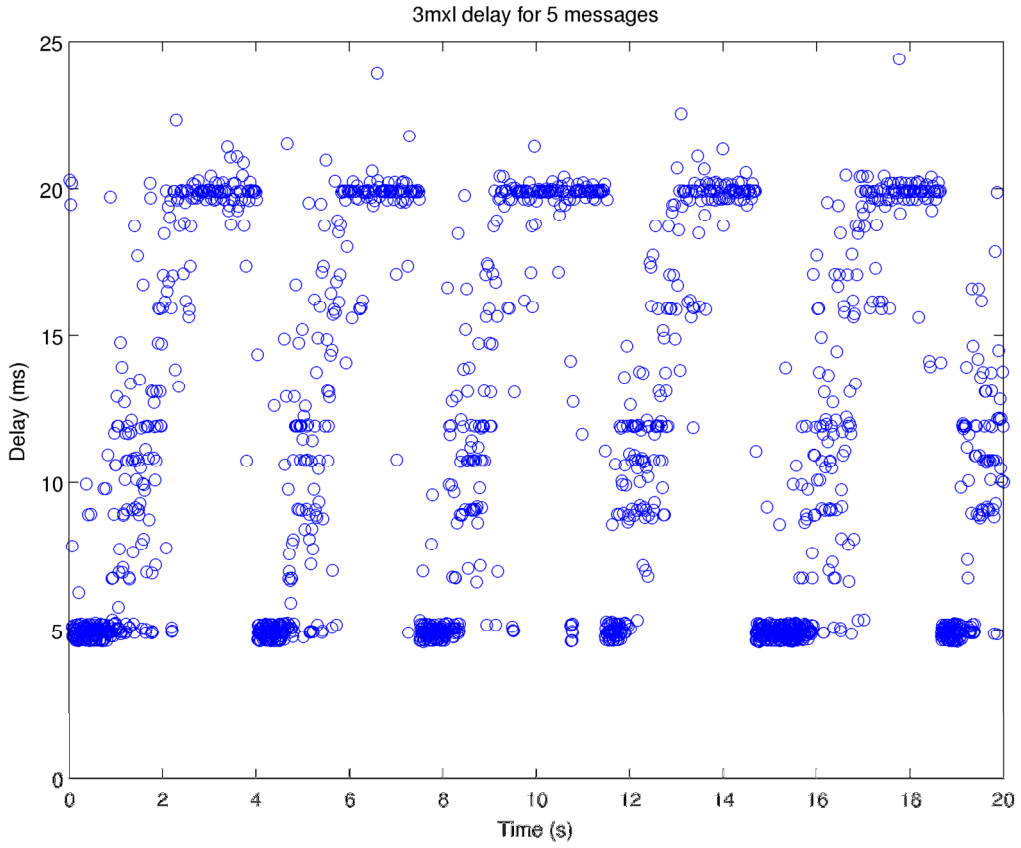

Figure A-25: The time it takes to receive 5 messages from the 3mxl through an USB port

A.2.4.1 UDP

UDP is a communication protocol that is able to send/receive packages between the xPC target and any other computer connected through Ethernet. UDP sends data to a remote ip address like TCP but differs in that sense that it sends packages and not series of data and that it does not confirm if the data reached its destination. Some have even described the difference as TCP is for a phone call as UDP is for a mail in a mailbox, the letter might get lost on its way when in a phone call you get feedback whether or not the message was delivered. Although UDP does not confirm successful deliveries it was chosen for its speed and in a master-slave real-time configuration the time is more important than successfully sending data that might already be outdated. When using UDP to communicate to/from the xPC target it is necessary to understand its limitations. For instance UDP blocks in Simulink run in the background task which is executed after the real-time tasks completes each time step. This might cause packages to be lost or dropped. The second limitation is the bandwidth. The UDP communications between the host and the target through the Ethernet cable is shared with the regular host-target communication. On the other hand while the

target is running, the regular host-target communication is minimal or none so it should not matter that much.

For the master-slave configuration it is essential for the software to react appropriately when a package has been lost or dropped. If that is not adequately done then the position/force of the master or slave goes to zero (if package does not arrive within the time step the data values goes to zero) and the other device will behave very strange (could even damage the device or be dangerous to people). Fortunately, that was not necessary because the Simulink model automatically uses the last received package from the other device.

The PentaGriph-DPR setup has 5 DOF and therefore 5 positions/forces data (double) to deliver to the other device. UDP needs to pack all the data (5*double = 40 bytes) into a single package (uint8) before sending it to the other end. At the other end the package is then unpacked into the same 5 numbers that were sent and used at that end, see Figure A-26 and Figure A-27.

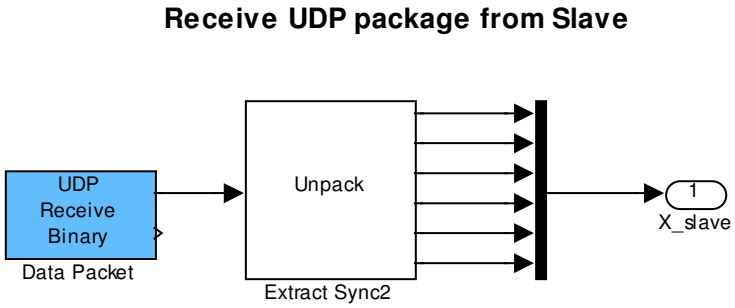

Figure A-26: UDP package received from the slave and unpacked

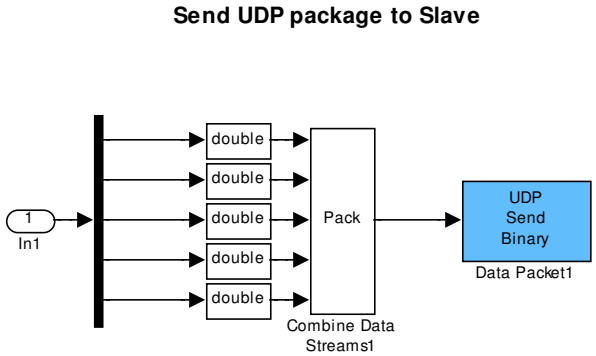

Figure A-27: Gathering data to pack and send to the slave through UDP communication protocol

Uploading and running a simple UDP send/receive model to the xPC target and running another send/receive model on the host provided the average running time of the target model to be $7.0*10^{-7}$ seconds. This turned out to be very low compared to the time step of the master-slave model which was 0.005 (200 Hz). Running the entire program on the xPC target was in the order of $1*10^{-5}$ seconds so one can see there is plenty of time for background tasks like UDP communication to operate during each times step.

The communication between the target and the slave through the Ethernet multiport switch was measured about 0.25 ms for each ping (message size usually 32 bytes). On the slave side the UDP communication was implemented in C++ as the slave was running ROS. The Slave was not running in hard real-time but soft real-time which means that if it was unable to finish one spin of the program in less time than the xPC´s sample rate it did not crash.

Please find the code for the UDP transmission at the slave side in the dpr2_slave package inside the dpr2_slave_stack.

Figure A-28: An operator controlling the Delft Personal Robot 1 (DPR1) with the Delft Hand 3 (DH3) to open a table top door. DH3 has here less degrees of freedom and less compliance because two fingers have been locked together with a plate.

Appendix B Unlatching Doors - Experimental Protocol

All subjects read this experimental protocol and followed the training schedule before starting the experiment.

B.1 Introduction

Welcome to the door opening experiment, were the goal is to investigate the influence of Haptic shared control and an underactuated hand, in a door opening task with a remotely controlled mobile robot. Such a robot could be used to save people in a burning house in the future. Haptic shared control is an automated function that assists the operator to approach and unlatch the door. An underactuated hand is a compliant hand that decreases the necessity of positioning the robot accurately during the rotation of the door handle. These two improvements are thought to improve the task performance of a human operator when opening a door. The experiment will be divided into 4 configurations which can be found in the table below and each has 8 repetitions. You´ll be trained to operate a remotely controlled robot before performing the experiment. The total procedure should take about 1-1½ hour. But before you operate let's look at a movie on how the robot is controlled.

	Haptic Shared Control Guided to the door	No Haptic Shared Control
Underactuated hand	8 repetitions	8 repetitions
Less-Underactuated hand	8 repetitions	8 repetitions

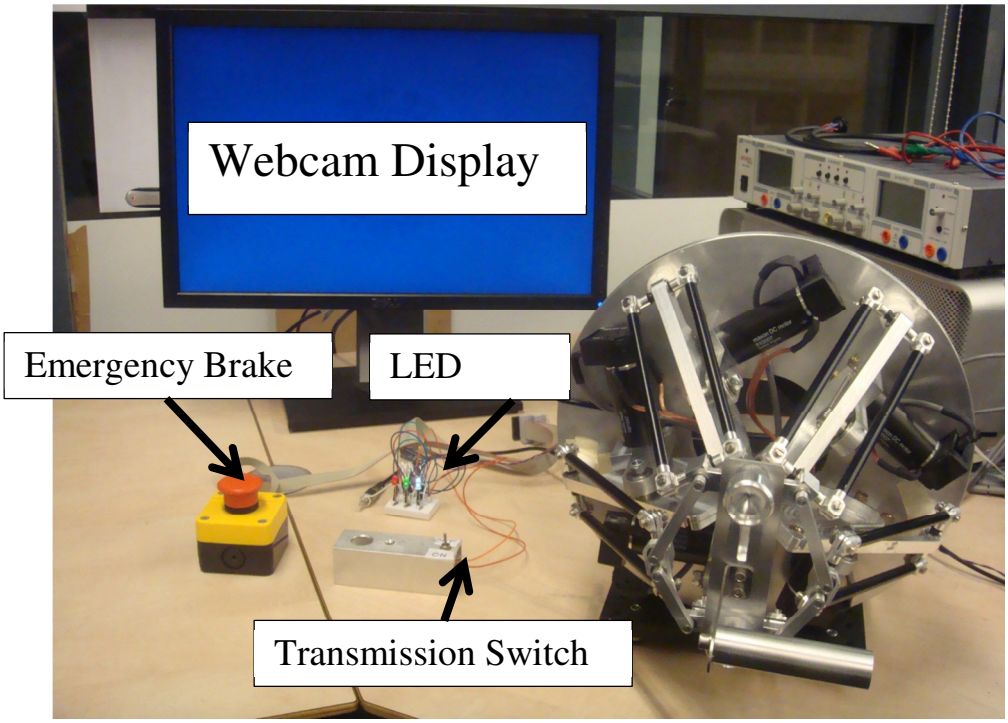

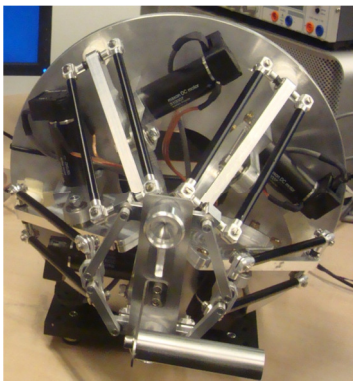

Data Transfer

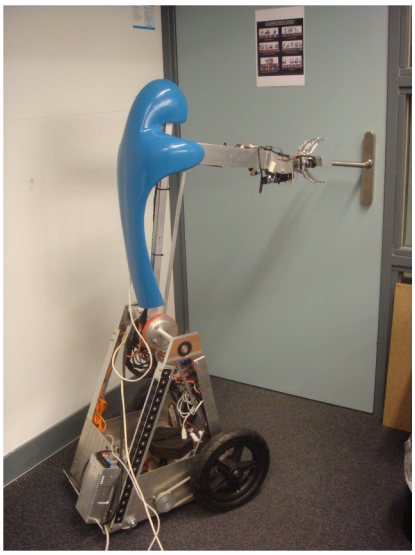

Master Device

Slave Device

B.2 Before Operating

- Run your hand through the sleeve.

1. Grasp the handle on the master device with your right hand.

- Place your index finger and thumb in the finger holders.
- Pull the device towards you, about half the way out.

2. Release the safety button.

- Try to be in the center of the workspace. You'll feel a small notch when you pass the center.

3. Switch on the communication to the slave robot when you´re ready to start the run, the red light should then appear and the timer starts.

- You should only look at the screen and not turn around.

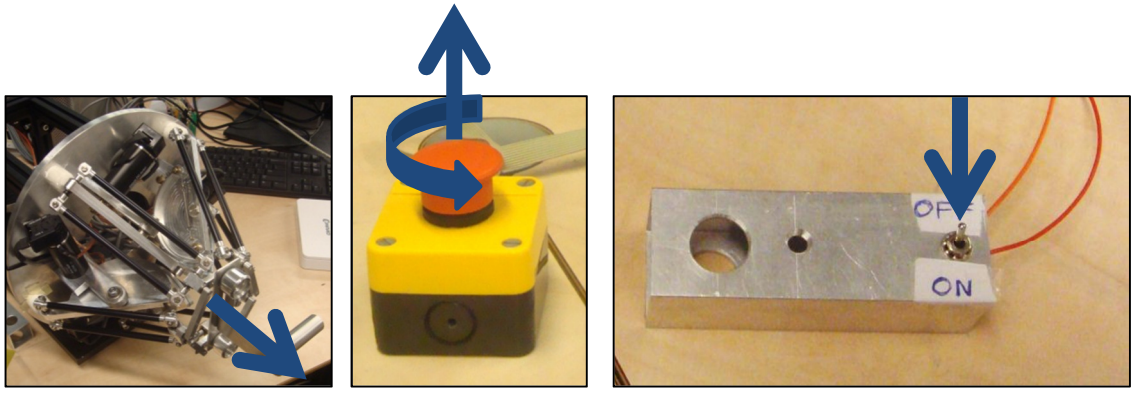

1. Pull device

2. Release

3. Switch ON

B.3 During Operation

- **Always keep your left hand on the transmission switch** in case you need to quickly stop the slave device. You can turn on and off the switch but remember the first time you switch it on the timer starts counting. You also might need to push the emergency brake to stop the master device if it starts behaving strange.
- **Always keep your fingers in the finger holders.**
- Always keep the gripper open unless you are about to grip the door handle.
- There is an unstable area located in the top right corner of the workspace of the master device which you should avoid going to.
- When the robot is in contact with the door the green light should appear.
- When the task is finished the white light should appear.

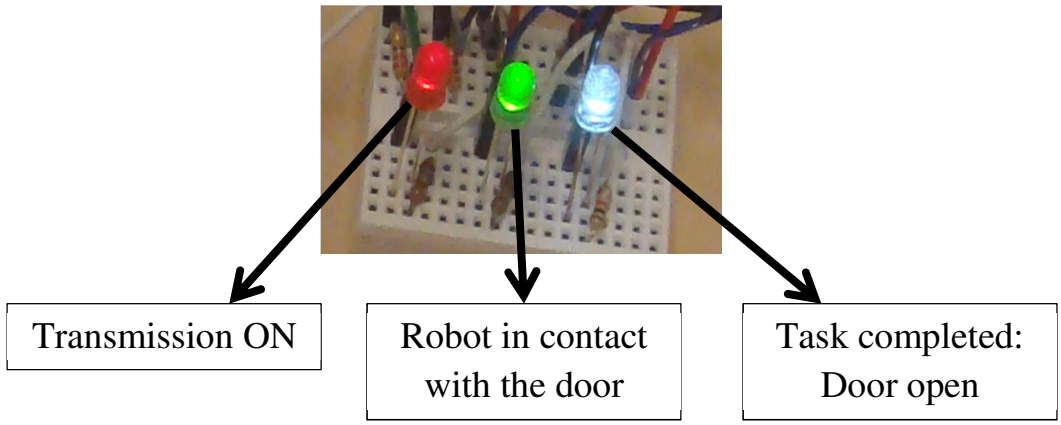

B.4 After Operation

1. First turn off the transmission switch.
2. Push hard on the emergency brake.
3. Then you can return the master device to its home position.

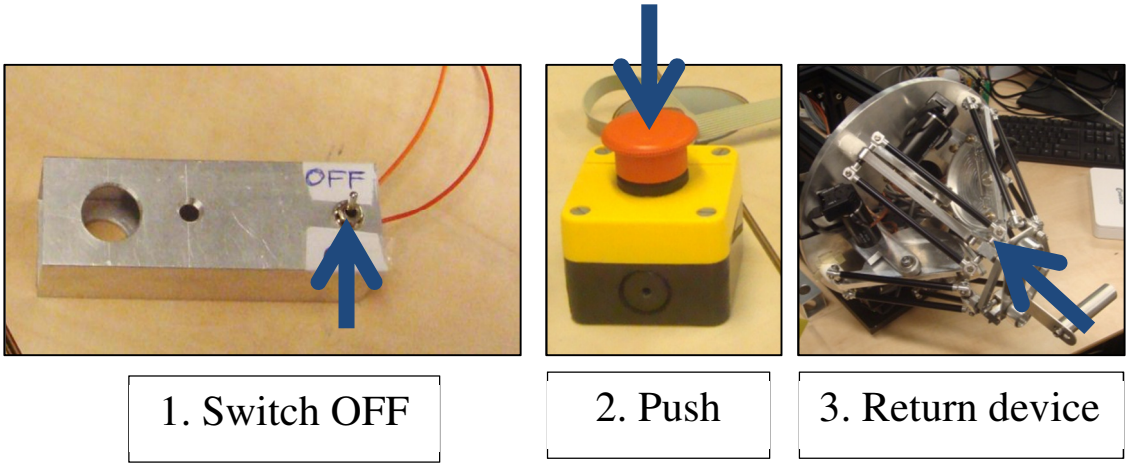

B.5 Task Description

- You should open the door as fast as possible, although without damaging the robot (might happen if you approach the door too fast).
- You will open the door 8 times for each of the 4 configurations

A. During the 8 rounds the robot´s position will change between two starting locations

B. First drive the robot towards the door and approach the door like you would do if you had to fully open the door later (approach)

C. Gently approach the door handle, don't push after contact is made.

- When the robot touches the door the green light should appear

D. Grasp the door handle (grasp)

D. Rotate the door handle (unlatch)

E. Slightly open the door till it hits the sensor (open), the white light should light up and you´ve finished one round.

A. 2 Starting

B. Drive as fast as possible towards the door handle

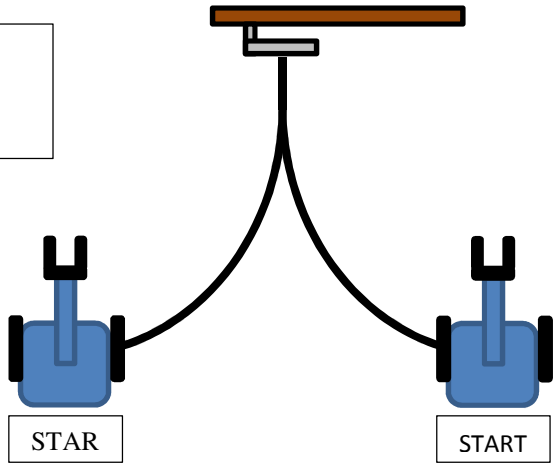

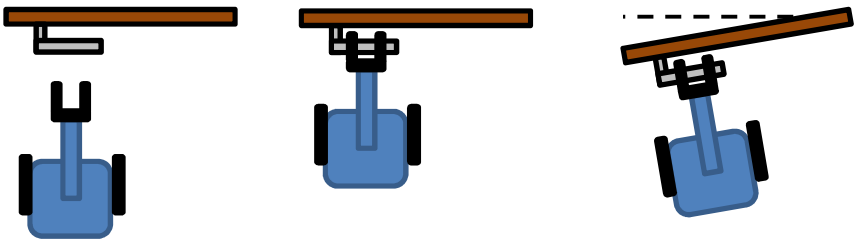

C. Drive gently when close to the handle

D. Grasp the handle in the middle and unlatch

E. Pull the door open

B.6 Training Schedule

Task Subject	1	2	3	4	5	6	7	8	9	10	11	12	13	14	15	16
Go around the master workspace																
Move base forward/backward																
Rotate base left/right																
Move arm up/down																
Rotate wrist left/right																
Rotate wrist left/right																
Close/open the hand																
Move slowly (2x each)																
F. Towards the door without touching in the right height																
- Backwards from the door																
G. Towards an object and gently touch it																
H. Grasp the object																
I. Release the object																
J. Backwards from the object																
Move medium speed (2x each)																
K. Towards the door, end slowly																
L. Gently touch the door handle																
M. Grasp the handle																
N. Release the handle																
O. Grasp the handle																
P. Rotate the handle																
Q. Pull the door open																
Move fast (2x each)																
R. Towards the door, end slowly																
S. Gently touch the door handle																
T. Grasp the handle																
U. Rotate the handle																
V. Pull the door open																

Appendix C Unlatching Doors - Experimental Results

The experimental results from the task of unlatching a door with haptic shared control and an underactuated hand are presented in this appendix. First the data management is described on how the raw measurement data was treated before the results are presented.

C.1 Data Managements

The experiment produces 512 trials from 16 subjects which performed 8 repetitions for each of the 4 configurations. From each trial 13 measures were recorded at 200 Hz and they are listed in Table C-1.

Table C-1: Measures that were recorded during each trial

Measures	Dim.	Description
time	1	Time
q	5	Encoder angles
X_m	5	End point values of x, y, z, θ and ρ
F_be	5	Motor torques to the motors on the master before transmission
n	1	Determines how many iteration needed to find the master's end point
F_af	5	Motor torques to the motors on the master after transmission
X_s	5	Outgoing velocity commands to the slave (turn, arm height, drive, wrist rotation and grasping)
X_s_in	6	Received position of the slave (global x pos, arm height, global z pos, wrist pos, gripper current, global angle)
F_master	5	Forces after the controller before inverse kinematics
HSC	5	Haptic shared control forces (or position if slave is grasping)
Sensors	3	Three sensory digital inputs
Global_pos	4	Global position of the slave (global x, global y, global z, global angle)
P_path	3	Points on the ideal path that were used during a trial

The performance and control effort metrics for the experiment were defined to be: time, number of grasps, distance travelled and the reversal rate (number of steering corrections per minute). To use the measured raw data to analyze the metrics they needed first to be organized for each subject and each configuration before calculating the metrics and perform statistical analyses. The following scripts are what I used to organize and analyze:

Script: *PG2_DPR1_Calculations.m*

- For each subject this is performed:
  - For each configuration this is performed:
    - Script: *Calculate_derived_data(User, user_number, set_number, [repetitions]).*
      - All 8 repetitions are loaded from the raw file.
      - The derived data are calculated.

        - The derived data are saved, *DER\Ui_Sj.mat*, where i is the user number and j is the set number.
    - Control effort is analyzed.
        - Script: *NASA_TLX(User).*
            - NASA_TLX scores are loaded and decoded.
            - Accumulated for each configuration.
            - Total score and score for each measure are returned.
        - Total NASA_TLX score and for each measure are accumulated for each user.
- NASA_TLX scores and measures are saved, *DER\TLX_Score.mat*
- Script: *Calculate_statistics(amount of sets, amount of users)*
    - For each set:
        - Derived data is loaded and accumulated for each subject.
        - Statistical analyses are performed.
        - The Statistical data are saved, *STAT\Si.mat*, where i is the set number.

Script: *PlotExp.m*

- Plots relevant figures of the analyses

Script: *CalcAnova(data,repetitions,alpha)*

- Calculates statistical differences (t-test) between columns in ‘data’

Script: animate_Global_pos(Global_pos,filename)

- Plots and records the motion of the slave robot performing the task, from above

C.2 Results

The results of the experiment are provided in this chapter. Results are presented for the performance and control effort metrics and the subjective measures. Analyses are then provided for the effect of learning (C.2.1), experience subject versus novice subject (0) and the driven path of the subjects (C.2.3).

Presented results are for 16 subjects that performed 8 repetitions for the 4 configurations.

To test the applicability to use the results for a normal distributed statistical analysis a normality assumptions was tested with a normal probability plot (Figure C-1) and a Lilliefors test. The Lilliefors test evaluates the null hypothesis that all the data in each configurations are normally distributed against that they are not normally distributed. The null hypothesis was not thrown, for the data in time to complete the entire task.

Please view the tables in the article which give a comprehensive overview of the analyses.

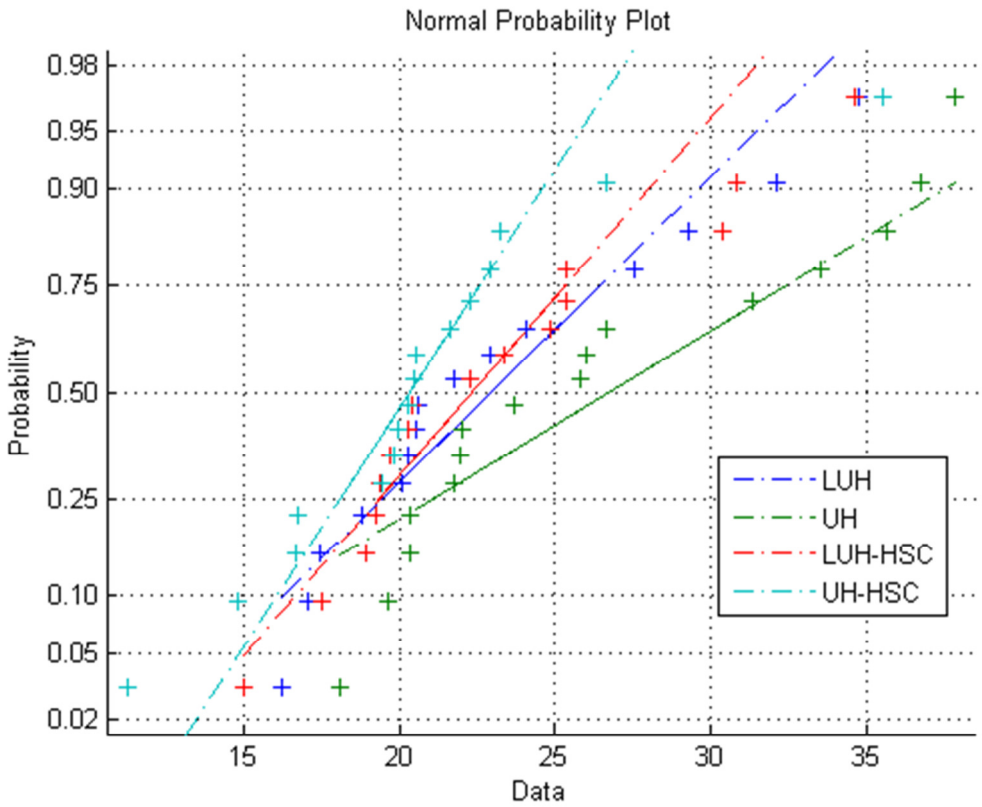

Figure C-1: A normal probability plot for the time to complete for the entire task, average of 8 repetitions for 16 subjects.

Time

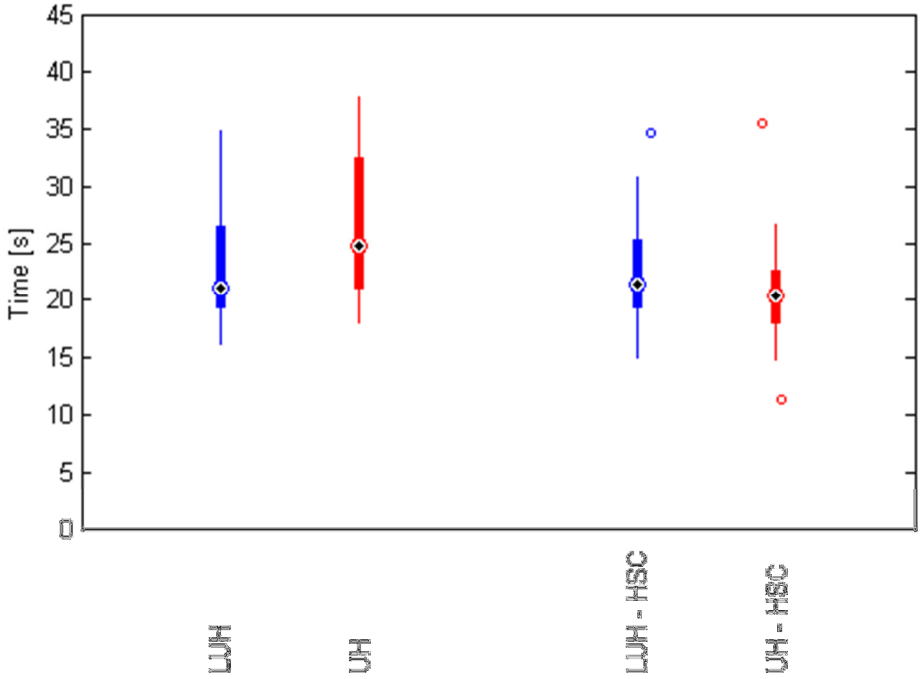

Figure C-2: Time to compete for the entire task for all configurations, average of 8 repetitions for 16 subjects.

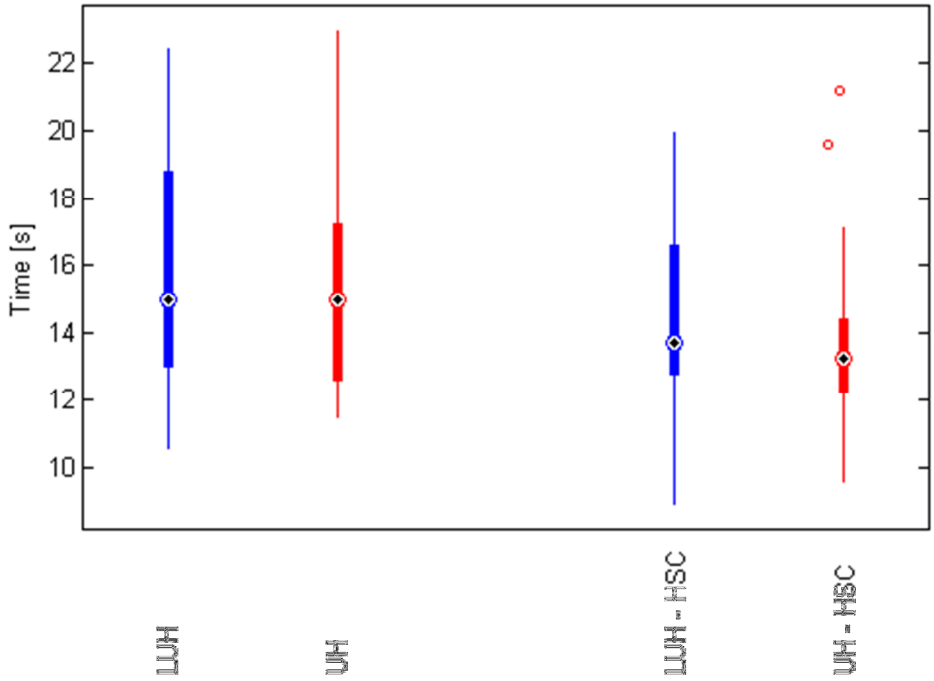

Figure C-3: Time to complete for subtask 1 (approach) for all configurations, average of 8 repetitions for 16 subjects.

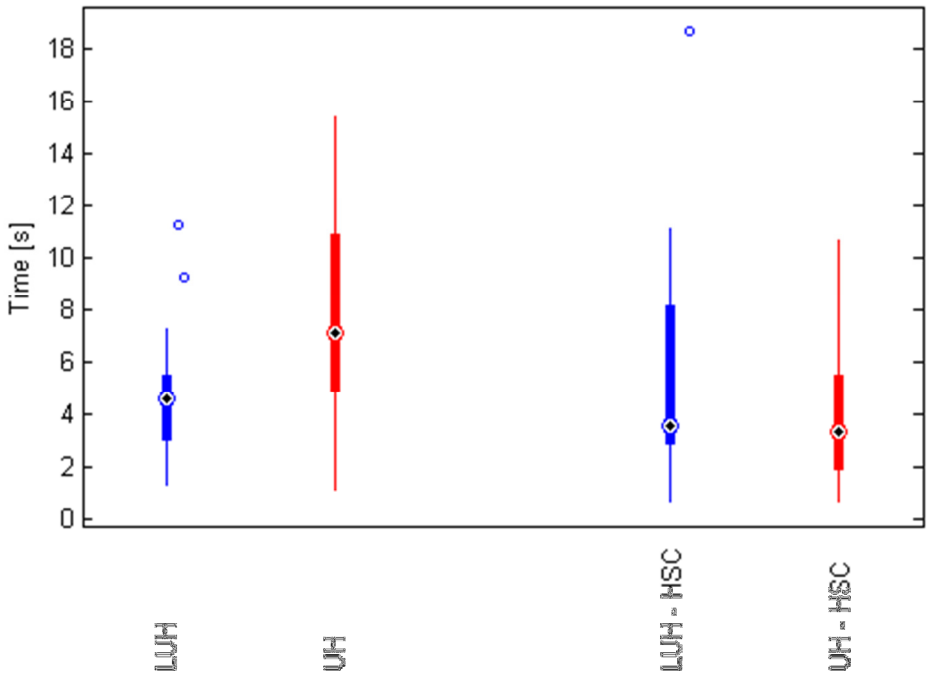

Figure C-4: Time to complete for subtask 2 (grasp) for all configurations, average of 8 repetitions for 16 subjects.

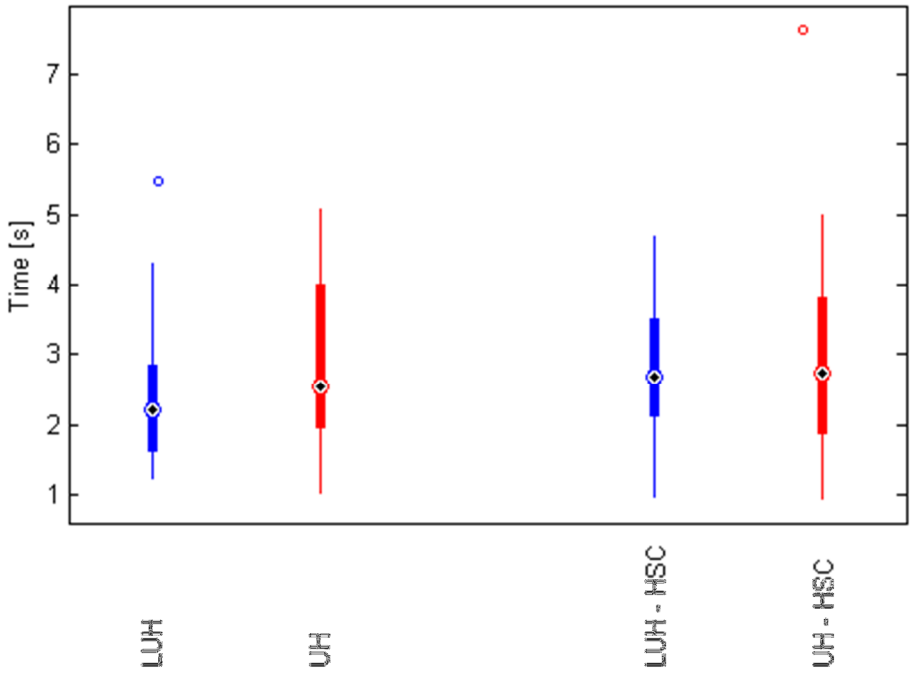

Figure C-5: Time to complete for subtask 3 (unlatch and open) for all configurations, average of 8 repetitions for 16 subjects.

Distance

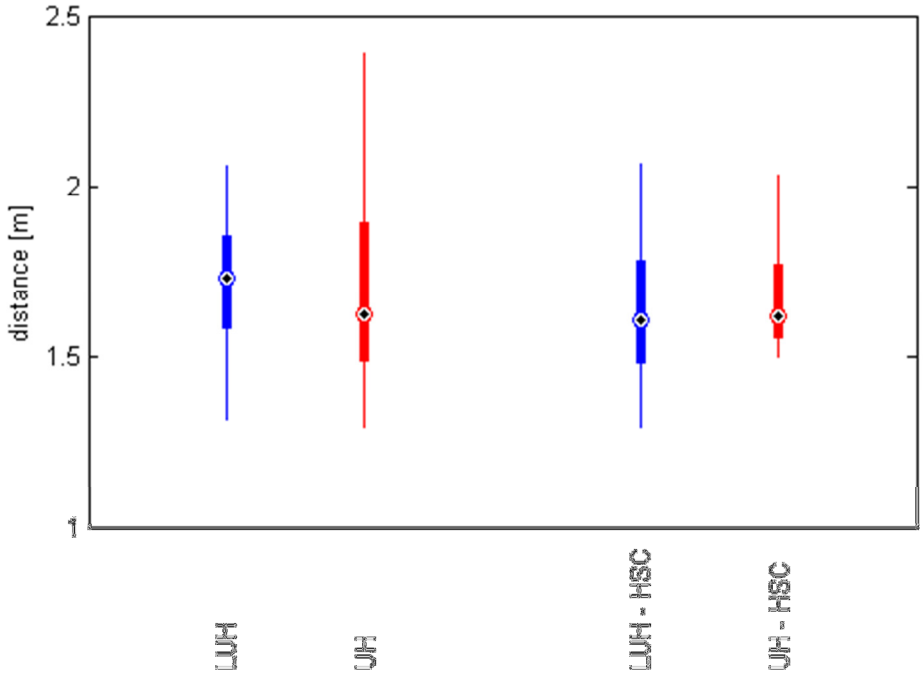

Figure C-6: The traveled distance for the approach subtask for all configurations, average of 8 repetitions for 16 subjects.

Reversal Rate

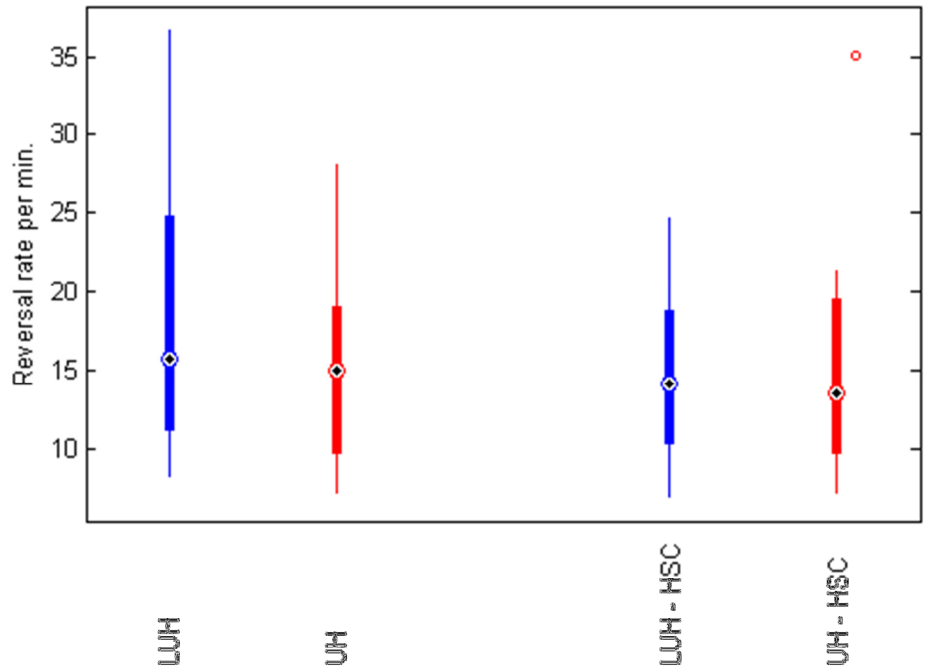

Figure C-7: Reversal rate in turning command (x-direction) for the approach subtask for all configurations, average of 8 repetitions for 16 subjects.

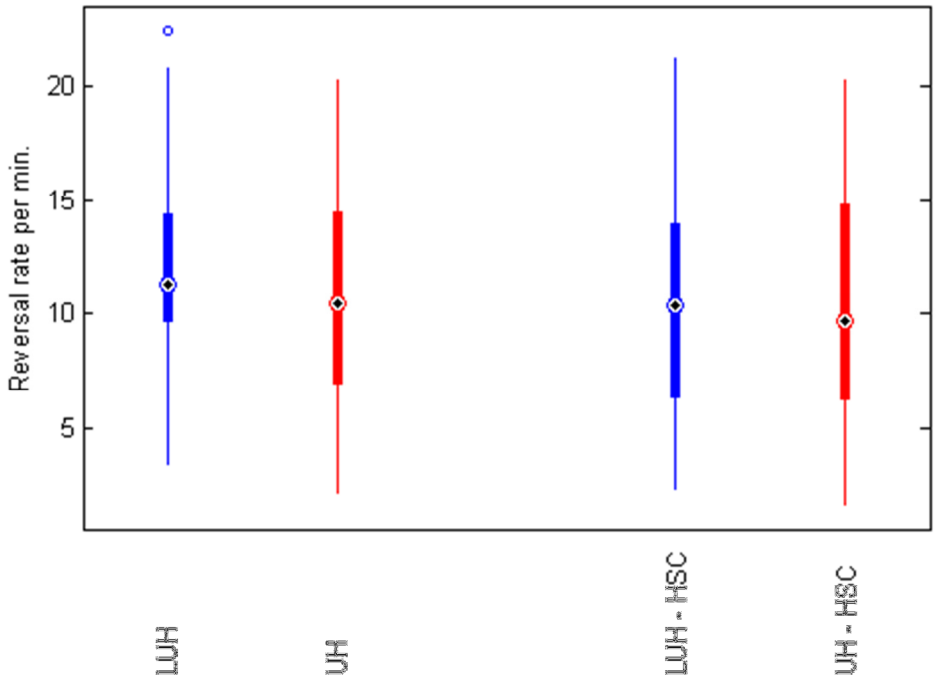

Figure C-8: Reversal rate in driving command (z-direction) for the approach subtask for all configurations, average of 8 repetitions for 16 subjects.

Angle

The angle between the robot and the door at contact was thought to provide evident results that haptic shared control guides the operator closer to being straight (closer to zero angle) to the door. It turned out to be non-significant. Interestingly thought, is that the mean of the UH and UH-HSC are higher than the corresponding LUH configurations (LUH: 6.43, UH: 7.91, LUH-HSC: 6.27 and UH-HSC: 6.42). This suggests that the underactuated hand enables the subject to successfully open the door at a wider angle.

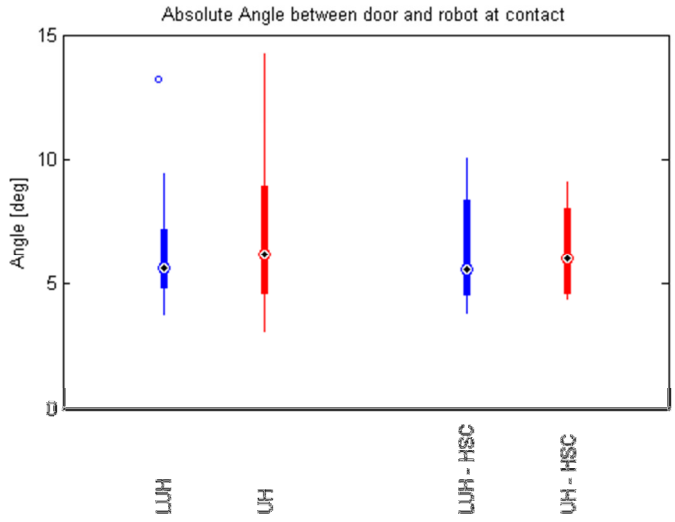

Figure C-9: Angle between the robot and the door at contact

Subjective Measures

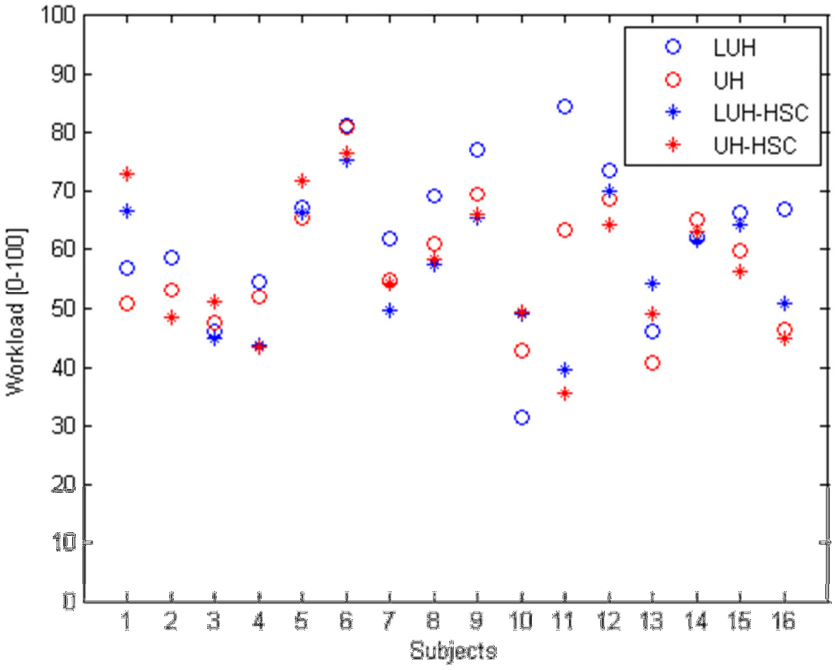

Figure C-10: Workload (NASA-TLX) for all 16 subjects. Low numbers represent lower workload.

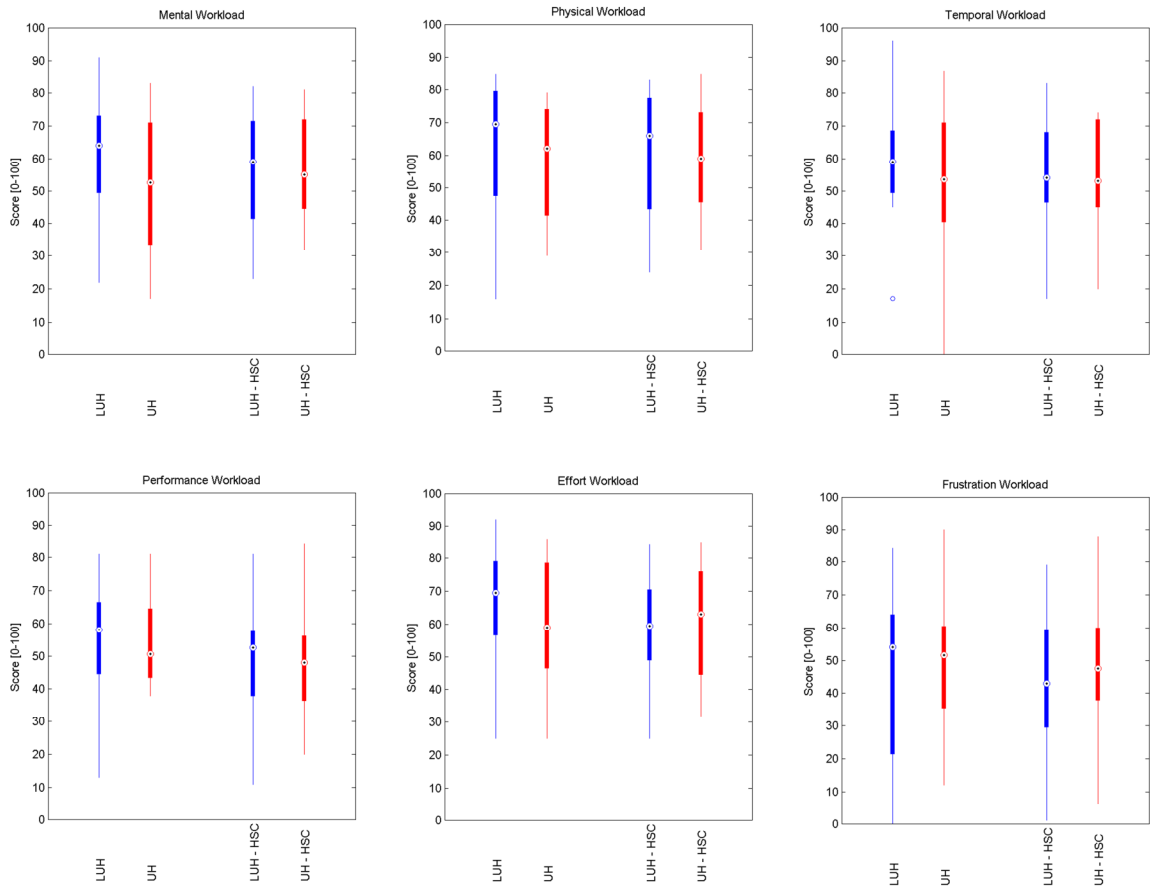

Figure C-11: Subjective workload (NASA-TLX) for all configurations is here divided into 6 measures (normal scores)

The subjective workload (NASA-TLX) was normalized as well where each datapoint from each of the 16 subjects was subtracted by the average value of the configuration.

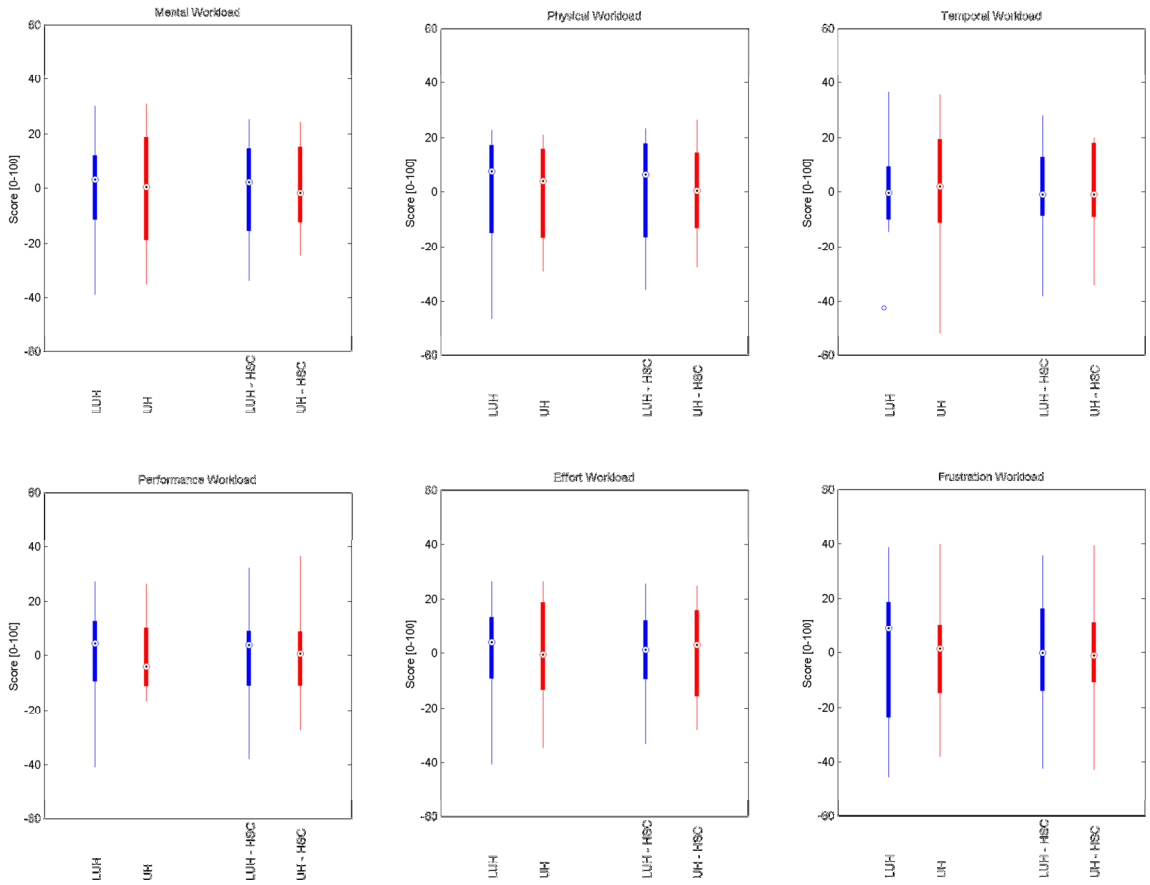

Figure C-12: Subjective workload (NASA-TLX) for all configurations is here divided into 6 measures (relative scores)

Failed attempts and problems with the master device

Subjects that did not firmly grasp the handle on the extended palm or pushed the door were counted as a failed attempt. Because of poor view on the handle, subjects grasped the handle sometimes too high or too low, which ended in the situation where the handle was beside the extended palm and not on it. Subjects performed the trial again after a failed attempt because then all subjects would have successfully completed 8 repetitions of all configurations.

Due to the implementation of the forward kinematics the end position of the master device got ´lost´ because the iterative search for the end position could not determine where it was. When that happened, the master device kept the last known position of the master device even though the operator moved the device. To the operator it felt like he had lost the communication with the slave device. At some occasions the position was found again and the operator could control it again but on other occasions a position was found that was completely wrong and outside the workspace of the master device. The position of the master was lost if the operator was on the outskirts of the workspace and especially if the device was pulled down and towards the operator.

Because the source of the lost communication, just described, between the master and the slave was not immediately found, the integrity of keeping track of the failed attempts was compromised due to frustration of the test conductor. Therefore the failed attempts were not used as one of the metrics for the experiment.

C.2.1 Learning Effects

The effects of learning can have tremendous effect on the analyzed data if proper precaution is not taken. First of all, the order of the configurations that subjects perform their experiment should be randomized to minimize the effect of learning. Because all configurations were not in the randomization during this experiment (HSC on or off only randomized) the effects of learning need to be analyzed and try to identify if it had any impact on the results. This chapter attempts to shed light on the learning effect by analyzing the effect of configuration order (Figure C-13), first and last 4 repetitions of each subject (Figure C-14) and the effect of subjects starting with or without HSC (Figure C-15 through Figure C-26). Subjects performed the experiment by either starting with HSC (1. UH-HSC 2. LUH-HSC 3. LUH and 4. UH) or without HSC (1. UH 2. LUH 3. LUH-HSC and 4. UH-HSC). Starting with HSC or without HSC was randomized and resulted in an equal amount of subjects (8) in both groups.

Table C-2: Performance metrics compared between subjects who started with guidance (HSC) and without guidance. The 4 configurations are compared and show the difference in mean and the significance (p-value). Shaded numbers present a significant difference. Negative difference in mean indicate that the mean of subjects starting with HSC is larger.

	HSC first vs HSC last [mean diff. (p-value)]			
	LUH	UH	LUH-HSC	UH-HSC
ttc [s]	-1.71 (0.550)	3.47 (0.967)	-0.15 (0.204)	-3.81 (0.162)
ttc – subtask 1	0.94 (0.615)	2.93 (0.051)	3.68 (0.035)	-1.45 (0.340)
ttc – subtask 2	-1.81 (0.185)	1.22 (0.099)	-3.32 (0.612)	-1.00 (0.488)
ttc – subtask 3	-0.84 (0.158)	-0.68 (0.401)	-0.51 (0.186)	-1.32 (0.127)
n_{grasps} [-]	-0.13 (0.141)	-0.11 (0.015)	-0.53 (0.419)	-0.063 (0.633)
d [m]	1.76 (0.295)	0.05 (0.062)	0.27 (0.645)	-0.03 (0.695)
r_{rate} -x [-]	8.01 (0.056)	0.49 (0.003)	8.96 (0.863)	3.30 (0.374)
r_{rate} -z [-]	5.77 (0.013)	4.20 (3.78e-4)	7.81 (0.098)	4.51 (0.099)
Nasa-tlx [0-100]	7.33 (0.305)	2.55 (0.601)	-3.13 (0.663)	-8.33 (0.190)

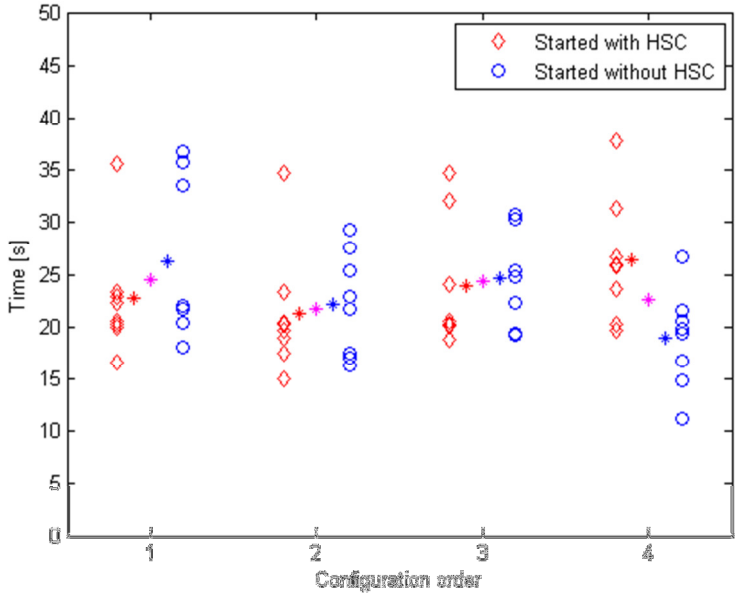

Figure C-13: Time to complete is compared between subjects that started with HSC (red diamonds) and those who started without HSC (blue circles). The stars represent the average of each group (red and blue) and the average of all subjects (pink). Subjects that started with HSC had the configuration order: 1. UH-HSC, 2. LUH-HSC, 3. LUH and 4. UH while the subjects that started without HSC had the configuration order: 1. UH, 2. LUH, 3. LUH-HSC and 4. UH-HSC.

Time

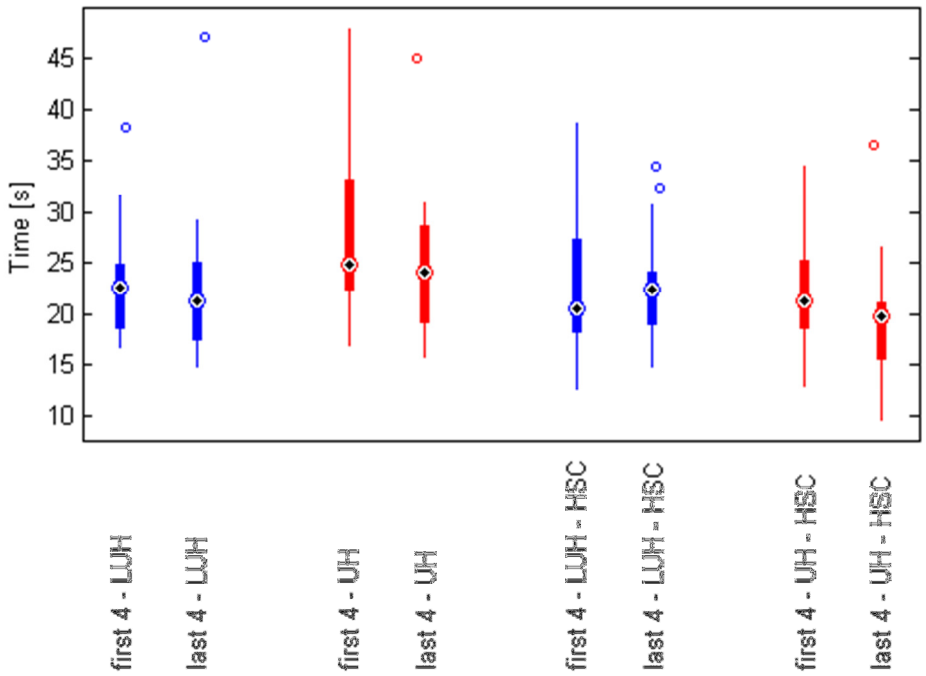

Figure C-14: Time to complete for the entire task for all configurations. The average of the first and last 4 trial of each of the 16 subjects are presented.

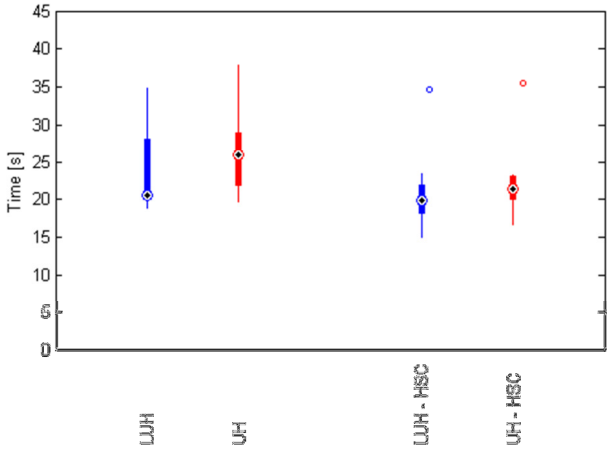

Figure C-15: Time to complete for the entire task for all configurations, average of 8 repetitions for 8 subjects that started with UH-HSC, then LUH-HSC, LUH and UH.

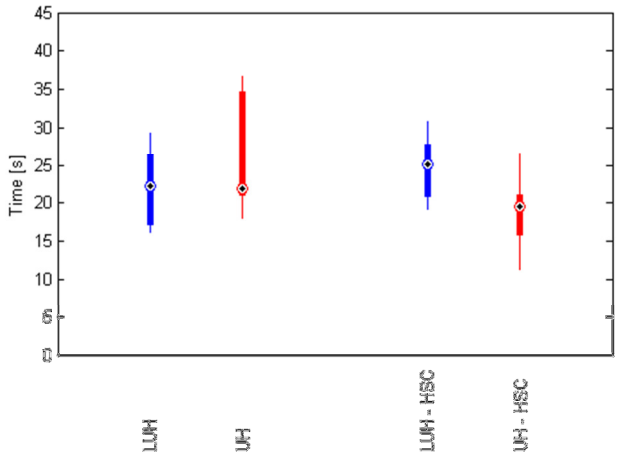

Figure C-16: Time to complete for the entire task for all configurations, average of 8 repetitions for 8 subjects that started with UH, then LUH, LUH-HSC and UH-HSC.

Grasps

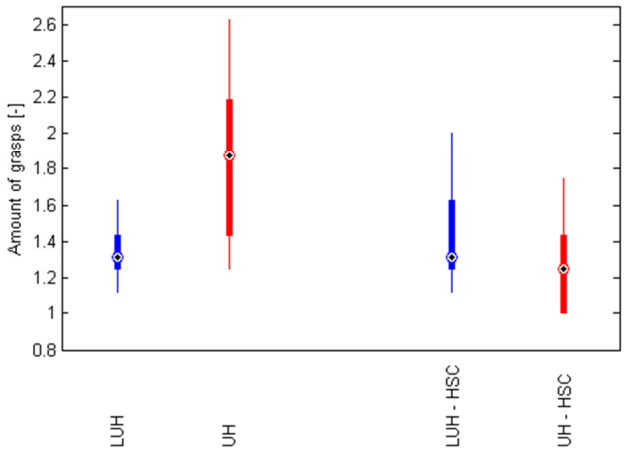

Figure C-17: Amount of grasps for all configurations, average of 8 repetitions for 8 subjects that started with UH-HSC, then LUH-HSC, LUH and UH.

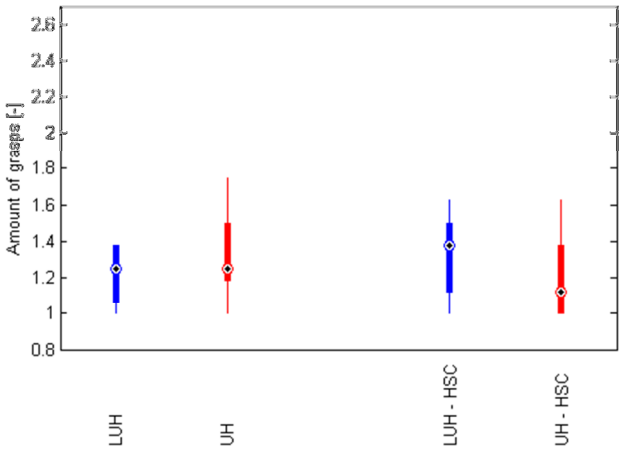

Figure C-18: Amount of grasps for all configurations, average of 8 repetitions for 8 subjects that started with UH, then LUH, LUH-HSC and UH-HSC.

Distance

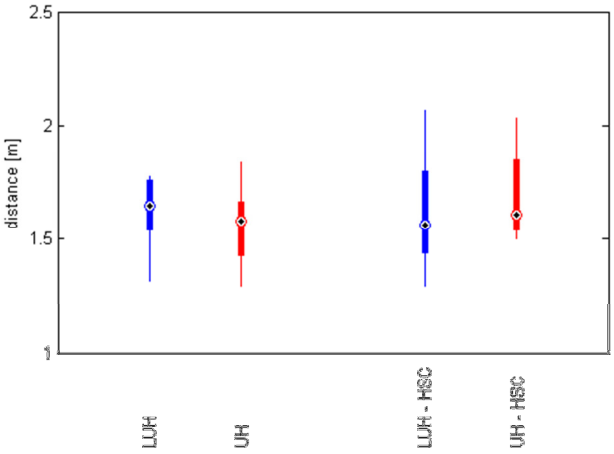

Figure C-19: Traveled distance for the approach subtask for all configurations, average of 8 repetitions for 8 subjects that started with UH-HSC, then LUH-HSC, LUH and UH.

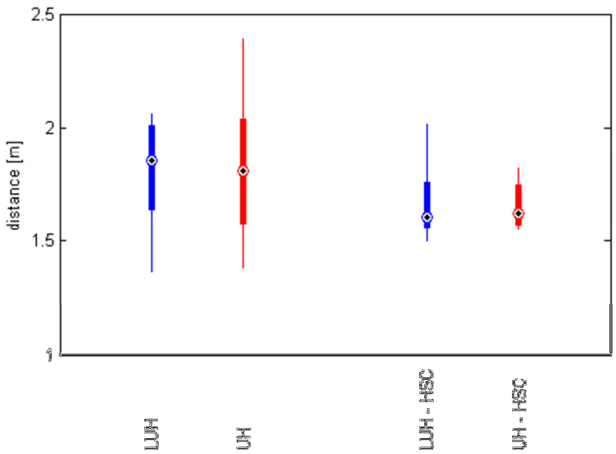

Figure C-20: Traveled distance for the approach subtask for all configurations, average of 8 repetitions for 8 subjects that started with UH, then LUH, LUH-HSC and UH-HSC.

Reversal Rate

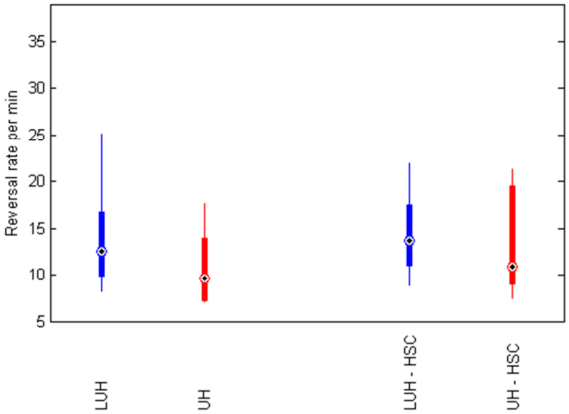

Figure C-21: Reversal rate in x-direction (turning) for the approach subtask for all configurations, average of 8 repetitions for 8 subjects that started with UH-HSC, then LUH-HSC, LUH and UH.

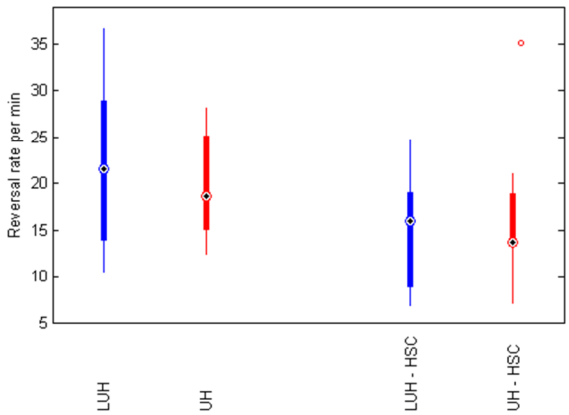

Figure C-22: Reversal rate in x-direction (turning) for the approach subtask for all configurations, average of 8 repetitions for 8 subjects that started with UH, then LUH, LUH-HSC and UH-HSC.

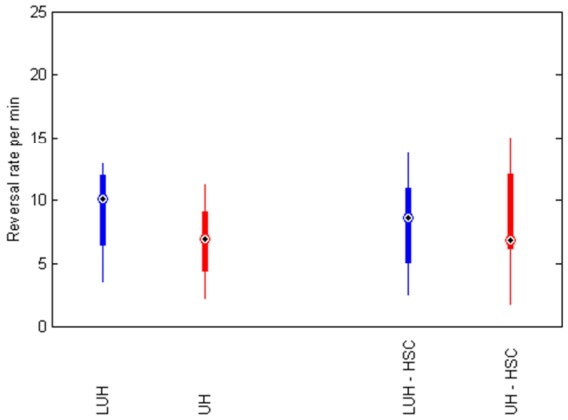

Figure C-23: Reversal rate in z-direction (drive) for the approach subtask for all configurations, average of 8 repetitions for 8 subjects that started with UH-HSC, then LUH-HSC, LUH and UH.

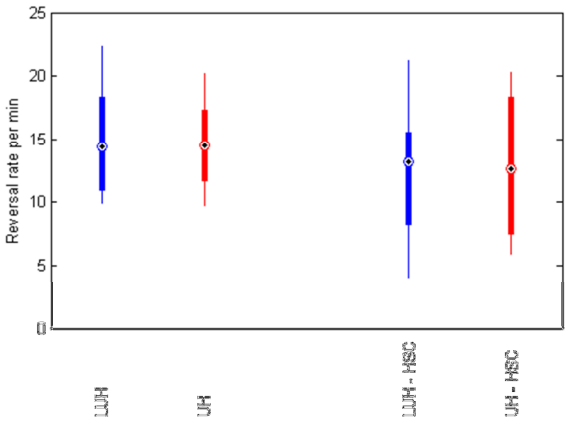

Figure C-24: Reversal rate in z-direction (drive) for the approach subtask for all configurations, average of 8 repetitions for 8 subjects that started with UH, then LUH, LUH-HSC and UH-HSC.

Subjective Measures

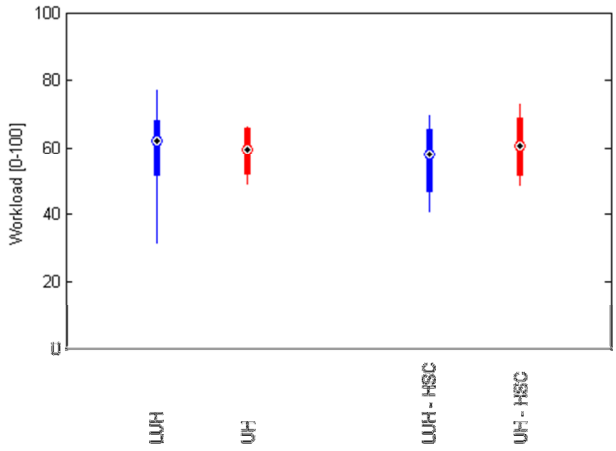

Figure C-25: Workload (NASA-TLX) for all configurations, average of 8 repetitions for 8 subjects that started with UH-HSC, then LUH-HSC, LUH and UH.

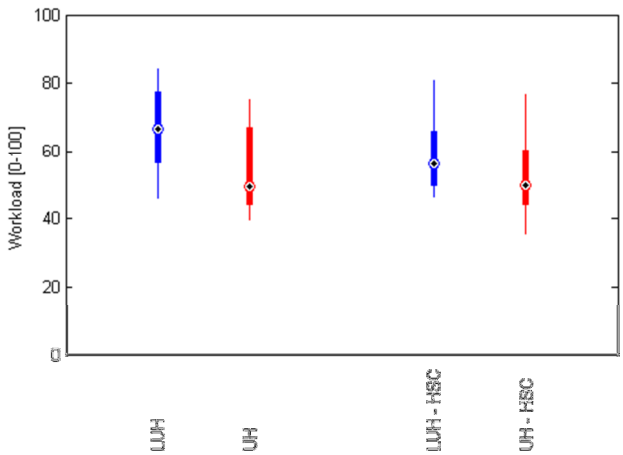

Figure C-26: Workload (NASA-TLX) for all configurations, average of 8 repetitions for 8 subjects that started with UH, then LUH, LUH-HSC and UH-HSC.

C.2.2 Experienced vs. Novice

Subjects that had previous experience in remotely controlling a robot might perform better or at least require less training. To find out if that is true a comparison between them and novice subjects, had no previous experience, was performed. The performance and control effort metrics and the subjective measures are analyzed. A comprehensive overview of the analysis can be seen in Table C-3. An Anova test was performed to see if any significant difference was between the subjects. No significant difference was found between an experienced subject and a novice subject. Although, it is quite interesting to see that novice subjects usually rated the subjective workload (Nasa-tlx) lower than experienced subjects.

Table C-3: Performance metrics compared between subjects with experience on remotely controlling a robot against subjects with no prior experience. The 4 configurations are compared and show the difference in mean and the significance (p-value). Negative difference in mean indicate that the mean of the experienced subjects is larger.

	Experienced vs. Novice subjects [mean diff. (p-value)]			
	LUH	UH	LUH-HSC	UH-HSC
ttc [s]	1.48 (0.620)	2.47 (0.531)	2.12 (0.505)	-1.71 (0.535)
ttc – subtask 1	-0.14 (0.948)	0.82 (0.617)	0.92 (0.694)	-0.68 (0.679)
ttc – subtask 2	1.19 (0.421)	1.34 (0.618)	0.96 (0.682)	-0.55 (0.718)
ttc – subtask 3	0.43 (0.525)	-0.03 (0.954)	0.56 (0.364)	-0.48 (0.601)
n_{grasps} [-]	-0.00 (0.958)	-0.09 (0.559)	0.27 (0.286)	-0.10 (0.497)
d [m]	0.06 (0.630)	-0.15 (0.222)	-0.06 (0.720)	-0.04 (0.620)
r_{rate} -x [-]	0.88 (0.685)	0.54 (0.824)	1.58 (0.281)	1.17 (0.537)
r_{rate} -z [-]	2.50 (0.404)	3.65 (0.241)	3.24 (0.277)	1.88 (0.527)
Nasa-tlx [0-100]	-9.37 (0.255)	-6.05 (0.303)	-4.58 (0.500)	-9.24 (0.183)

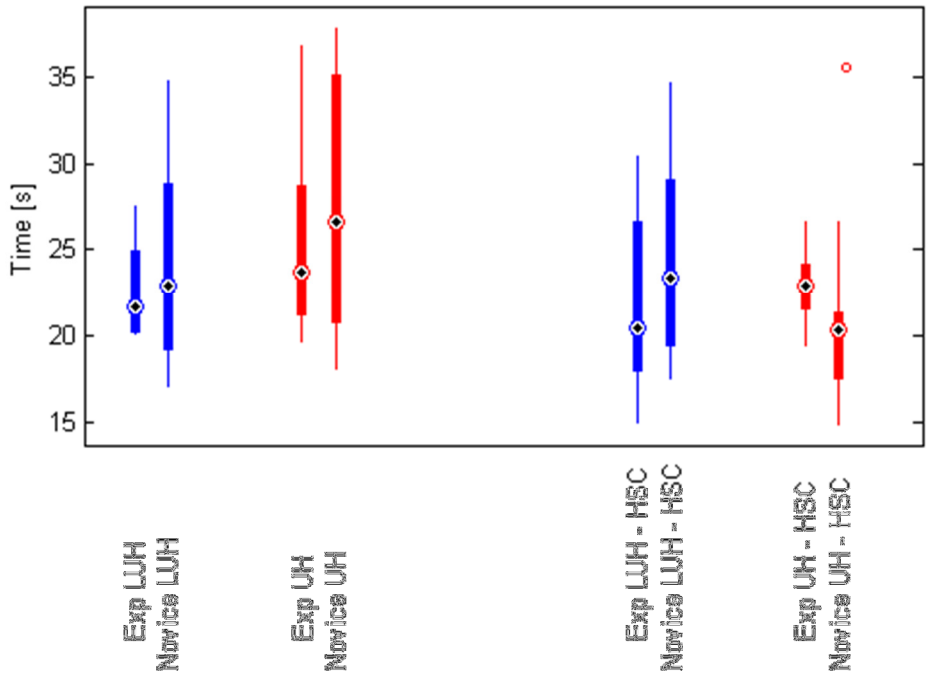

Figure C-27: Time to complete compared between subjects with some experience remotely controlling a robot against novice subjects.

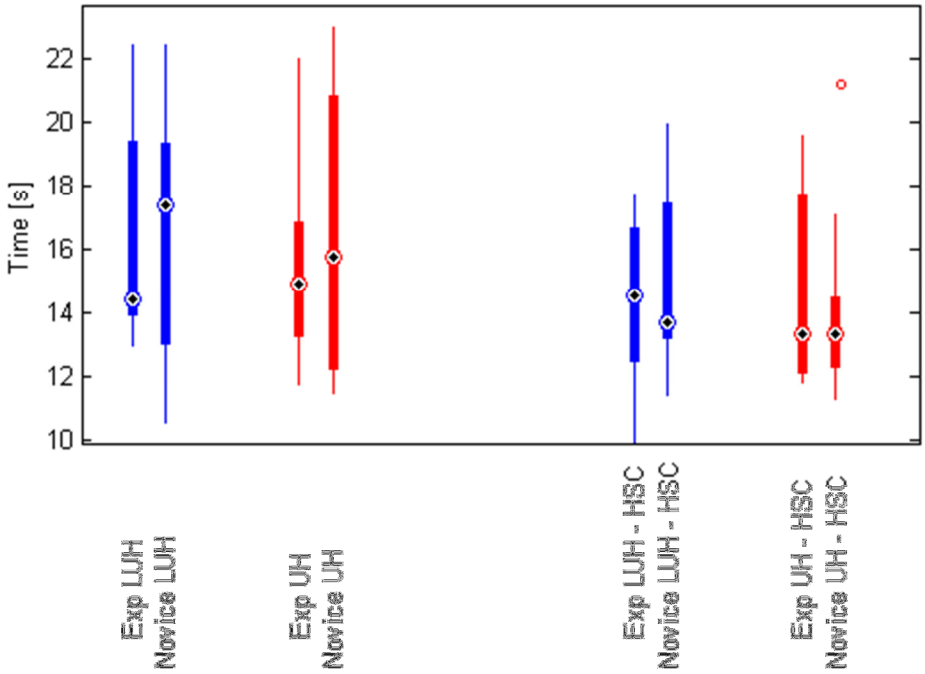

Figure C-28: Time to complete for subtask 1 (approach) compared between subjects with some experience remotely controlling a robot against novice subjects.

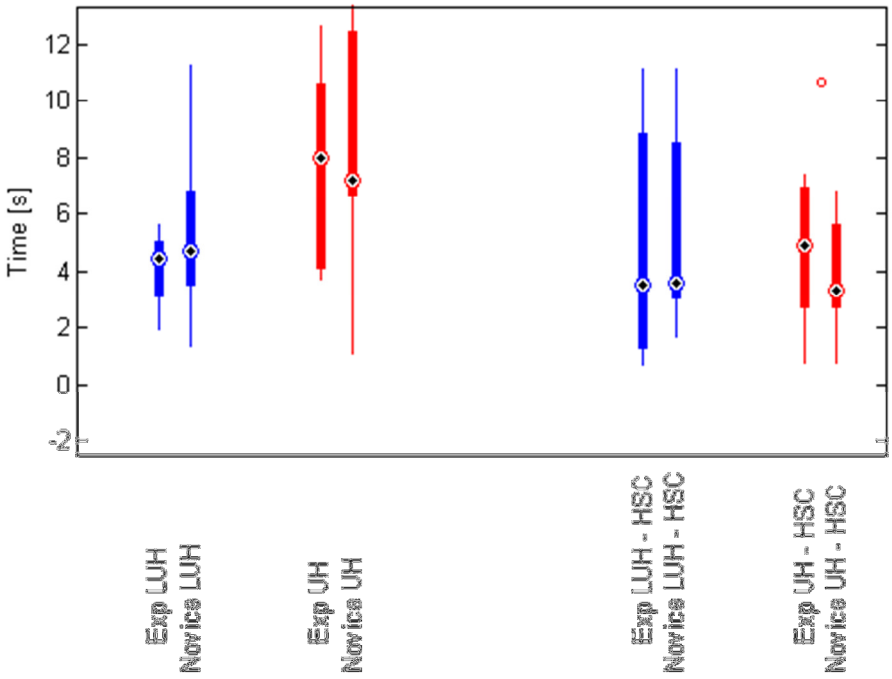

Figure C-29: Time to complete for subtask 2 (grasp) compared between subjects with some experience remotely controlling a robot against novice subjects.

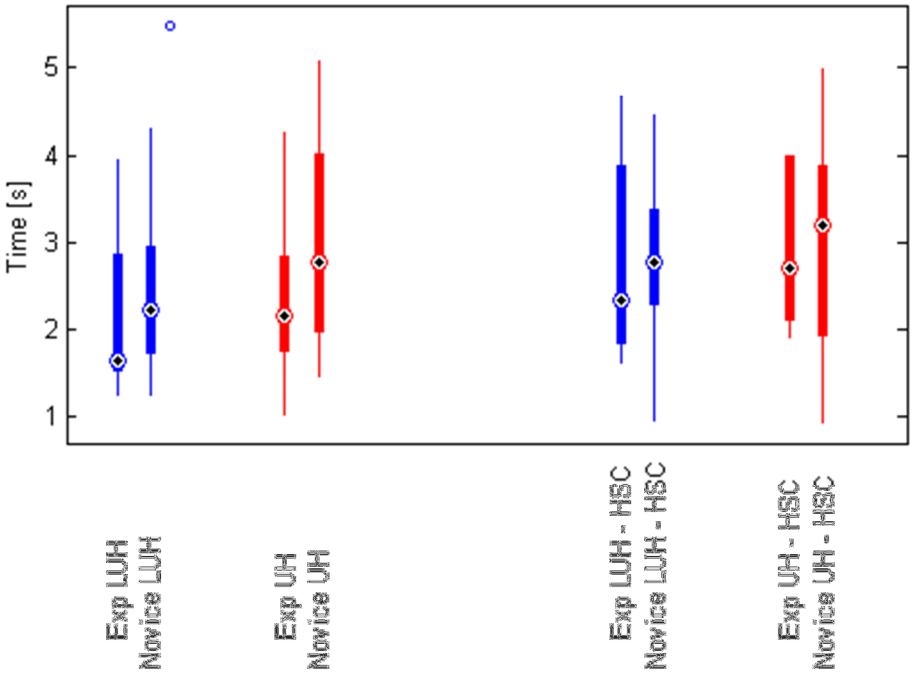

Figure C-30: Time to complete for subtask 3 (unlatch and open) compared between subjects with some experience remotely controlling a robot against novice subjects.

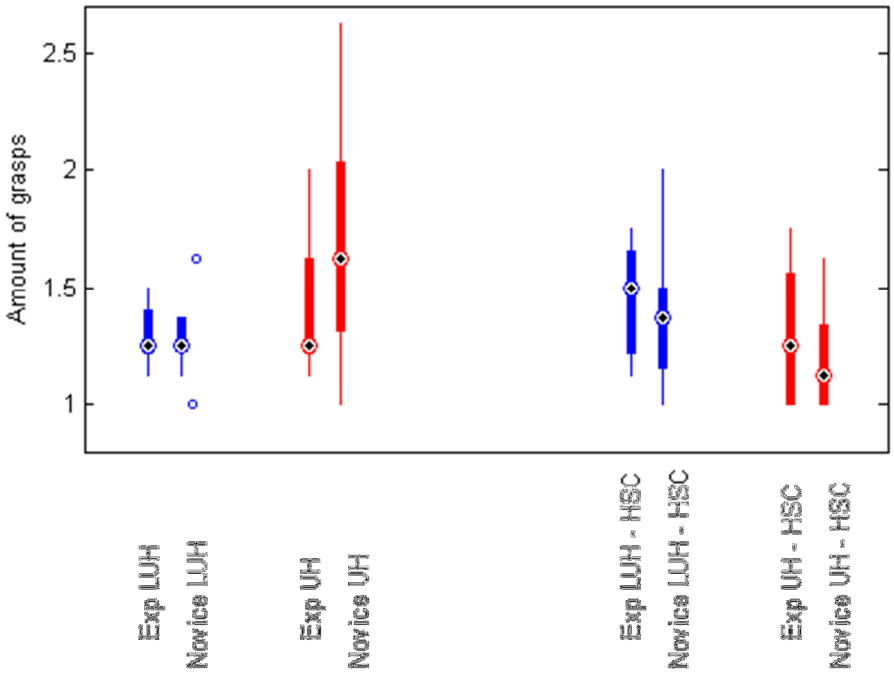

Figure C-31: Amount of grasps compared between subjects with some experience remotely controlling a robot against novice subjects.

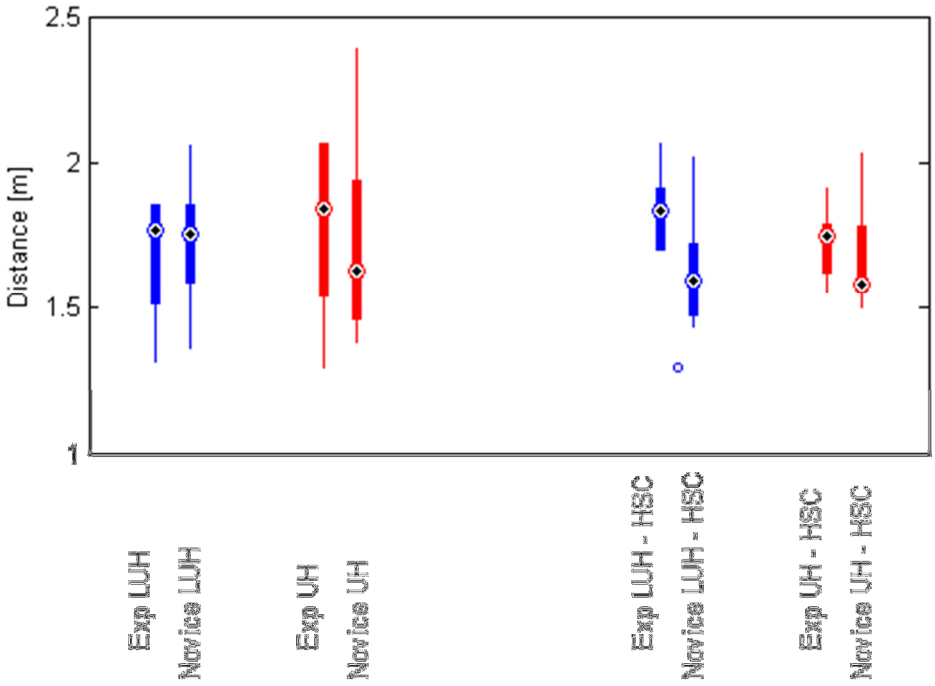

Figure C-32: Distance travelled compared between subjects with some experience remotely controlling a robot against novice subjects.

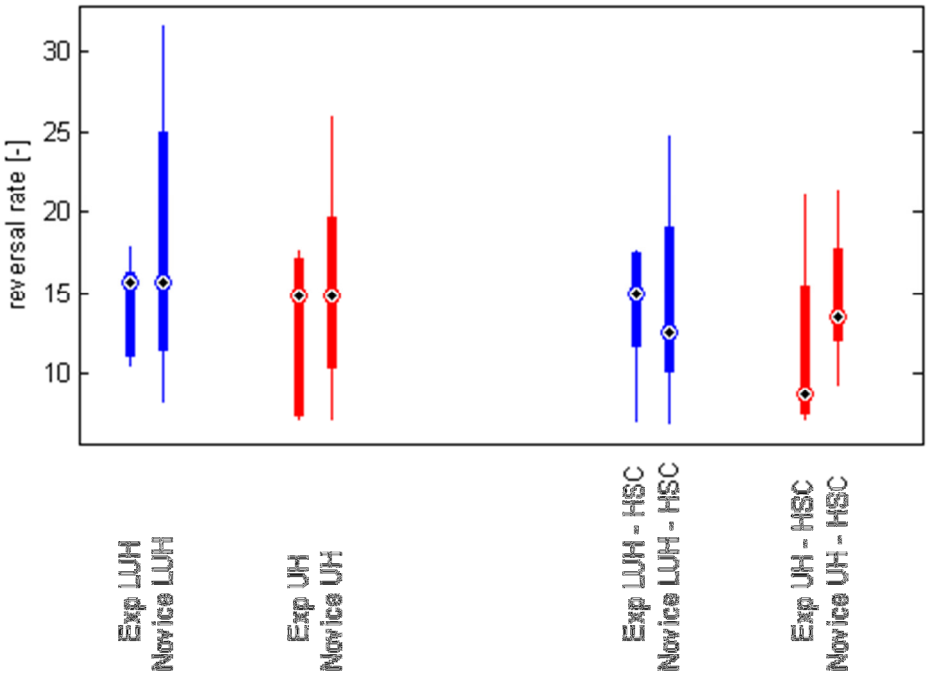

Figure C-33: Reversal rate, steering corrections, compared between subjects with some experience remotely controlling a robot against novice subjects.

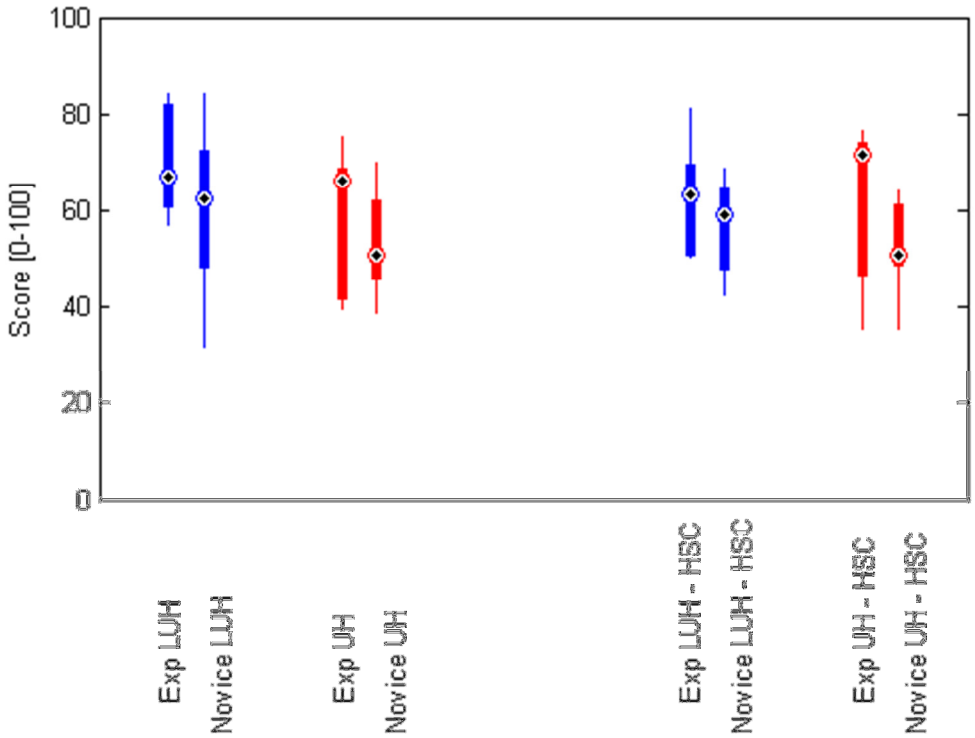

Figure C-34: Subjective workload (NASA-TLX) compared between subjects with some experience remotely controlling a robot against novice subjects.

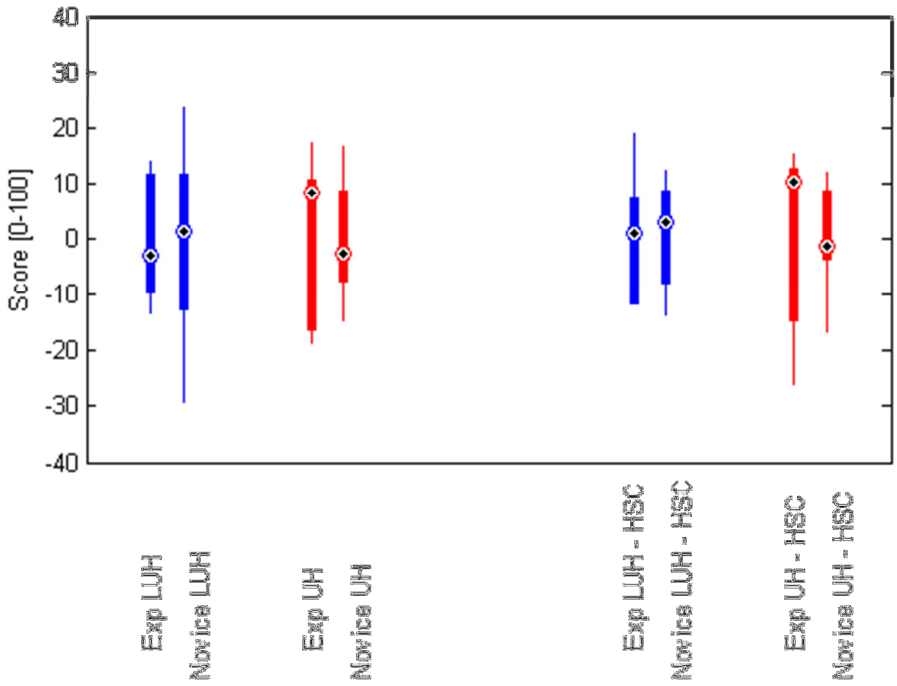

Figure C-35: Subjective workload (NASA-TLX) compared between subjects with some experience remotely controlling a robot against novice subjects (relative measures, each value is subtracted by the average of each group).

C.2.3 Path

Subjects travelled to the door with a certain path and looking at that path can show how well haptic shared control guided the subjects to the door. Figure C-36 and Figure C-37 show a path of a typical subject during all of his trials, divided into two starting location. The ideal path that subjects were guided towards was a straight line from (0, 0) to (1.3, 0). In the figures the line is a horizontal line in the middle of the figures.

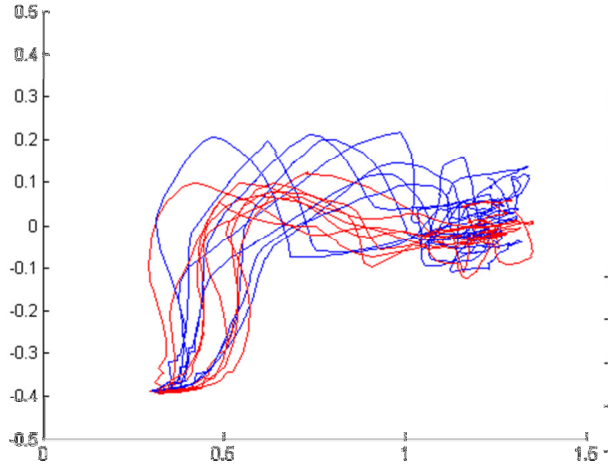

Figure C-36: End-effector path of a typical subject with haptic shared control (red) and without haptic shared control (blue) from one starting point. Horizontal axis is x-direction [m] and vertical axis is y-direction [m]. Robot started from (0.4, -0.395) and ended at the door at (1.3, 0).

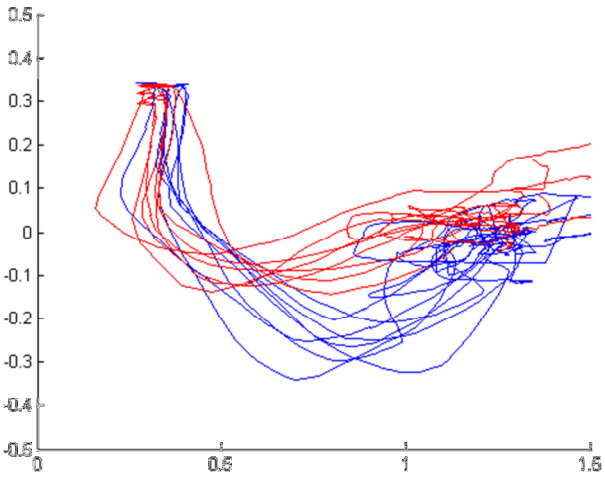

Figure C-37: End-effector path of a typical subject with haptic shared control (red) and without haptic shared control (blue) from one starting point. Horizontal axis is x-direction [m] and vertical axis is y-direction [m]. Robot started from (0.4, 0.35) and ended at the door at (1.3, 0)

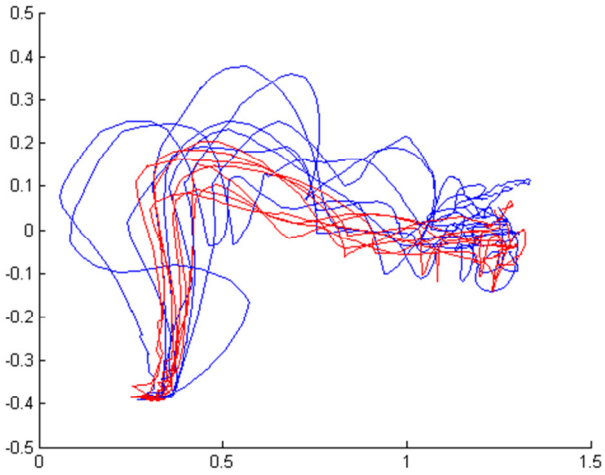

Figure C-38: End-effector path of a typical subject with haptic shared control (red) and without haptic shared control (blue) from one starting point. Horizontal axis is x-direction [m] and vertical axis is y-direction [m]. Robot started from (0.4, -0.395) and ended at the door at (1.3, 0).

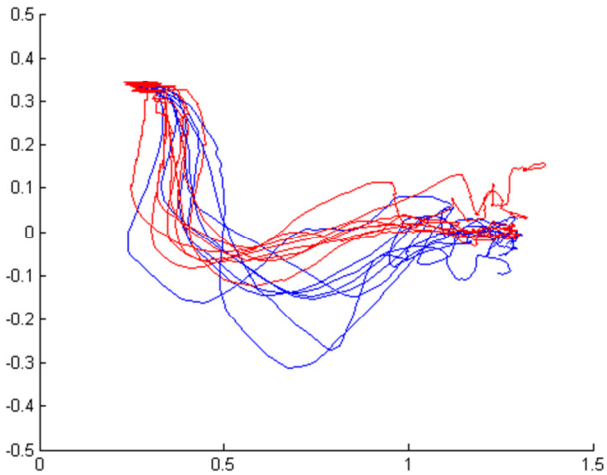

Figure C-39: End-effector path of a typical subject with haptic shared control (red) and without haptic shared control (blue) from one starting point. Horizontal axis is x-direction [m] and vertical axis is y-direction [m]. Robot started from (0.4, -0.395) and ended at the door at (1.3, 0).

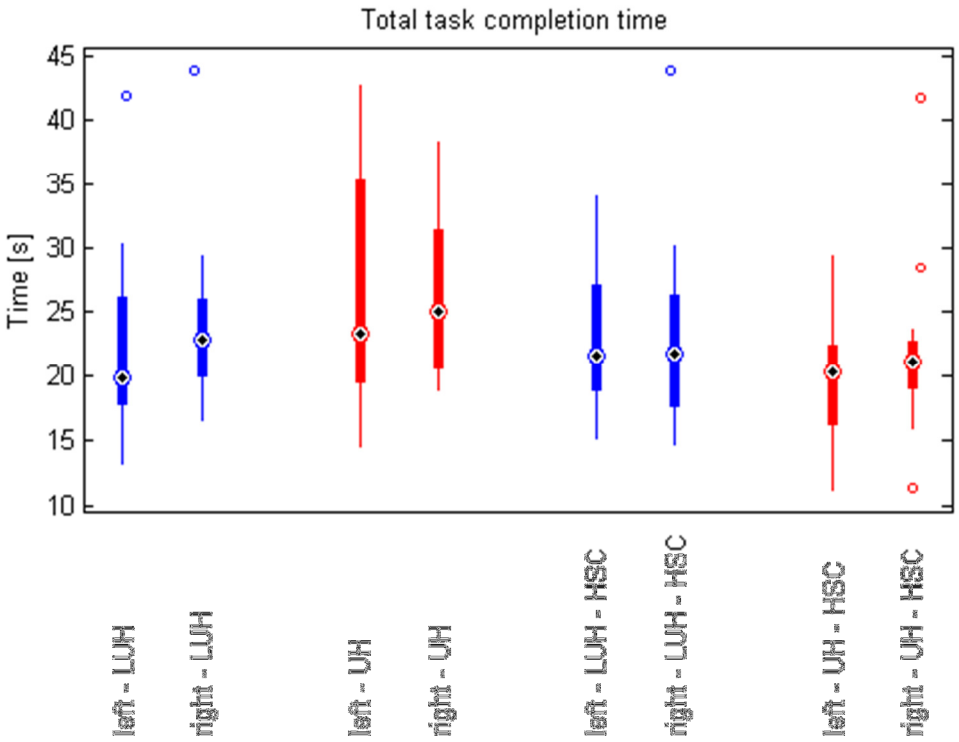

Figure C-40: Time to complete for the entire task separated by the two starting locations, left or right of the door.

Subjects seemed to be influenced by from which starting locations they started, whether it was approaching the door from left or right. Figure C-40 illustrates that effect and shows quite some change in behavior of the subjects. Table C-2 provides a comprehensive overview of the results.

Table C-4: Performance metrics compared between starting from the left or right of the door. The 4 configurations are compared and show the difference in mean and the significance (p-value). Shaded numbers present a significant difference. Negative difference in mean indicate that the mean of starting from left is larger.

	Left vs Right [mean diff. (p-value)]			
	LUH	UH	LUH-HSC	UH-HSC
ttc [s]	1.73 (0.484)	0.15 (0.942)	0.20 (0.950)	2.05 (0.314)
ttc – subtask 1	0.55 (0.692)	0.34 (0.321)	1.44 (0.754)	2.04 (0.085)
ttc – subtask 2	0.59 (0.687)	0.08 (0.579)	-1.07 (0.969)	-0.18 (0.869)
ttc – subtask 3	0.59 (0.222)	-0.27 (0.737)	-0.172 (0.500)	0.18 (0.782)
n_{grasps} [-]	1 (1)	0.02 (0.497)	-0.16 (0.904)	0.09 (0.421)
d [m]	-0.36 (0.762)	-0.04 (0.986)	0.00 (0.682)	-0.01 (0.930)
r_{rate} -x [-]	-0.64 (0.849)	3.52 (0.389)	2.33 (0.120)	3.10 (0.260)
r_{rate} -z [-]	0.16 (0.935)	-0.39 (0.545)	1.30 (0.852)	2.33 (0.276)
Nasa-tlx [0-100]	-	-	-	-

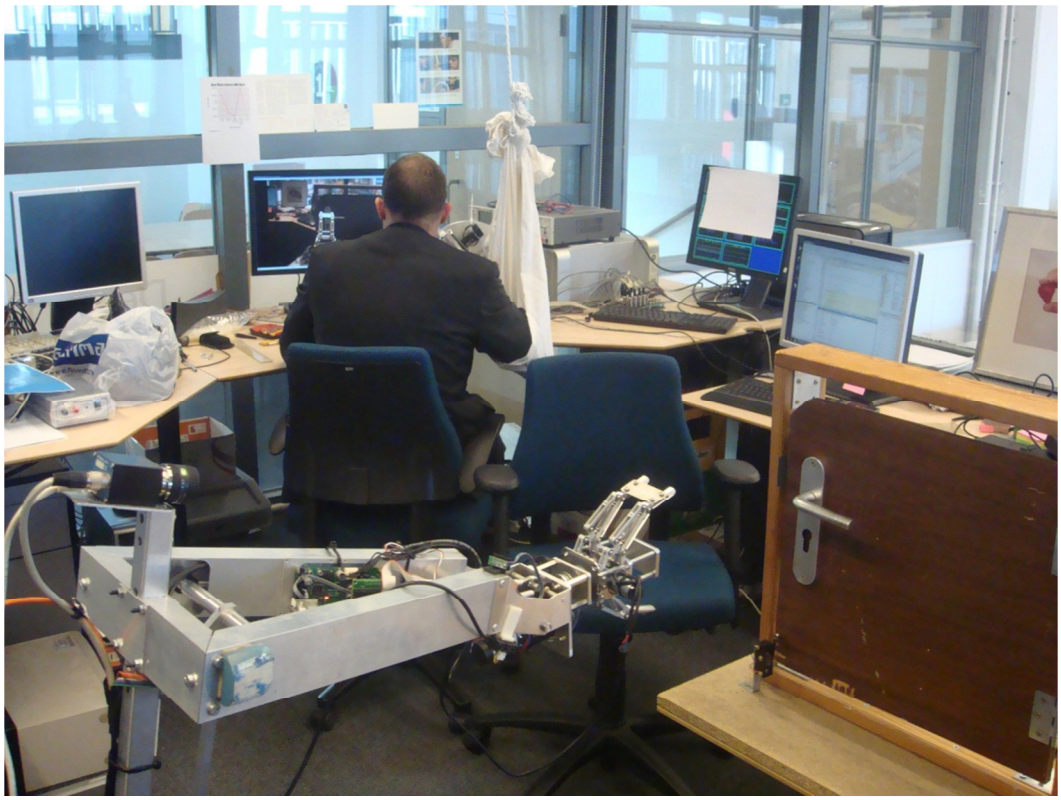

Figure C-41: A subject executing the task.

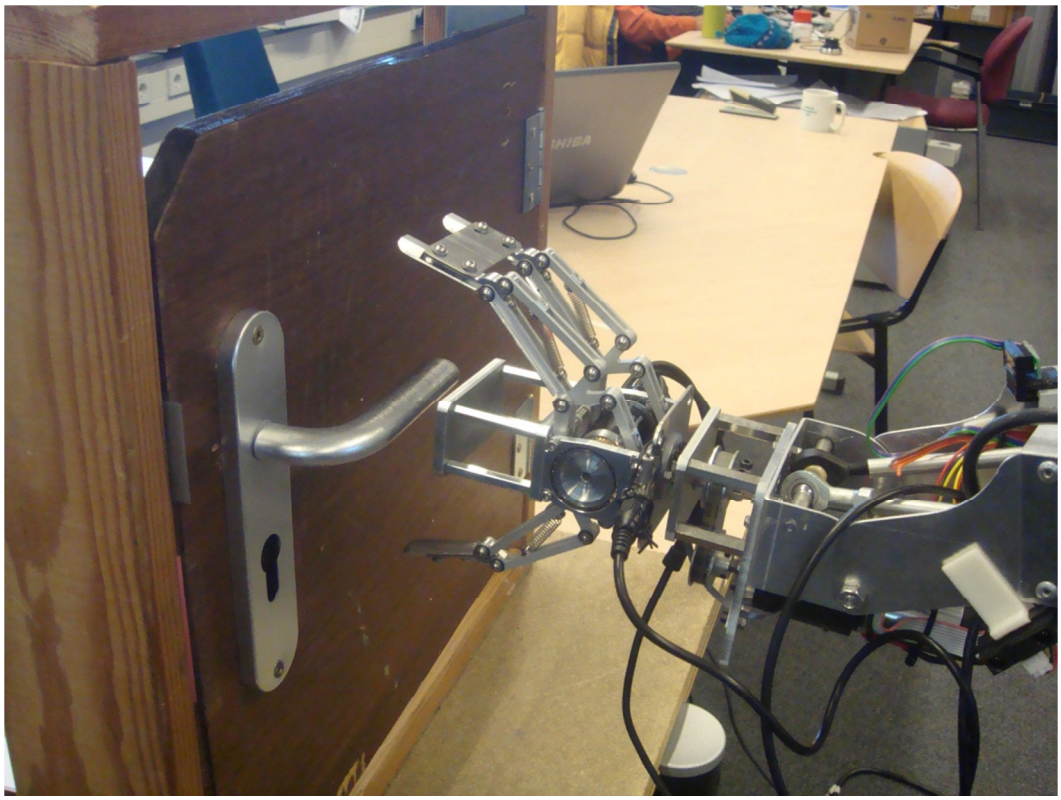

Figure C-42: A subject about to grasp the door handle to unlatch the door.

Appendix D Experiment on Underactuated Hand

Underactuated hands are usually not used in telemanipulation because they lack the exact position of the fingers to provide such feedback information. An underactued hand developed at TU Delft, Delft hand 3 (DH3), was used in the telemanipulation task described in the paper. The DH3 is without any positional sensor which makes things even harder to estimate the finger position. An idea came up to use motor current to know the state of the hand because it was known that when the hand gripped an object the current rises. This information could then be sent over to the master side as force feedback. Using the motor current, an already given information at the slave robot, no extra sensors was needed, positional or force. An experiment was done to get better familiar with the current behavior while gripping and releasing a door handle and quantify the current-force relationship of the hand.

D.1 Delft Hand 3 (DH3)

The DH3 has three fingers, each with two phalanges and the underactuation is provided by a differential and a motor that can rotate its shaft and housing. The motor housing is connected to one finger, the shaft to the differential and then each side of the differential to the other two fingers.

Some modification was needed on the DH3 so it could firmly grip a door handle. The fingers touched the door itself before the palm contacted the door handle and the hand gripped the handle with a caging grip, very loose grip. Both was solved by extending the palm about 40 mm, see Figure A-14 and Figure A-15.

D.2 Experimental setup

The experiment was done to test if the motor current is a feasible choice for a haptic feedback. When the fingers cannot move further (fully open, fully closed or is gripping an object) the motor current peaks to a certain level depending on the PWM control signal. To perform this experiment a force sensor and a current sensing multimeter were required to properly calibrate the current signal from the slave and also to see the force-current relationship. The force sensor was a Mini loadcell S beam 111 N and was placed along with a stiff sponge in between two aluminum plates. Pressing the plates together gave a voltage signal from the loadcell that already had been calibrated. The output voltage signal from the loadcell was then sent through an analog signal conditioner (amplifier) CPJ-CPJ2S and then picked up by a National Instrument DAQ which communicated with LabView 8.2.1. on a laptop. Parallel to this setup the DH3 was operated through a 3Mxel v2.0 microprocessor by the same laptop and both current and PWM signal from the 3Mxel were recorded. The multimeter displaying the current was connected in series with the DH3 motor and a voltage measuring multimeter connected parallel to the motor.

In the experiment, both a pinch and power grasps were analyzed to better understand the force distribution in the fingers. Also when gripping a door handle with the extended palm it is very hard to read out the exact force because some of the force push the handle onto the palm and the rest towards the other fingers, see Figure D-1. Force-current relationship of such a grip was significantly lower than for a pinch grasp because a great deal of the force went into pushing against the opposing finger(s) and not onto the force sensor.

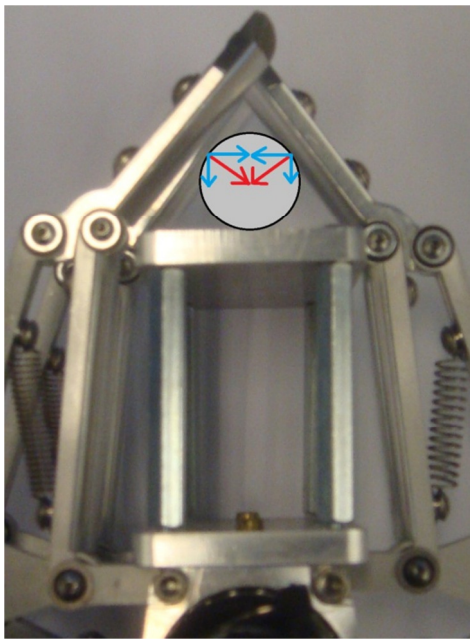

Figure D-1: Grasping forces acting on a door handle (red). If they are separated into an x and y components, a large part of the force can be seen acting against another similar force.

D.3 Results

The motor uses a current of 0.035 A (measured by 3mxel) when opening or closing the gripper at any PWM, see Figure D-3. Different PWM determines however the maximum (high) current and voltage when in contact or fully open gripper, see Table D-1.

Table D-1: Different PWM signals sent to the motor of DH3

PWM	Multimeter Current [A]	Multimeter Voltage [V]	Power [W]	3Mxel Current [A]	Power Grasp [N]	Pinch Grasp [N]
100						
200	0.04	0.91	0.0364	0.035	1.26357	0.21714
300	0.07	1.51	0.1057	0.052	3.68175	0.774185
400	0.10	2.21	0.212	0.070	6.7966699	1.80854
500	0.12	2.74	0.3288	0.087	8.153249	2.5921
600	0.15	3.35	0.5025	0.105	9.2997544	3.4604
700	0.18	3.97	0.7146	0.122	10.38951	4.43951
800	0.20	4.58	0.916	0.145	13.77246	5.26238
900	0.23	5.20	1.196	0.157	14.744	5.66238
1000	0.25	5.82	1.455	0.186	15.9191	5.9486
1100	0.28	6.43	1.8004	0.190	17.3432	5.9631
1200	0.30	7.04	2.112	0.205	20.022	5.91338

One can see in Table D-1 that there is a difference in measured current by the multimeter and the 3Mxel, see also Figure D-2. By now it has been fixed with a new firmware.

The current increases rapidly when in contact with a hard object as can be seen in Figure D-3. The signal goes sometimes to 0 because the hand was controlled with a 3 position switch (open-off-close) and was not operated fast enough. By using the switch the opening and closing of the hand does not show the negative current that the microcontroller is able to provide. The microcontroller can therefore know when it is opening or closing the hand by determining the sign of current.

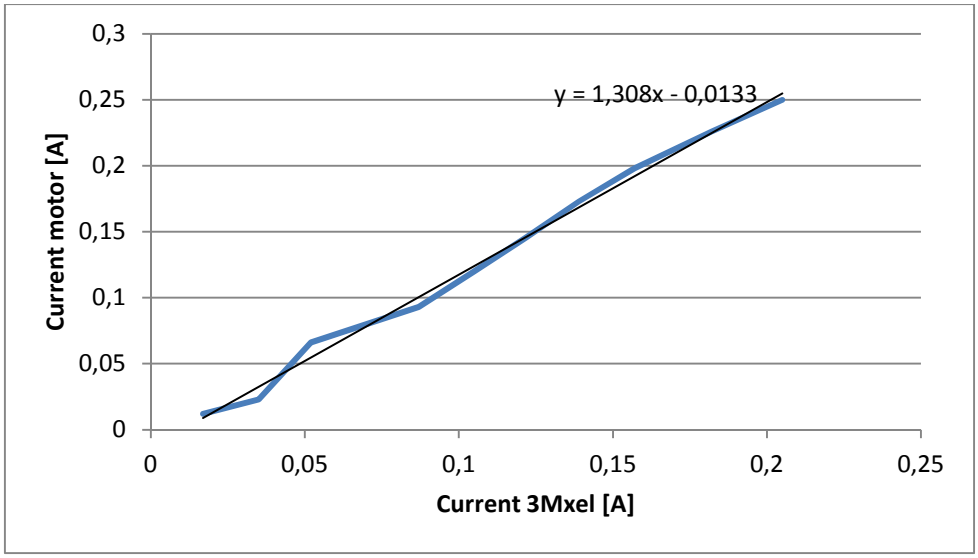

Figure D-2: Motor current measured by 3Mxel and a multimeter

The two grips are presented in Figure D-4 where the force is a function of current. For the experiment the grasps for different PWM signals where always the same because if the object was grasped differently the forces would be different. Power grasp was measured to receive the maximum force that the hand can produce while pinch grasp was to see the forces in the fingertips. The pinch force is a better estimation of the forces that will occur while gripping a door handle. When an object was gripped and pulled out of the gripper the current did not increase.

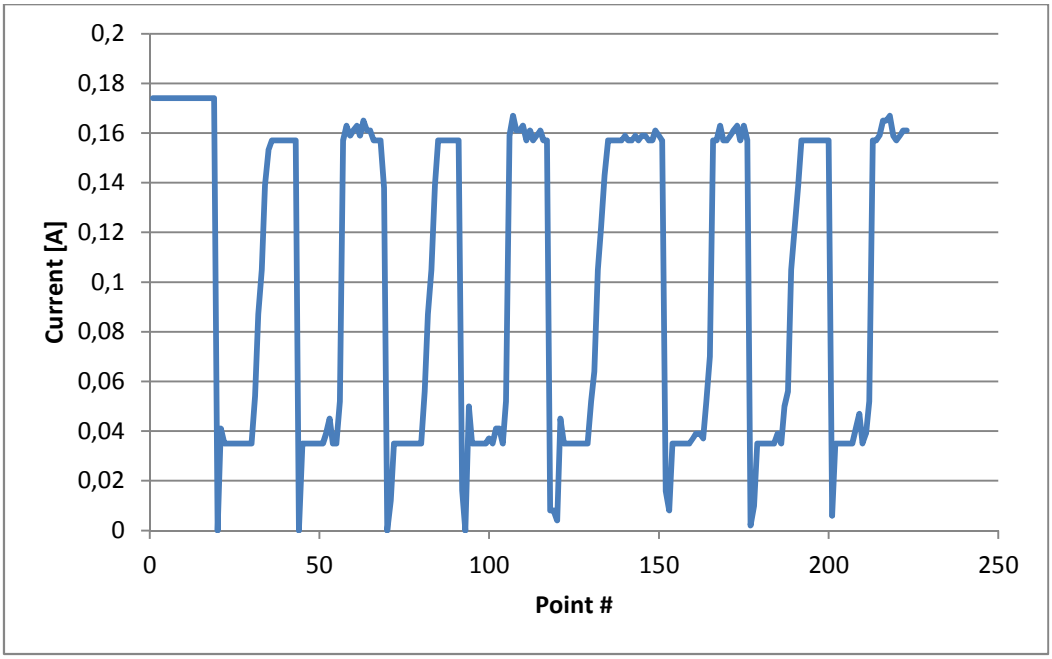

Figure D-3: 900 PWM current signals to the motor of DH3 when grasping an object 4 times using a 3 position switch

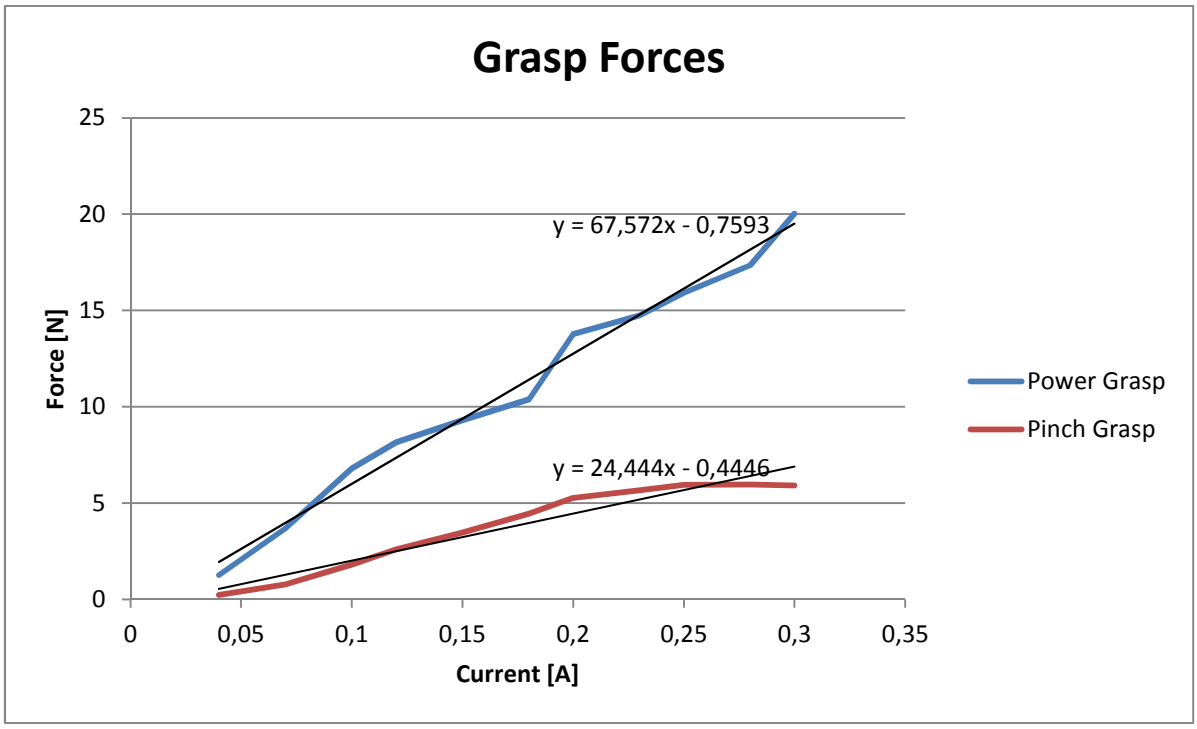

Figure D-4: Current versus force for both power and pinch grasps

D.4 Discussion

Using an underactuated hand in a telemanipulator is not so trivial. Such hands have always been controlled by switching them either on or off but never position controlled. Mainly because they don´t have position sensors. The results show that the motor current is usable

for feedback information. The electrical current can provide the current state of the fingers, fully open, closed or moving. That information can be used to provide the operator some knowledge of what is going on at the slave side.

The only downfall is that the position of the fingers are not know, only if they are fully open, fully closed or if they are moving. An improvement could be realized to know the finger positions without any additional sensors, by adding springs to the fingers with a very low spring constant that will just barely change the motor current linearly depending on how extended they are. The springs would make it linearly harder for the motor to close the hand and therefore would increase the motor current depending on the fingers position. Although the springs should not decrease the gripping force excessively.

D.5 Conclusions

The experiment on gripping a door handle with DH3 has provided us with valuable information on how to create a controller for the DH3 that is able to provide force feedback. The conclusions from the experimental results are mainly these:

- Current
    - Current rises and drops quickly in hard contact.
    - Current signal is repeatable and is almost constant at its maximum or minimum value.
    - Current drop suggest that fingers are about to move away from an object or an end stop.
    - Current less than 0.04 A indicates that fingers are moving. Although dependent on how tightly screwed the screws are in the fingers.
    - Current rise suggest that fingers are about to move towards an object or an end stop.
    - Current that is about constant and above 0.04 A indicate that an object or an end stop are blocking the fingers movement.
- Force
    - Measuring force in underactuated grasps is difficult because different finger positions generate different forces and force directions.
    - Power grasp produces almost three times higher forces than a pinch grasp.
    - Pinch grasp forces are a good estimation on the forces that occur during door handle grasping because proximal phalanges are not in contact with the handle.

To successfully create a force feedback controller for DH3 the controller needs to know the current that is being used and convert that to an estimate force with equation F=24.444*I-0.446 (for opening doors).

Adding springs to the fingers should make it possible to provide some indication on finger position due to increase in motor current.